2020

Characterizing the requirements for the matricellular protein, dCCN, in nervous system function

Elizabeth L. Catudio Garrett
University of Montana

Recommended Citation

CHARACTERIZING THE REQUIREMENTS FOR THE MATRICELLULAR

PROTEIN *dCCN* IN NERVOUS SYSTEM FUNCTION

By

ELIZABETH LEILANI CATUDIO GARRETT

Bachelors of Art, University of Montana, Missoula, Montana, 2014

Thesis

presented in partial fulfillment of the requirements
for the degree of

Master of Science
in Cellular, Molecular and Microbial Biology

The University of Montana
Missoula, MT

July 2020

Approved by:

Scott Whittenburg,
Graduate School Dean

Dr. Sarah Certel, Research Advisor
Division of Biological Sciences, Professor

Dr. Mark Grimes, Committee Member
Division of Biological Sciences, Professor

Dr. Allen Szalda-Petree, Committee Member
Department of Psychology, Professor

Table of Contents

Acknowledgements

There is so much gratitude and appreciation I hold for so many ancillaries who have helped me and encouraged me along my academic journey. In all honesty, throughout my undergraduate and graduate career, I have endured many distractions and hardships that were out of my control. Oftentimes, I amaze myself thinking that I have made it this far. This is the biggest accomplishment of my life, and there are so many people I owe credit to for assisting me, and continually supporting me along the way.

First and foremost, I'd like to express a million *thank yous* to Dr. Sarah Certel, who unconditionally believed in me, supported me, and assisted me with many challenging spells in my life; all while patiently mentoring me during my time in her lab. Words simply cannot describe the deep appreciation, immense gratitude, and gratefulness I feel for Dr. Certel. I learned so much about being a better student, researcher, and overall scientist from her. I would not be where I am today without the assistance, enthusiasm, patience, guidance, and care I received from Dr. Certel. I will never forget you, and I am forever indebted to you. I am in awe to have had this opportunity to work in your lab, and grow under your tutelage. ***Thank you again, for everything!!!***

Next, I would like to thank my committee, Dr. Certel, Dr. Grimes, and Dr. Szalda-Petree for their valuable insight, guidance, suggestions, challenging questions, and mentorship. Additionally, I'd like to thank the numerous professors, mentors, instructors, teaching assistants, and lab mates I had worked with and learned from while at the University of Montana. A special thanks goes to Dr. Szalda-Petree, Dr. Lawrence, Dr. Hansen, Dr. Bridges, Dr. Hay, Dr. Kavanaugh, Dr. Yi, Dr. Duley, Dr. Wilhelm, Dr. Gabriel, Dr. Cochran, Dr. Yoonhee-Jang, Dr. Hall, Dr. Campbell, Dr. Foltz, Dr. Henderson, Dr. Farnsworth, Dr. Lind, Dr. Andrews, Dr. Palacios-Moreno, and many others. I gained invaluable research exposure while working with you, in your labs, or while taking courses from you. Lastly, I would like to give a resounding thank you to Dr. Diane Friend, who would pull me out of high school classes and bring me to her lectures at the University of Montana to inspire me to try college. It worked, so thank you so much for believing in me and encouraging me! All of these experiences, words of encouragement, and lessons contributed to molding me into the scientist I am today. Thank you all!

Next, I would like to thank my family. I am the first in my family to graduate high school, college, and now graduate school. I want to give a special thanks to my Mom, Arlene Catudio Garrett, for always encouraging me to explore novel academic opportunities, and who persuaded me to keep pushing forward, no matter how tough times became. I also want to thank my Dad, Timothy Garrett, for being excited about the sciences with me, and always being interested in hearing me discuss biology. It is a wonderful feeling to break the cycle, and lead by example to my younger family members. I hope my academic accomplishments will continue to inspire my family members into pursuing education, and I now have this particular academic experience to share with my family members in inspiring, mentoring, and guiding them.

Catudio Garrett, Elizabeth, M.S., Spring 2020   Cellular, Molecular and Microbial Biology

Characterizing the requirements for the matricellular protein *dCCN* in nervous

system function

Chairperson: Dr. Sarah J. Certel

The brain is organized as a complex network of specialized neurons that communicate via a combination of electrical and chemical signals. Our brains function to generate movement, control organ function, or direct complex behaviors; all of which requires the ability to regulate the flow of communication between circuits and networks. Work in this thesis addresses two areas of neuron communication: first, *how does the release of more than one neurotransmitter from a single neuron impact behavior*, and second, *are matricellular proteins* (MCPs) *key contributors to synaptic transmission and neuron function*? The conserved CCN family of MCPs have a unique mosaic structure consisting of a secretory signal peptide followed by four conserved functional domains. This complex mosaic structure provides CCN proteins with key signaling and regulatory roles that are required for many vital biological functions, however, our understanding of the function of CCN proteins in the central nervous system (CNS) is quite limited. The goal of this study was to characterize *dCCN* expression, the sole *Drosophila melanogaster* CCN member, and determine how *dCCN* contributes to neuron function. We determined that *dCCN* expression in the CNS begins during embryogenesis and continues into mature adult neurons. In the adult, *dCCN* expression was found in a number of neuron types including sensory neurons, neurons innervating the crop and gut of the gastrointestinal system, and neurons innervating the ovaries and uterus indicating a multi-faceted role in neuron function in this invertebrate member. Furthermore, I describe co-expression between *dCCN* and neurons that express the monoamines octopamine (OA), dopamine (DA), and serotonin (5-HT), and in neurons that are sexually dimorphic, including *fruitless* (*fru*), and *double-sex* (*dsx*). Lastly, we demonstrate for the first time a requirement for *dCCN* in synaptic transmission at the larval neuromuscular junction (NMJ), and female fertility. Our results demonstrate *dCCN* is expressed in a diverse set of neurons that respond to a variety of external and internal signals, direct synaptic transmission at the neuromuscular junction, and are critical for the function of reproductive and behavioral circuits.

Abbreviations

Name:	Abbreviation:
Extracellular matrix	ECM
Extracellular space	ECS
Matricellular protein	MCP
CCN	Cellular Communication Network Factors
CCN family of matricellular proteins	CCN family of MCPs
Drosophila melanogaster CCN	*dCCN*
CYR61/CTGF/NOV *original gene names*	CCN (former/current CCN nomenclature)
CYR61	Cysteine rich 61
CTGF	Connective tissue growth factor
NOV	Nephroblastoma overexpressed
WISP1-3 *older names*	CCN4-6 *current names*
Traumatic brain injury	TBI
Octopamine	OA
Dopamine	DA
Serotonin	5-HT
Central nervous system	CNS
Peripheral nervous system	PNS
Ventral nerve cord	VNC
fruitless	*fru*
double-sex	*dsx*
Neuromuscular junction	NMJ
Signal Peptide	SP
Insulin-like growth factor binding protein	IGFBP
von Willebrand factor type C repeat	VWC
Thrombospondin type 1 repeat	TSP
Cysteine knot	CK
Lipoprotein receptor-related protein 1	LRP-1
Wnt inducible signaling protein	WISP
Heparan sulfate proteoglycans	HSPG
Bone morphogenetic protein 4	BMP4
Transforming growth factor β	TGFβ
Insulin-like growth factor	IGF
Subesophageal zone	SEZ
Accessory mesothoracic neuropil	AMNp
Abdominal neuropil	ANp

Table of figures

Chapter 1: Introduction

The monoamine neurotransmitters and extra-synaptic release

Monoamine neurotransmitters, also known as the biogenic amines, are a class of key neuromodulators important for numerous biological processes in a wide range of animals including humans. The biogenic amines each contain an amino group attached to an aromatic ring, making these biological compounds highly stable and susceptible to many enzymatic interactions (Dougherty, 2007; Grouleff et al., 2015). The monoamine neurotransmitters include dopamine (DA), serotonin (5-HT), norepinephrine (NE), and octopamine (OA), the invertebrate homologue to NE. Monoamine neurotransmitters, monoamine receptors, and aminergic-modulated neuronal circuits are highly conserved between vertebrates and invertebrates, and carry out a diverse set of physiological functions (Kravitz and Huber, 2003; Spielman et al., 2015; Swallow et al., 2016; Kamhi, 2017).

Within the conserved anatomical structure and physiological function of monoamine-expressing neurons, there is diversity in the behaviors and organs modulated by monoamines. For example, monoamine neurotransmitters modulate complex mood states and govern behaviors including sleep, appetite, attention, arousal, locomotion, stress response, sexual drive and reproduction, learning and memory, addiction formation, and eusocial behaviors (Dishman 1997; Libersat and Pflueger 2004; Kamhi and Traniello 2013; Bubak et al., 2014; De Boer et al., 2015; Swallow et al., 2016). Second, dysregulation of monoamine signaling is a significant component of psychiatric and neurodegenerative disorders such as sleep dysfunction (Watson, 2010), major depression (Nutt, 2008; Hamon and Blier, 2013; Yukiori et al., 2016), bi-polar spectrum disorders (Walderhaug et al., 2011), attention deficit hyperactivity disorder (ADHD; Manor et al., 2002; Reddy, 2013), schizophrenia and schizoaffective spectrum psychoses (Issa et al., 1994; Sedvall, 1990; Yukiori et al., 2016; Leppik et al., 2018), Alzheimer's Disease (Liu et al., 2016), and Parkinson's Disease (Bruno et al., 2016). Third, monoamine neurotransmitters are critical in the regulation of heart rate and blood pressure (Watts et al., 2012), smooth muscle function (Gilloteaux, 1979), the gastrointestinal system (Meirieu et al., 1986; Eisenhofer et al., 1997; Mittal et al., 2017), female reproduction (Hansson et al., 2009), and thermoregulation (Cook et al., 2017; Sinakevitch, 2018). In summation, monoamine neurotransmitters are involved in many

physiological, neurological, and behavioral processes in both vertebrates and invertebrates.

In addition to release at the synapse, monoamine neurotransmitters are released extra-synaptically; from non-synaptic sites including the soma, somatic dendrites, and axons (De-Miguel et al., 2005; Fuxe et al., 2015; Grygoruk et al, 2014; Borroto-Escuela et al., 2014; De-Miguel and Nicholls, 2015; Del-Bel and De-Miguel, 2018; Svensson et al., 2018). Extra-synaptic release is a separate method of signaling that occurs by diffusion as monoamines and neuropeptides move from the releasing source to the target receptor in a process termed volume transmission (De-Miguel et al., 2005; Fuxe et al., 2015; Grygoruk et al, 2014; Borroto-Escuela et al., 2014; De-Miguel and Nicholls, 2015; Del-Bel and De-Miguel, 2018; Svensson et al., 2018). Signaling through volume transmission impacts time and anatomical space considerations within the central nervous system (CNS; De-Miguel et al., 2005; Ludwig, 2006; Fuxe et al., 2015; Grygoruk et al., 2014; Borroto-Escuela et al., 2014; De-Miguel and Nicholls, 2015; Del-Bel and De-Miguel, 2018; Svensson et al., 2018). Extra-synaptic, and in particular, somatic exocytosis, is slower than synaptic terminal release and affects the CNS for several hours (Ludwig, 2006; Trueta and De-Miguel, 2012; De-Miguel et al., 2015; De-Miguel and Nicholls, 2015). Therefore, extra-synaptic release can prolong the effect of a signal with a slow-onset and long-lasting timing to the modulation of hardwired circuits (Ludwig, 2006; Trueta and De-Miguel, 2012; De-Miguel et al., 2015; De-Miguel and Nicholls, 2015).

Results from many animal systems indicate that specific neuron populations primarily signal extra-synaptically. Ridet et al. in 1993, and Van Bockstaele et al. in 1993, examined 5-HT neurons in the dorsal horns of rat spinal cords (Ridet et al., 1993) and in the rat nucleus accumbens (Van Bockstaele and Pickel, 1993), and both research groups found over half of the 5-HT neurons they examined do not form any classical synapses. Both Ridet et al. and Van Bockstaele et al.'s findings show evidence that specific 5-HT neurons largely communicate extra-synaptically. Another example of extra-synaptic release is found with oxytocin, a powerful neuropeptide. Although there is little innervation of oxytocin containing projections observed in rodent brains, dendritic extra-synaptic release of oxytocin contributes profound long-lasting impacts on social

bonding behavior (Nicholson and Rice, 1991; Kawagoe et al., 1992; DeVries et al., 2006; Ludwig, 2006; Syková and Nicholson, 2008; Wang et al., 2011; Naskar and Stern, 2014; Dyakonova et al., 2019). In addition, although glutamate mediates point-to-point transmission at the synapse, recent studies indicate that glutamate spillover from the synaptic cleft may accumulate in the extra-synaptic space, and signal through volume transmission to regulate crucial brain functions (Okubo and Iino, 2011; Tabor and Hurley, 2014). Collectively, these findings demonstrate that extra-synaptic signaling is a widespread phenomenon, and importantly for this thesis, is that extra-synaptic signaling can be modified by the dynamic microenvironment that surrounds each neuron. Such dynamic processes include ECM turnover, ionic changes due to neural activity, changes in intercellular adhesion machinery, and changes in MCP function in response to variations in environmental cues (Wong and Rustgi, 2013; Barnes et al., 2017; Nicholson and Hrabětová; 2017).

Once monoamine neurotransmitters are released into the extracellular space, they bind to post-synaptic receptors to elicit a physiological response. In addition, monoamine activated receptors are also expressed on pre-synaptic neurons and called autoreceptors (Timmermans and Thoolen, 1987). Activation of autoreceptors has been shown to be important for conveying feedback regulation of neurotransmitter release (Göthert, 1985; Xie et al., 2008; Langer, 2008; García-Fuster, and García-Sevilla, 2015; Rutigliano et al., 2018). Monoamine receptors are G-protein coupled receptors (GPCRs), with the exception of the serotonin 5-HT$_3$ receptor, which is the sole ionotropic-gated receptor (Martin et al., 2010). In summation, the combination of synaptic and extra-synaptic release provides monoamine-expressing neurons the capability of communicating both at high speeds with spatial precision, as well as at slower speeds with an anatomically broader impact and longer-lasting effects on the CNS. Both communication modes are important for brain function in health, disease states, and behavior.

The extracellular environment and neurotransmission

Monoamine neurotransmitters, neuropeptides, and neuromodulatory transmitters are released from neurons or glia, and travel within the synaptic cleft or diffuse extra-synaptically into the extracellular fluid to reach their receptor molecule targets. The

microenvironment surrounding cells, or the space between individual cells, is known as the extracellular matrix (ECM). The ECM is a non-cellular medium composed of water and filled with many characterized proteins and macromolecules that form a three-dimensional network (Bornstein, 1995; Bornstein and Sage, 2002; Frantz et al., 2010; Schultz et al., 2011; Kular et al., 2014; Murphy-Ullrich and Sage, 2014; Kusindarta and Wihadmadyatami, 2018; Adams, 2018). Matrix components bind each other as well as cell adhesion receptors to form a complex web-like network into which cells reside (Bornstein, 2009; Kular et al., 2014; Kusindarta and Wihadmadyatami, 2018; Adams, 2018). Cell surface receptors transduce signals into cells from the ECM, which regulate diverse cellular functions, such as survival, growth and shape, adhesion and de-adhesion, migration, proliferation, and differentiation (Bornstein, 1995; Bornstein and Sage, 2002; Schultz et al., 2011; Murphy-Ullrich and Sage, 2014; Kusindarta and Wihadmadyatami, 2018; Adams, 2018). Thus, similar to how a flourishing garden requires nutritious and enriched soil to give rise to healthy plants that yield high quality produce, so too, do cells or neurons and glia in their ECM environment.

One principle role of the ECM is to provide a space for ECM proteins and macromolecules to physically support cells. The ECM consists of numerous cell secreted molecules within a dynamically and reciprocally rapidly changing environment (Frantz et al., 2010; Schultz et al., 2011; Kusindarta and Wihadmadyatami, 2018; Adams, 2018). Cells modify the surrounding ECM, and can readily secrete and orient structurally supportive molecules (Alberts et al., 2002; Adams, 2018). The primary job for many cell secreted molecules of the ECM is to provide critical structural support for cells to assist with cellular growth and shape, development, injury repair, and cell stabilization (Bornstein, 1995; Bornstein and Sage, 2002; Frantz et al., 2010; Schultz et al., 2011; Kular et al., 2014; Murphy-Ullrich and Sage, 2014; Kusindarta and Wihadmadyatami, 2018; Adams, 2018). Some examples of cell secreted ECM proteins include collagens, proteoglycans, glycosaminoglycans, elastin, fibronectin, laminins, and several other glycoproteins. These structural ECM proteins attach to the cytoskeleton of cells and give tissues their structural integrity and durability, allowing tissues to be flexible or hard, and withstand pulling, stretching, twisting, and various other mechanical movements (Frantz et al., 2010; Kular et al., 2014; Kusindarta and Wihadmadyatami, 2018; Adams, 2018).

Thus, the ECM is essential for creating the dynamic, complex, three-dimensional meshwork environment into which cells embed into. Additionally, the overall composition of a tissue's ECM is responsible for giving tissues their shape, flexibility, and firmness.

The second fundamental role of the ECM is to provide a medium for intercellular signaling to occur. Intercellular signaling is "the transfer of information from one cell to another, which is accomplished by a cell releasing a substance that is taken up by another cell" (National Cancer Institute, 2020). Matricellular proteins (MCPs) are non-structural cell secreted proteins that are critical in modulating intercellular signaling and ECM:cell communication within any tissue type in both vertebrates and invertebrates (Bornstein, 1995; Bornstein and Sage, 2002; Frantz et al., 2010; Schultz et al., 2011; Kular et al., 2014; Murphy-Ullrich and Sage, 2014; Kusindarta and Wihadmadyatami, 2018; Adams, 2018). Secreted MCPs are sometimes found along the edges of cells, interacting with cell surface receptors and structural ECM proteins (Bornstein, 2009; Schultz et al., 2011; Kular et al., 2014; Malik et al., 2015; Adams, 2018). MCPs can also modulate regulatory and growth factors, hormones, and other bioeffector molecules (Bornstein, 2009; Schultz et al., 2011; Kular et al., 2014; Morris and Kyriakides, 2014; Malik et al., 2015; Adams, 2018). Intercellular communication or cell:ECM signaling is crucial for proper cell migration, anchoring, differentiation, wound healing, apoptosis, growth, proliferation, and many other important cellular processes within a variety of tissues (Bornstein, 2009; Schultz et al., 2011; Kusindarta and Wihadmadyatami, 2018; Adams, 2018). This critical and delicate balance of structural remodeling and stabilization requires cell:ECM interactions to reciprocally signal, which allow for dynamic and rapid appropriate structural changes in the development of many tissues throughout an organism's lifespan.

There are several distinct MCP families which are highly conserved and found across many different animal phyla (Bornstein and Sage, 2002; Bornstein, 2009; Adams, 2018). One family of MCPs are the thrombospondins, which have been shown to be important for cell processes involved with angiogenesis, cancer progression, inflammation regulation, immune system regulation, formation of myotendinous junctions, maintenance of the myocardium integrity and function, and synaptogenesis (Bornstein and Sage, 2002; Bornstein, 2009; Stenina-Adognravi, 2014; Adams, 2018).

Another class of MCPs is the SPARC family, which has eight members and has been shown to be vital for ECM assembly, counter-adhesion, ECM protease regulation, and regulation of growth factor and cytokine activation pathways (Bornstein and Sage, 2002; Bornstein, 2009; Bradshaw, 2012; Adams, 2018). Finally, I will discuss below the CCN family of MCPs which are critical for cellular development, differentiation, and cell:ECM communication (Bornstein and Sage, 2002; Rachfal, 2005; Katsube et al., 2009; Chen and Lau, 2009; Bornstein, 2009; Perbal, 2013; Adams, 2018; Perbal, 2018).

The CCN family of matricellular proteins

The CCN family of MCPs is currently known as the family of *Cellular Communication Network* Factors (previous nomenclature: **C**YR61/**C**TGF/**N**OV; the term was coined by Bork P. in 1993 and was named after the first three discovered proteins to create the original *CCN* acronym; Bork, 1993; Brigstock et al., 2003; Perbal, 2018). There are six CCN family members in vertebrates (*H. sapiens, M. musculus, X. tropicalis, and D. rerio*) and a sole CCN family member in invertebrates (*B. floridae, D. melanogaster, E. multilocularis*; Hu et al, 2019). CCN proteins are secreted as well as found in the nucleus of cells (Holbourn et al., 2008; Jun and Lau, 2011; Malik et al., 2015; Krupska et al., 2015; Perbal, 2018). CCN family members are unique as they contain a signal peptide and four well conserved domains that can be found in ECM or signaling protein families (Planque and Perbal, 2003; Rachfal, 2005; Leask and Abraham, 2006; Holbourn et al., 2008; Perbal, 2013; Malik et al., 2015; Krupska et al., 2015; Xia et al., 2016; Takigawa, 2017; Perbal, 2018; Hu et al., 2019). Following the export signal peptide (SP), the four highly conserved domains of CCN proteins include the insulin-like growth factor binding protein (IGFBP), a von Willebrand factor type C repeat (VWC), thrombospondin type-1 repeat (TSP-1), and a cysteine knot-containing domain (CK) (see figure 1A; adapted from figure 1 of Malik et al., 2015; Hu et al., 2019). CCN5 is the only exception, in that this particular CCN family member is missing the CK domain (Planque and Perbal, 2003; Holbourn et al., 2008; Malik et al., 2015; Krupska et al., 2015). Examples of CCN domain interacting partners include integrins, Notch 1, Fibulin C1, Collagen V, Fibronectin, Wnts, Bone morphogenetic protein 4 (BMP4), Transforming

growth factor β (TGFβ), Lipoprotein receptor related protein 1 (LRP1), Insulin-like growth factor (IGF), and heparin sulfate proteoglycans (HPSG) (see Figure 1C; adapted from Malik et al., 2015). These canonical interacting partners and receptors of CCN proteins allow for the regulation of many cellular processes important for the growth, development, maintenance, and ECM:cell communication (Leask and Abraham, 2006; Katsube et al., 2009; Chen and Lau, 2009; Jun and Lau, 2011; Malik et al., 2015; Krupska et al., 2015; Takigawa, 2017; Perbal, 2018). One example of a CK domain-mediated interaction is signaling between CCN3 and Notch 1, which is required for neuronal differentiation in the chick retina (Laurent et al., 2012; Malik et al., 2015). In summation, the CCN family of MCPs have the unique ability to interact with numerous receptors and ligand partners due to their four highly conserved domains.

Figure 1:
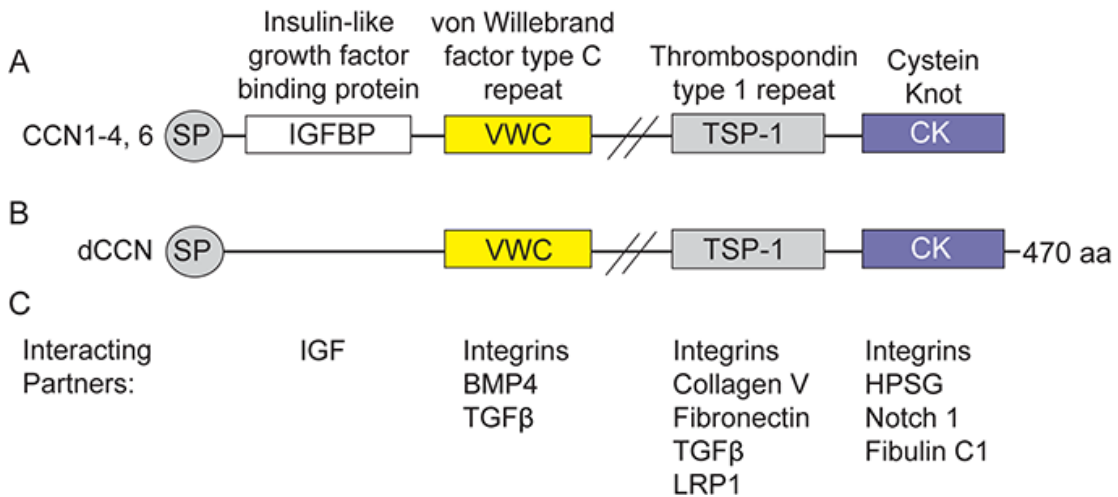
Figure 1: **The functional domains of the CCN family of matricellular proteins**. (**A**) Functional domains of a vertebrate CCN protein. (**B**) Functional domains of a *dCCN* protein. (**C**) Select examples of interacting partners aligned with their associated interactive domain. Adapted from Malik et al., 2015.

The CCN family of MCPs is often thought of as "traffic coordinators" – recruiting various molecular workers to the area at specific times, and modulating intercellular signaling to regulate cell function, gene expression, development, angiogenesis, apoptosis, differentiation, ECM structural remodeling, cell stabilization and anchoring, injury repair, overall cell homeostasis, and ECM:cell communication (Leask and

Abraham, 2006; Katsube et al., 2009; Chen and Lau, 2009; Jun and Lau, 2011; Malik et al., 2015; Krupska et al., 2015; Takigawa, 2017; Perbal, 2018).

CCN family members can initiate many diverse cellular responses when interacting with the same receptor. For example, CCN1 can interact with the αvβ3 integrin of fibroblasts to initiate DNA synthesis or proliferation, but activating the same receptor in microvascular endothelial cells via CCN1 will inspire chemotaxis to occur (Jun and Lau, 2011). The CCN family of MCPs can also coordinate opposing actions as well. For example, CCN1 promotes chemotaxis in smooth muscle cells whereas CCN3 prohibits migration in the same cells (Jun and Lau, 2011). Lastly, CCN proteins can synergistically change cellular responses when paired with other bioeffector molecules. For example, α6β1 activation via CCN1 alone influences cell adhesion in fibroblasts, but when CCN1 is paired with TNF-α and activates the same receptor, apoptosis in fibroblasts occurs (Jun and Lau, 2011). These pleiotropic behaviors are dependent on the cell type, the cell's receptor composition, the presence of additional bioeffector molecules, and the cell's current status in development (Jun and Lau, 2011; Malik et al., 2015). In summation, the CCN family of MCPs has the extraordinary ability to function in a pleiotropic manner, and can govern numerous different cellular responses among many different tissues.

Numerous studies demonstrate that alterations in CCN function, or disruptions in cell:CCN family of MCPs communication results in a wide range of disorders. Examples include developmental disorders such as cardiac diseases and heart vasculature developmental defects (Frangogiannis, 2012; Xia et al., 2016; Klenotic et al., 2016; Díez et al., 2016), bone development disorders (Kubota and Takigawa, 2011, Takigawa, 2013; Chen et al., 2014; Kubota and Takigawa, 2015), fibrotic diseases (Kubota and Takigawa, 2015; Díez et al., 2016; Chen et al., 2017), kidney disease and glomerulosclerosis (Sawai et al., 2007), and dysregulation of inflammation throughout development (Leask and Abraham, 2006; Jun et al., 2011; Kular et al., 2011; Chen et al., 2014). In addition, CCN dysfunction has been linked to numerous types of cancer including glioblastoma where CNN1 levels are used as a prognostic factor (Dhar and Ray, 2010; Li et al., 2015; Ishida et al., 2015; Kim et al., 2018).

Within the CNS, CCN dysregulation has been reported in psychiatric disorders such as schizophrenia (Ito et al., 2007), depression, bi-polar spectrums, and post-partum

psychosis (Malik et al., 2015; Dazzan et al., 2018; Davies, 2019). A role of CCN proteins in neurodegenerative diseases such as dementia, Alzheimer's Disease, or Parkinson's Disease has been reported. An increase in CCN2 expression levels leads to the promotion of chronic inflammation and the formation of neuritic plaques and neurofibrillary tangles; all of which are associated with neurodegenerative diseases (Ueberham et al., 2003; Zhao et al., 2005; Jun and Lau, 2011; Malik et al., 2015; Jayakumar et al., 2017). Changes in CCN transcript levels occur in response to traumatic brain injuries (TBIs) as well. Increased levels of CCN2 transcripts and protein was induced in rodent neurons and glia after TBI lesions were made (Schwab et al., 2000; Hertel et al., 2000; Schwab et al., 2001; Jones and Bouvier, 2014; Malik et al., 2015; Abu Hamdeh et al., 2018). Lastly, CCN proteins have also been associated with CNS viral infections such as the Zika virus, in which CCN1 and astrocytes have reportedly played a role as an infection mechanism through manipulations by the Zika virus (Sun et al., 2019). In summation, the CCN family of MCPs has implications in many developmental disorders, mood states, diseases, cancers, and many other pathologies.

As CCN family members are critical for development, ECM modeling, and intercellular communication, it comes as no surprise that CCN proteins are highly expressed within the developing and mature CNS. The Allen Mouse Brain Atlas and Allen Human Brain Atlas has characterized CCN expression patterns in the rodent and human CNS. High expression levels of CCN1-6 members are found in the hippocampus, cortical regions, caudate nucleus, cerebellum, and spinal cord (Lein et al., 2007; Hawrylycz, 2012; Malik et al., 2015; Jayakumar et al., 2017; Kusindarta and Wihadmadyatami, 2018). Although the functional role for CCN proteins within the CNS has been largely understudied, new results indicate a complex role in neuron development and differentiation. For example, Malik et al. demonstrated that CCN1 is required for dendritic branching in rat hippocampal neurons *in vitro*, and acts downstream of the Ras, ERK, and PI3K signaling pathways (Malik et al., 2013). In other examples, Khodosevich et al. in 2013, demonstrated that CCN2 regulated and promoted apoptosis in rodent olfactory bulb newborn neurons in an activity-dependent manner (Khodosevich et al., 2013; Malik et al., 2015), and CCN3 suppresses myogenesis through Notch 1 signaling (Sakamoto et al., 2002). In addition, CCN3 plays a role in

neuroinflammation by upregulating CCL2 and CXCL1 expression in astrocytes through β1 and β5 integrins; acting through the Rho/ROCK/JNK/NF-kappaB and Rho/qROCK/p38/NF-kappaB signaling pathways (Le Dréau et al., 2010). These few examples demonstrate a portion of the ways that the CCN family of MCPs contribute to CNS function. However, it is largely unknown how CCN family members contribute to neuronal circuit formation or function.

dCCN

The model organism, *Drosophila melanogaster*, is an excellent animal model to examine CCN function in the CNS for several reasons. The first reason being that only a single CCN family member is encoded by the *Drosophila* genome, thus eliminating concerns about redundancy or overlapping functional roles. Other advantages include a well-established genetic toolbox, an easy to use genetically amenable system, and *Drosophila* have a simplified CNS with approximately ~100,000 neurons. The sole *Drosophila* CCN member, *dCCN*, has a signal peptide and three of the four domains present, including the VWC, TSP-1, and CK domains (see figure 1B). The focus of this thesis project was to determine and characterize *dCCN* expression throughout development and into the adult stage, as well as identify neuron populations that co-express *dCCN*. In addition, I determined *dCCN* is required for female fertility and through collaboration, *dCCN* is a requirement in synaptic transmission.

Significance

The narrow microenvironment that surrounds every cell of the CNS provides a reservoir for the dynamic intercellular structure and signaling communication that is required for neuron development and function. Many signaling molecules including classical neurotransmitters, neuropeptides, and monoamine neuromodulators are released by neurons or glia and disperse by volume transmission to reach their receptor targets. Our long-term goal is to understand how CCN proteins impact monoamine signaling via volume transmission in wildtype and disease conditions. The experiments in this thesis provide the frame to address this question by: (1) characterizing the expression pattern of the single *Drosophila* family member, (2) determining a subset of monoaminergic neurons express *dCCN*, (3) demonstrate *dCCN* is required for female fertility and thus

exhibits a sex-specific function, and (4) by collaboration I report that *dCCN* is required for synaptic transmission at the neuromuscular junction (NMJ). My findings support and advance the previously published work in vertebrates while providing a strong genetically manipulatable platform that will allow future studies addressing neuron-specific requirements for *dCCN* during development as well as in the mature nervous system. Together, results from this project are expected to significantly enhance the potential to address MCP function in distinct cellular contexts that could lead to novel ways of manipulating neurotransmitters of volume transmission, the efficacy of drug delivery, and the remodeling of neuronal networks.

Chapter 2: Identification and Characterization of *dCCN*

dCCN expression begins during embryogenesis

The CCN family has a common primary structure consisting of a secretory signal peptide at the N-terminus followed by four conserved functional domains: insulin-like growth factor binding protein domain (IGFBP), von Willebrand factor type-C domain (VWC), thrombospondin type-1 repeat domain (TSP-1), and a cysteine-knot-containing (CK) domain (Fig. 2A) (Perbal 2004; Yeger and Perbal 2007; Holbourn et al., 2008). A recent comparative analysis of the CCN gene family (Hu et al., 2019) as well as our own homology searches indicates the *Drosophila* genome encodes a single CCN family member, *dCCN* (*Drosophila CCN*). While lacking the IGFBP domain, *dCCN* contains the VWC, TSP-1, and CK domains as well as a signal peptide within the transmembrane domain, and up to 7 glycosylation sites (Fig. 2A-B, SFig. 1) (Hu et al., 2019).

Specific CCN family members in zebrafish, xenopus, and mice are required for embryonic viability (e.g., mammalian CCN1, 2 and 5) (Latinkic et al., 2003; Jun and Lau 2011; Krupska et al., 2015), while other members are not essential for development (e.g., mammalian CCN3, 4 and 6) (Jun and Lau 2011; Ono et al., 2018), possibly due to functional redundancy and/or specialization during evolution (Holbourn et al., 2008; Krupska et al., 2015). *dCCN* transcripts were detected at embryonic stage 13 and predominantly confined to the developing ventral nerve cord (VNC) (Fig. 2C). Within the segmentally-repeated VNC neuromeres at stage 15, *dCCN* transcripts accumulate in differentiating neurons including cells at the midline (arrow, Fig. 2D). To facilitate the identification of *dCCN*-expressing cells, we generated a *dCCN-Gal4* line through MiMIC insertion-conversion at the endogenous *dCCN* chromosomal locus. MiMIC-converted Gal4 drivers are under control of the complete regulatory region of each gene and thus reliably reflect endogenous gene expression (Diao et al., 2015). Expression of a UAS-driven membrane GFP reporter, *UAS-CD8:GFP*, by *dCCN-Gal4* (hereafter *dCCN*>GFP) confirmed predominant expression in the VNC (stage 17, Fig. 2E). Based on qRT-PCR quantification, our *dCCN-Gal4* line is also a severe hypomorphic allele (hereafter *dCCN^{Gal4}*) (SFig. 2). *dCCN^{Gal4}/ dCCN^{Gal4}* embryos develop to larval stages, indicating that *dCCN* is not required for embryonic viability. However, the number of homozygous

Figure 2:

A

CCN1-4, 6 (SP) — IGFBP — VWC //— TSP-1 — CK

dCCN (SP) — VWC //— TSP-1 — CK —470 aa

B

```
Mou CCN1  CEYNSRIYQNGESFQPNCKHQCTCIDGAVGCIPLCPQELSLP----NLGCPNPRLVKVSGQCCEEWVCD   67
    VWC   C   +   + +G +F+ +CK QC C +G   C  LCP E  LP      + C +PRLV+V G CC+ W+C+
    dCCN  CSVGNTTFAHGVTFKLDCKTQCVCENGRHACSTLCPNE-QLPAPEDTISCRSPRLVEVPGHCCKMWLCE   70


Mou CCN1  CIVQTTS--WSQCSKSCGTGISTRVTNDNPECRLVKETRICEVRPC   45
   TSP-1  C   TTS  W+ CS+SCG G +TR T + C  +   R+CE R C
    dCCN  CHNSTTSGNWTACSRSCGLGTATRHTTTHAGCHQLSNLRLCENRRC   46


Mou CCN1  PVRFTYAGCSSVKKYRPKYCGSCVDG-RCCTPLQTRTVKMRFRC   52
     CK    P R    C S K YRPK CG C  G +CC P  + T+++    C
    dCCN  PARIRLGECVSRKLYRPKLCGRCHRGVKCCAPAVSTTIQVELLC   52
```

C Stage 13 **D** Stage 15 **E** Stage 17 dCCN^GFP

Figure 2: Vertebrate CCNs and *Drosophila* CCN share domain homology. (**A**) *dCCN* contains the signal peptide (SP) and three of the four conserved modules, von Willebrand factor type C (VWC), thrombospondin type 1 (TSP1) repeat, and a C-terminal cysteine knot (CK). *dCCN* is lacking an insulin-like growth factor binding protein (IGFBP) domain. (**B**) Sequence alignment of mouse CCN1 and *dCCN*. (**C**) *dCCN* transcripts accumulates in the developing CNS (arrow) beginning at stage 14. (**D**) Midline cells accumulate *dCCN* transcripts in a stage 15 dissected CNS (arrow). (**E**) CNS expression (arrow) in a *UAS-CD8:GFP; dCCN^Gal4* stage 17 embryo. Scale bar represents 50 μm.

Supplemental figure 1:


```
        10         20         30         40         50
MLILLPLLGI FGNGFVAEVE ANLSLGFKAI KLPRHPNPAN CSVGNTTFAH
        60         70         80         90        100
GVTFKLDCKT QCVCENGRHA CSTLCPNEQL PAPEDTISCR SPRLVEVPGH
       110        120        130        140        150
CCKMWLCENP TADVYATCHN STTSGNWTAC SRSCGLGTAT RHTTTHAGCH
       160        170        180        190        200
QLSNLRLCEN RRCDKDDHED NKWSRSRPLT HKRKQHRAHS HSHQRYHHHK
       210        220        230        240        250
EHEEPAHRIR KGHECRSIQR LGPARIRLGE CVSRKLYRPK LCGRCHRGVK
       260        270        280        290        300
CCAPAVSTTI QVELLCPLNA VDPINYVQRR QANKKRQMKE PQDDEDDDDD
       310        320        330        340        350
DDGDDNVEPE PVLQSAQLWD TVALEPIDQE FLQSHQIQIE NKFIAVEWIL
       360        370        380        390        400
KCECSTKNCN AGSSNISSNS NSNDNMANTN KYGYYNYKNN NRGRNHETNG
       410        420        430        440        450
EPNEPTNNNA GNNKDNEEDV VDSGNNLDHN DVDNMSSEQQ PDIIPYPPSV
       460        470
GESSWKAEKL RQQHHWQQNT
```

Signal Peptide TSP-1 domain
VWC domain CK domain

Figure S1: *dCCN* sequence and domains. The *dCCN* sequence contains a signal peptide (SP), a von Willebrand Factor type C repeat domain (VWC), a thrombospondin type-1 repeat domain (TSP-1), and a cysteine knot-containing domain (CK).

Supplemental figure 2:
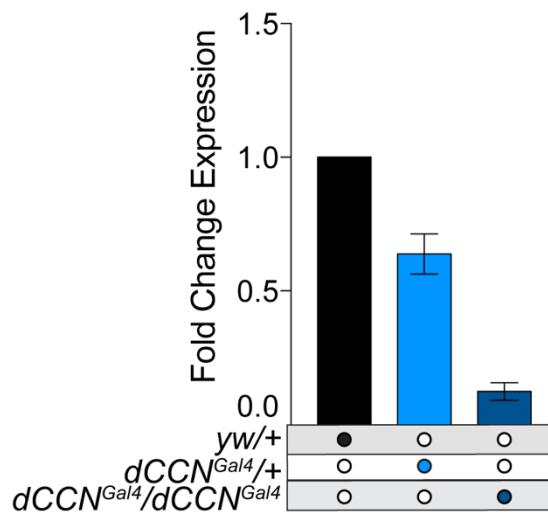
Figure S2: *dCCN* **transcript expression.** Quantification of *dCCN* transcripts. A significant reduction of *dCCN* transcripts is observed in homozygous *dCCN*^Gal4 flies (dark blue column) when compared with heterozygous *dCCN*^Gal4 (light blue column) flies and *yw* controls (black column). Error bars denote S.E.M.

progeny is less than expected, suggesting that *Drosophila* development is compromised with reduced *dCCN* function.

dCCN is required for synaptic transmission at the larval neuromuscular junction

Within the central nervous system (CNS), CCN family members are expressed in neurons and glia (Malik et al., 2015; Jayakumar et al., 2017). For example, CCN1 has been found in rat hippocampal and cortical neurons, whereas CCN2 and CCN3 are expressed in subtypes of glia as well as neurons (Kondo et al., 1999; Schwab et al., 2000, 2001). To determine the neuronal vs. glial identity of *dCCN*-expressing cells, we double-labeled dissected larval CNSs from *dCCN^Gal4^>UAS-dsRed* progeny with the neuronal marker, Elav, and separately the Repo glial marker (SFig. 3) (Koushika et al., 1996; Kaplow et al., 2008). Widespread but distinct *dCCN* expression was found in the central brain minus the optic lobe regions, and also present in the VNC (Fig. 3B). Extensive co-localization between *dCCN>dsRed* and Elav indicate the majority of *dCCN+* cells are either inter- or motor neurons (SFig. 3 A-B''). Co-localization was not observed between *dCCN>dsRed* and the Repo glial marker (SFig 3C-D''). Additional methods of identifying possible glial co-expression includes the use of the *repo-flp* line in combination with *dCCN^Gal4^,* and two separate split-Gal4 combinations with different *dCCN* split gal4 lines and the glia-expressing excitatory amino acid transporter (EAAT1)-Gal4 lines did not identify *dCCN*-expressing glia (see Materials and Methods). Thus, using *in situ* hybridization and *dCCN^Gal4^*, we determined that *dCCN* is expressed during development, comparable to vertebrate CCN gene expression levels during development. However, in contrast to the vertebrate CCNs, the expression of *dCCN* appears limited to the CNS and neurons.

As in the embryo, the *Drosophila* larval VNC is composed of segmentally repeated neuromeres with motor neurons extending outside of the VNC to innervate body wall muscles (Fig. 3A) (Keshishian et al., 1996; Landgraf et al., 1997, 2003; Landgraf and Thor 2006). Using *dCCN>GFP*, we determined *dCCN*-expressing neurons include motor neurons that innervate muscles 6 and 7 among others at the larval neuromuscular junction (NMJ) (Figure 3C). During larval stages, *dCCN^Gal4^* mutants have a morphologically

Supplemental figure 3:
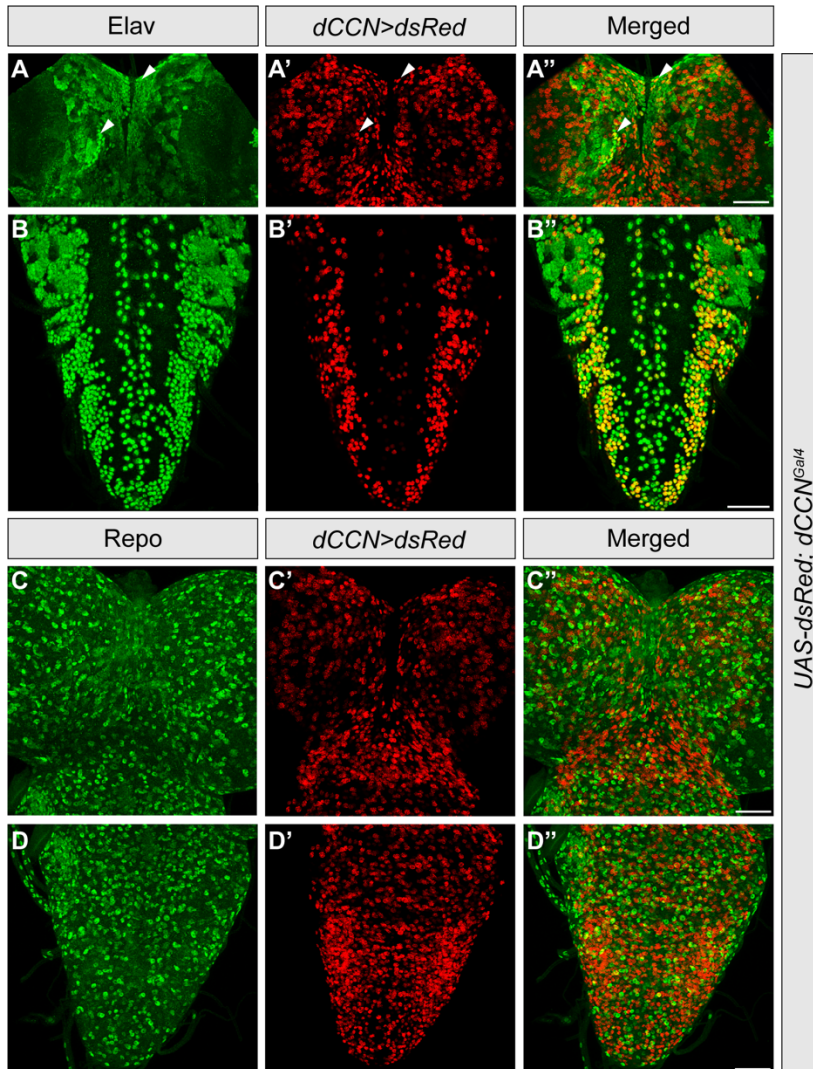
Figure S3: *dCCN^Gal4* expression is found within neurons and not glia. (**A-A''**) Larval brain lobes stained with Anti-Elav of a *UAS-dsRed; dCCN^Gal4* CNS reveals co-expression of *dCCN* and Elav (see arrowheads). (**B-B''**) Consistent co-expression of Elav and *dCCN* of the larval VNC are either inter- or motor neurons. (**C-D''**) No co-expression was found among Repo and *dCCN* in the brain lobes and VNC of a *UAS-dsRed; dCCN^Gal4* larval CNS. Scale bars represent 50 μm.
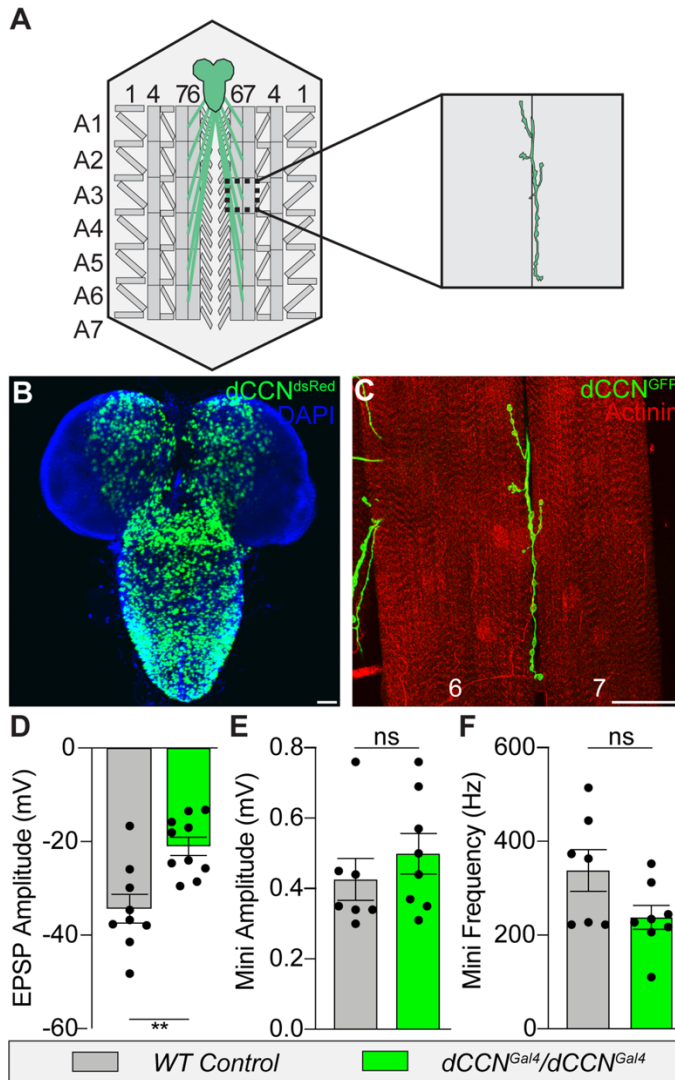
Figure 3:

Figure 3: *dCCN* is required for neurotransmission at the larval neuromuscular junction. (**A**) A schematic displaying a filet of a larvae exposing the central nervous system (CNS). Motor neuron projections from the CNS innervate the body wall muscles. The inset shows a zoomed in schematic representation of a motor neuron innervating the body wall muscles at a neuromuscular junction (NMJ). (**B**) Pseudo colored green nuclei is seen in the larval CNS of *dCCN^{Gal4}>UAS-dsRed*. Blue represents DAPI staining. Scale bar represent 50 μm. (**C**) An image displaying a *dCCN* expressing motor neuron innervating the body wall muscles 6 and 7 at an NMJ of an *dCCN^{Gal4}>UAS-CD8:GFP* larvae enhanced with anti-GFP. Red represents anti-actinin staining (invertebrate muscle marker). Scale bar represents 50 μm. (**D-F**) Electrophysiology kinetics detailing a significant decrease in the neurotransmission of homozygous *dCCN^{Gal4}* mutants when compared with wild type (WT) controls. (**D**) A measurement of excitatory post-synaptic potential amplitude shows a significant decrease in neurotransmission at the NMJ of homozygous *dCCN^{Gal4}* mutants when compared with WT controls. (**E**) A measurement of mini-amplitude reveals no significant difference between homozygous *dCCN^{Gal4}* mutants and WT controls. (**F**) A measurement of mini-frequency reveals no significant difference between homozygous *dCCN^{Gal4}* mutants and WT controls. Error bars denote S.E.M. Statistical tests conducted were two-tailed Mann-Whitney tests (*$p<0.05$, **$p<0.01$, ***$p<0.001$, ****$p<0.0001$).

normal NMJ without readily apparent structural defects in boutons or bouton numbers (SFig. 4A-B). However, the few adults that eclose exhibit locomotor defects. While it is well-established that ECM molecules derived from both neurons and glial regulate different aspects of synaptic differentiation and synaptic function (Rohrbough et al., 2007; Eroglu 2009; Jayakumar et al., 2017), a role for CCN family members in synaptic function has been limited to acting as immediate early genes in response to events that alter synaptic activity. For instance, CCN protein expression is altered in response to neuroinflammation by the cytokines Tβh/TNFα and to facilitate synaptic plasticity via the activity of muscarinic acetylcholine receptors (Albrecht et al., 2000; Kular et al., 2011), and increased expression of CCN1 via β1-integrin induces dendritic growth (Malik et al., 2013). To ask if *dCCN* itself is required for synaptic transmission, we used two-electrode voltage clamp recordings to examine NMJ neurotransmission. We find from our recordings of evoked excitatory junction currents (EJCs) and spontaneous miniature events (mEJCs) that EJC amplitudes of *dCCN* mutants are reduced by 38.8% versus controls (P<0.001) (Fig. 3D-F). A reduction in miniature event frequency of 33.4% compared to controls (P<0.001, data not shown) was seen without a change in miniature event amplitude. Given these results, quantal content is reduced by 40.3% (P<0.001) in *dCCN* mutants versus controls. Taken together, these results indicate that *dCCN^{Gal4}* mutants have a significant presynaptic evoked neurotransmission defect.

Adult peripheral and central nervous system neurons expression of *dCCN*

To ask if *dCCN* expression is maintained in the adult nervous system and putatively required for neuron function as well as neuron differentiation, we examined *dCCN>GFP* expression in the mature adult *Drosophila* peripheral nervous system (PNS) and CNS (Fig. 4A). While widespread, *dCCN>UAS-stingerGFP* (hereafter *dCCN>UAS-nlsGFP*) is not ubiquitous and is instead found in distinct brain and VNC regions (Fig. 4B-C). For example, although absent in the larva optic lobe, extensive *dCCN>UAS-nlsGFP* expression is visible in the adult optic lobe, as well as the subesophageal zone (SEZ), the superior protocerebrum, and the ventromedial and ventrolateral neuropils (Figure 4B). Additionally, we dissected both heterozygous and homozygous *dCCN^{Gal4}* adult brains, and

Supplemental figure 4:
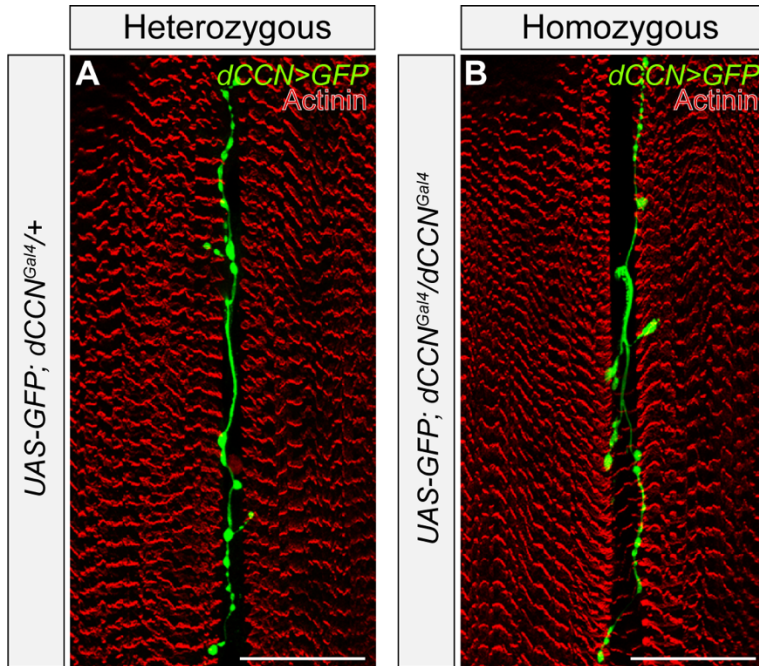
Figure S4: Significant morphological differences were not observed in heterozygous vs homozygous *dCCN^Gal4* **larval neuromuscular junctions.** (**A**) *dCCN>GFP* expressing projections and boutons can be seen making synaptic contact points on muscles 6 and 7 of a heterozygous *20XUAS-6XGFP; dCCN^Gal4* larval neuromuscular junction (NMJ). (**B**) *dCCN>GFP* expressing projections and boutons can be seen making synaptic contact points on muscles 6 and 7 of a homozygous *20XUAS-6XGFP; dCCN^Gal4/dCCN^Gal4* NMJ. No obvious or significant differences between heterozygous vs homozygous *dCCN^Gal4* NMJs are observed. Red represents actinin staining. Scale bars represent 50 µm.
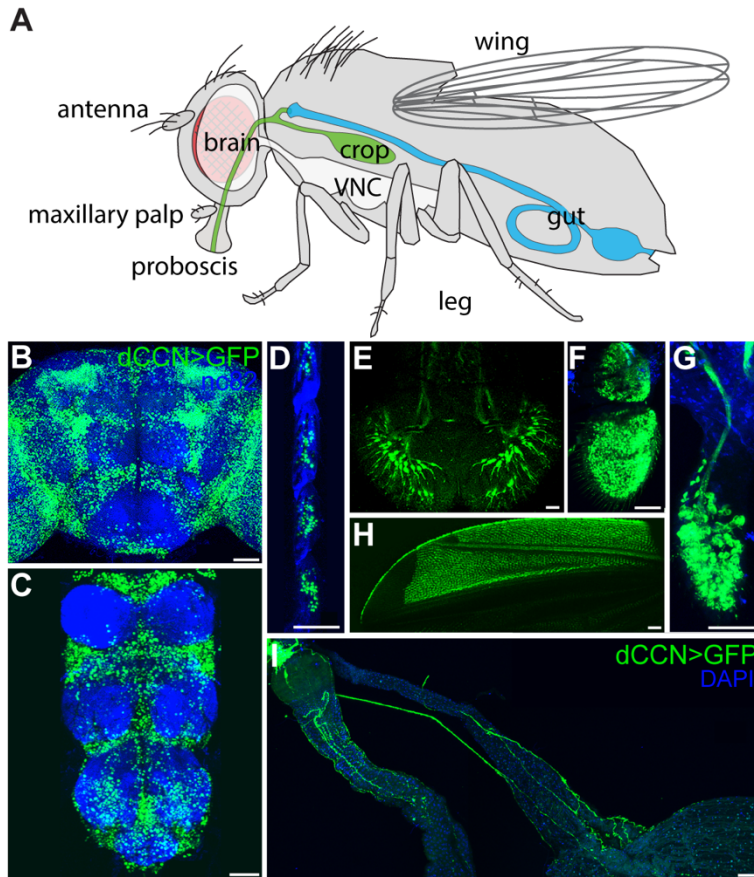
Figure 4:

Figure 4: *dCCN* is expressed in a diverse set of neurons in the adult nervous system. (**A**) Schematic overview of selected *Drosophila* adult organs. (**B-C**) Widespread nuclear GFP expression in the brain and VNC of a *dCCN^{Gal4};UAS-nlsGFP* adult visualized with the neuropil marker BRP (blue) and anti-GFP by immunohistochemistry. (**D**) Nuclear *dCCN* expression in the adult male foreleg. Blue represents DAPI staining. (**E**) *dCCN^{Gal4}* -driven GFP expression in proboscis neurons (*UAS-GFP.S65T;dCCN^{Gal4}*). (**F**) Olfactory sensory neurons in the antennae express *dCCN^{Gal4}* -driven GFP. (**G**) GFP-expression in maxillary palps neurons of *UAS-6X-GFP;dCCN^{Gal4}* adults. (**H**) *dCCN^{Gal4}* -driven GFP expression along the wing margin (*UAS-GFP.S65T;dCCN^{Gal4}*). (**I**) Projections from *dCCN* expressing neurons located in the brain innervate the crop and proventriculus of the intestinal system (*UAS-6X-GFP;dCCN^{Gal4}*). Blue represents DAPI staining. For all panels, scale bars represent 50 μm.

Supplemental figure 5:
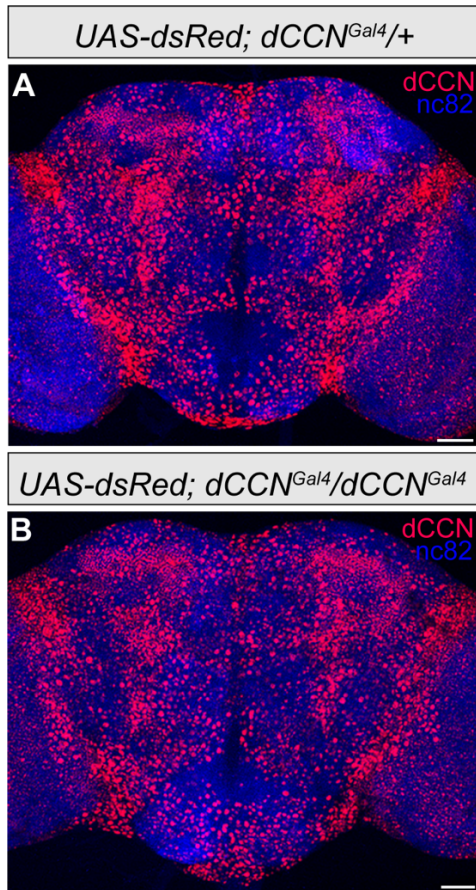
Figure S5: No significant differences in neuron number are observed in heterozygous vs homozygous *dCCN*[Gal4] adult brains. (**A**) Widespread dsRed nuclei can be seen in a heterozygous *UAS-dsRed; dCCN*[Gal4]/+ brain. (**B**) Widespread dsRed nuclei can be seen in a homozygous *UAS-dsRed; dCCN*[Gal4]/ *dCCN*[Gal4] brain. No significant differences are observed between heterozygous vs homozygous *dCCN*[Gal4] adult brains. Blue represents anti-brp (nC82) neuropil staining. Scale bars represent 50 μm.

found no obvious morphological differences in the number of *dCCN* expressing neurons of *dCCN>UAS-dsRed* adults (SFig. 5A-B). The thoracic segments of the VNC house motor neurons that coordinate limb actions and thus control complex behaviors such as walking (Burrows et al., 1988; Laurent and Burrows 1988; Yellman et al., 1997), escape jumping, courtship tapping, aggressive lunges, and grooming (Chen et al., 2018). Within the VNC, *dCCN*-expressing neurons are located in the five major neuropils—prothoracic, mesothoracic, and metathoracic neuropils (which correspond to the three thoracic segments), the accessory mesothoracic neuropil (AMNp), and the abdominal neuropil (ANp) (Figure 4C) (Venkatasubramanian and Mann 2019; Court et al., 2020).

   dCCN expression is also prevalent within neurons located in the periphery that mediate complex sensory processes such as olfaction, chemoreception, and mechanosensation. *dCCN>dsRed* cell body expression is apparent in sensory neurons located within the first to fifth tarsal segment of the foreleg (Fig. 4D). Different classes of leg sensory neurons respond to sugar, water, and contact chemosensory information including male and female pheromones (Inoshita and Tanimura 2006; Fan et al., 2013; Ling et al., 2014). Additional experiments will be required to determine the identities of *dCCN*-expressing leg neurons. Contact chemical perception in adult *Drosophila* is also mediated by sensory neurons in the wings and the proboscis, the insect feeding organ used for both taste cue detection and food ingestion (Raad et al., 2016; Jeong et al., 2016). Using the *UAS-GFP.S65T* reporter, we identified *dCCN*-expressing neurons within the labellum (Fig. 4E) as well as along the row of sensilla on the anterior wing margin (Fig. 4H) that receives pheromonal input and impacts sexually-dimorphic behavior (He et al., 2019).

   In mice, CCN2/CTGF is found in the mitral cell and glomerular layers of the main and accessory olfactory bulb where it controls the survival of newly generated neurons (Khodosevich et al., 2013). To determine if *dCCN* is expressed in the insect olfactory system, we examined the antenna and maxillary palp from *dCCN>20XUAS-6XGFP* adults. *dCCN*-positive neurons are found in the funiculum and pedicel (including in Johnston's organ) of the antenna (Fig. 4F), and projections from *dCCN*-positive neurons in the maxillary palp that terminate in the brain are visible (Fig. 4G). Finally, the crop and proventriculus structures of the gastrointestinal system are innervated by projections from *dCCN*-positive neurons located in the central brain (Fig. 4I). Collectively, these results

demonstrate a significant number of neurons with different anatomical specialties and functions express the invertebrate CCN family member suggesting *dCCN* may be required for neuronal function in a diverse set of contexts.

Subsets of aminergic neurons express *dCCN*

To determine the neurotransmitter identities of *dCCN* neurons in the adult nervous system, we began with neurons that express the neuromodulatory neurotransmitters: dopamine (DA), serotonin (5-HT), and octopamine (OA; the invertebrate equivalent to norepinephrine). While relatively few in number, monoaminergic systems have different patterns of widespread innervation across brain areas (Niens et al., 2017; Kasture et al., 2018; Pauls et al., 2018), heterogeneity in synaptic organization (Dori et al., 1998), as well as distinct neuromodulatory actions (Okaty et al., 2019). The *Drosophila* DA system consists of a relatively small number of neurons clustered throughout the brain and VNC (Mao and Davis 2009; Hartenstein et al., 2017; Kasture et al., 2018) (Fig.5A-A'). Within the anterior adult brain, DA neurons are found in the lateral anterior protocerebrum (PAL) cluster, the medial anterior protocerebrum (PAM) cluster, and a pair of individual neuron called tritocerebrum 1 (TC1) flanking the PENP (Fig. 5A) (Nässel and Elekes 1992). Ventrally, three protocerebral posterior medial clusters (PPM1-3), two posterior protocerebral lateral clusters (PPL1-2) and three neuron pairs located in the lateral (SP1-2) and medial (SVP) parts of the SEZ (SEZ1-3) (Figure 5A') are identifiable (Friggi-Grelin et al., 2003; Niens et al., 2017). Lastly, there are two unpaired neurons in the medial SEZ: one dorsal (VUM1) and one ventral (VUM2) (Nässel and Elekes 1992).

dCCN expression in DA neurons was determined by labeling GFP-expressing *dCCN* neurons (*dCCN>UASnlsGFP*) with an antibody for tyrosine hydroxylase (TH), the rate-limiting step in DA synthesis. In the dorsal region, we found *dCCN* co-expression in the PAL (Figure 5B-D'', G) and the SVP pair (Figure 5B, E, G) while in the ventral region, *dCCN*/TH neurons were identified within the PPM3 (Figure 5C, F-F'', H) and PPL1 (Figure 5C, G-G'', H). Within the adult VNC, *dCCN*/TH co-expression was detected in all thoracic segments except T3 (SFig 6A-C), with the highest number of *dCCN*-expressing neurons being expressed in the abdominal ganglia (SFig 6C, D-D'' and 6C, E-E''). These results demonstrate that *dCCN* is expressed in subsets of DA neurons within the adult CNS.

Figure 5:
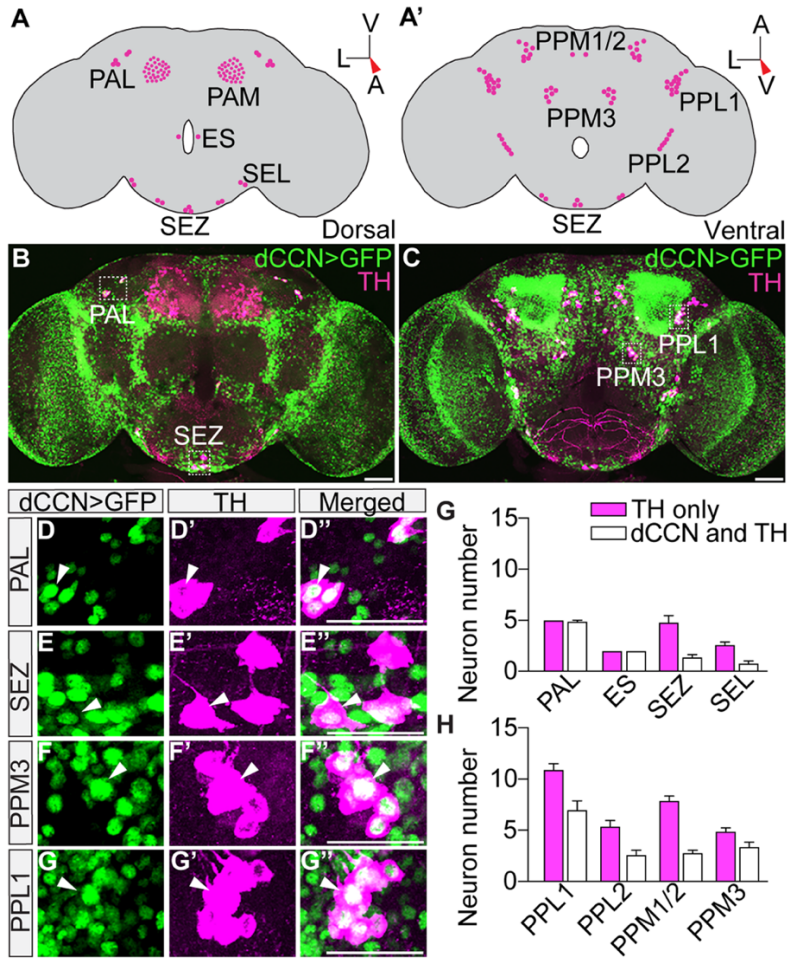
Figure 5: DA neurons express *dCCN*. (A-A') Dorsal (**A**) and ventral (**A'**) schematic views of the major DA neuronal clusters (magenta). (**B**) $dCCN^{Gal4}>nlsGFP$ expressing TH in dorsal sections of the adult brain (anti-TH, magenta). Dotted boxes outline higher magnification images of clusters in D and E. (**B'**) $dCCN^{Gal4}>nlsGFP$ expressing TH in ventral optical sections. Dotted boxes outline higher magnification images of clusters in F and G. (**D-G**) Co-expression of TH and $dCCN^{Gal4}>nlsGFP$ in higher magnification confocal images from dotted boxes in B-B'. Arrowheads point to dCCN/TH co-expressing neurons. Scale bars represent 50 μm. (**D-D''**) Neurons co-expressing TH and $dCCN^{Gal4}>nlsGFP$ in the PAL cluster. Channels are separated in C-C', and merged in C''. (**E-E''**) Co-expression of TH and $dCCN^{Gal4}>nlsGFP$ in SEZ neurons. (**F-F''**) Neurons co-expressing TH and $dCCN^{Gal4}>nlsGFP$ in the PPM3 cluster. (**G**) Neurons co-expressing TH and $dCCN^{Gal4}>nlsGFP$ in the PPL1 cluster. (**H**) Quantification of *dCCN*+ dorsal DA neurons per cluster. (**H**) Quantification of *dCCN*+ ventral DA neurons per cluster. Error bars denote S.E.M. PAL: dorsolateral anterior protocerebral neurons, PAM: dorsalmedial anterior protocerebral neurons, PPL1: dorsolateral posterior protocerebral neurons, PPL2: lateral posterior protocerebral neurons, PPM: dorsomedial posterior protocerebral neurons, SEZ: subesophageal zone. Nomenclature from Friggi-Grelin et al., 2003.

Supplemental figure 6:
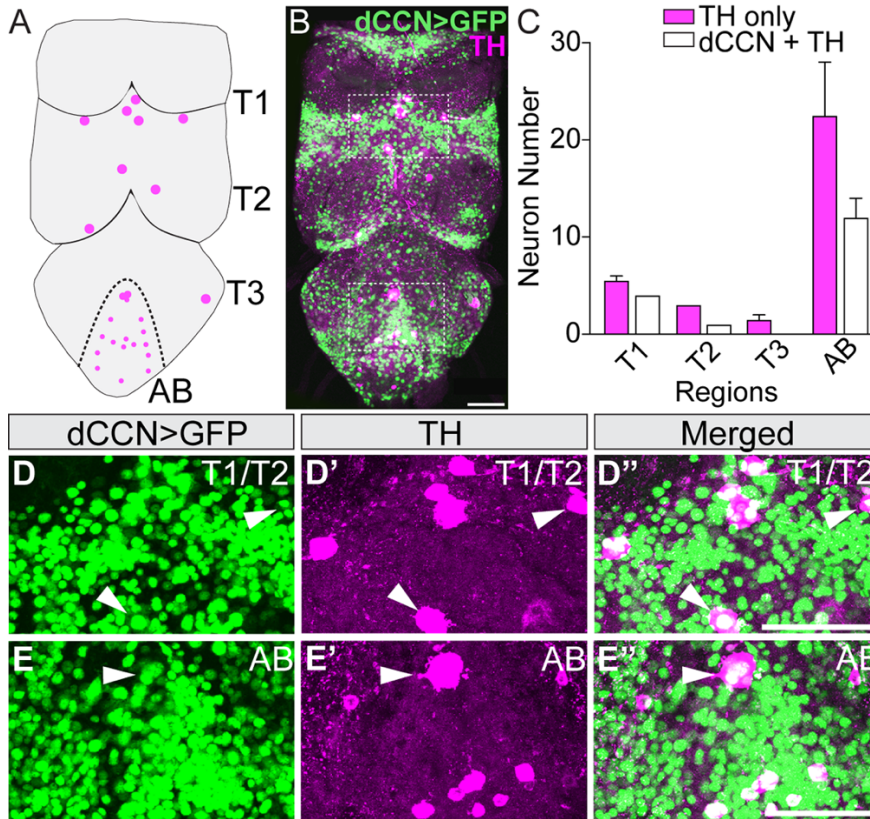
Figure S6: Co-expression of DA and *dCCN* in adult ventral nerve cords. (**A**) A schematic representation of an adult ventral nerve cord (VNC) with magenta dots representing prominent dopamine (DA) neurons. The VNC is divided into regions T1, T2, T3, and AB. (**B**) GFP nuclei of a *dCCN^(Gal4)^>UAS-nlsGFP* VNC is seen. Anti-TH staining appears in magenta. (**C**) Quantification of TH only and TH - *dCCN* co-expressing neurons per region. (**D-D''**) A closer examination at the T2 region of the VNC highlighting TH immunoreactive neurons co-expressing *dCCN*. Arrows point to examples of co-expressing neurons. (**E-E''**) A closer examination at the T3/AB region of the VNC highlighting TH immunoreactive neurons co-expressing *dCCN*. Arrows point to examples of co-expressing neurons. Scale bars represent 50 µm.

The serotonergic system in the adult consists of approximately 12 major clusters, with 7 dorsal clusters and 4 anterior clusters (Giang et al., 2011). The dorsal region contains a neuron pair in the dorsal protocerebrum (DP), a cluster in the anterior protocerebrum (AP), three clusters in the lateral protocerebrum (LP1-3), and 2 clusters in the subesophageal ganglion (SE1-2) (Figure 6A-A') (Giang et al. 2011). There are also 2 single deutocerebral neurons (CSDs) that project contralaterally and innervate the antennal lobes (Figure 6A) (Dacks et al., 2009; Giang et al., 2011). The ventral region contains 2 clusters in the superior protocerebrum (SP1-2), as well as the inferior medial protocerebrum (IP) and the subesophageal ganglion (SE3) (Figure 6A') (Giang et al., 2011). To examine *dCCN* expression in 5-HT neurons, we labeled GFP-expressing *dCCN* neurons (*dCCN>UAS-nlsGFP*) with an antibody for 5-HT. Dorsally, *dCCN*/5-HT co-expression was identified in the DP pair (Figure 6B, C-C'',G) and in the SE2 cluster (Figure 6B, F-F'',H). Ventrally, the LP1 (Figure 6B, D-D'', H) and SP2 (Figure 6B, E-E'', H) clusters contain *dCCN*/5-HT neurons. We also determined *dCCN*/5-HT co-localization occurs in all thoracic segments within the adult VNC (SFig 7A-D'') as well as the abdominal ganglion (SFig 7A-C, E-E'').

Finally, we asked if *dCCN* is expressed in the octopaminergic neuromodulatory system by labeling the CNS of *dCCN>UAS-nlsGFP* progeny with an antibody to Tdc2, the rate-limiting enzyme required for the synthesis of OA. Tdc2-positive neuronal clusters are located in the periesophageal neuropil (PENP), the subesophageal zone (SEZ), and the anterior superior medial protocerebrum (ASMP) in the dorsal part of the brain and in the SEZ and the posterior medial protocerebrum (PSMP) in the ventral part (Figures 7A-A'). *dCCN* co-expression in Tdc2 neurons occurs in each cluster (Figures 7B-B'). We quantified *dCCN*/Tdc2 co-expression in the PENP (Fig. 7B, C-C'', G), SEZ (Fig. 7B-B', D-D'', H), ASMP (Fig. 7B, E-E'', G), and PSMP (Fig. 7B', F-F'', H). In the adult VNC, Tdc2-positive clusters in the thoracic segments innervate skeletal muscle and facilitate motor activity in males and females, while Tdc2-positive neurons in the abdominal ganglia innervate the ovaries and control oviposition in females (Pauls et al., 2018; Masuzzo et al., 2019). Within the VNC, neurons located in the thoracic clusters T1, T2, and T3 co-expressed Tdc2 and *dCCN* (SFig. 8A-D''), as did Tdc2-positive neurons in the abdominal ganglia (SFig. 8A, E-E''). Together these results indicate *dCCN* is expressed in a

Figure 6:
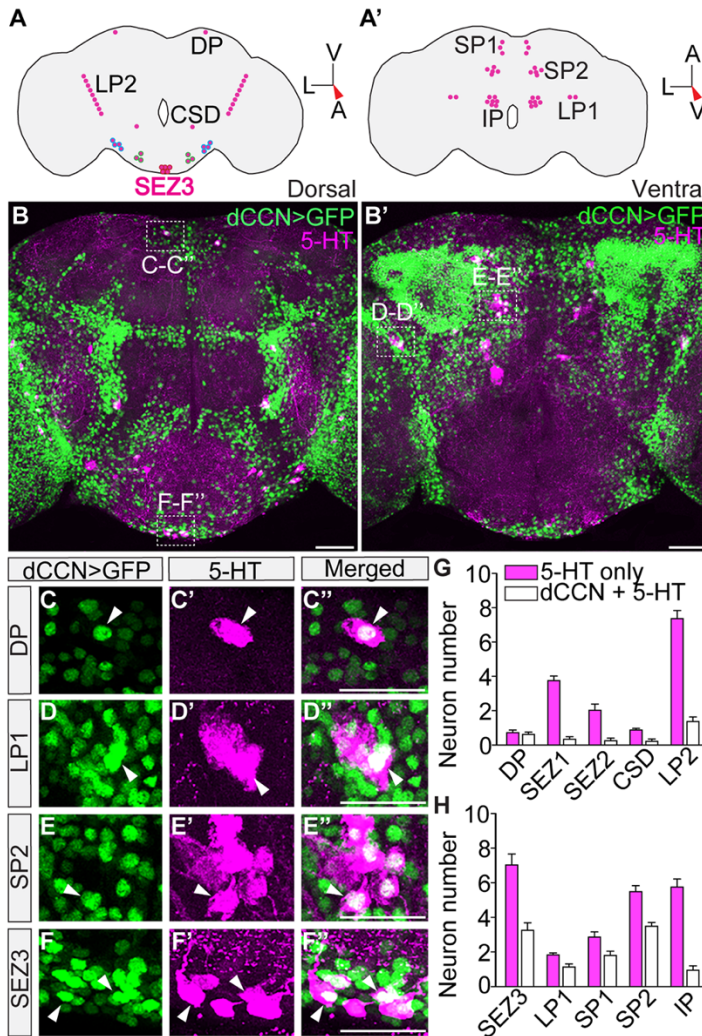
Figure 6: 5-HT neurons express *dCCN*. (**A-A'**) Dorsal (**A**) and ventral (**A'**) schematic views of the major 5-HT neuron clusters. SEZ2= black outlined circles, SEZ3=blue outlined circles. (**B**) Co-expression of 5-HT and *dCCN*^{Gal4} *>nlsGFP* in dorsal optical sections of an adult brain (anti-5-HT, magenta). Dotted boxes outline higher magnification images of clusters in D and G. (**C**) *dCCN*^{Gal4}*>nlsGFP* expressing 5-HT in ventral optical sections. Dotted boxes outline higher magnification images of clusters in E and F. (**C-F''**) Co-expression of 5-HT and *dCCN*^{Gal4}*>nlsGFP* in higher magnification confocal images from dotted boxes in B-C. Arrowheads point to *dCCN*/5-HT co-expressing neurons. Scale bars represent 50 μm. (**D-D''**) Co-expression of 5-HT and *dCCN*^{Gal4}*>nlsGFP* in the DP cluster. (**E-E''**) Co-expression of 5-HT and *dCCN*^{Gal4}*>nlsGFP* in the LP1 cluster. (**F-F''**) Co-expression of 5-HT and *dCCN*^{Gal4}*>nlsGFP* neurons in the SP2 cluster. (**G-G''**) *dCCN*^{Gal4}*>nlsGFP* neuons express 5-HT within the SEZ3 cluster. (**H**) Quantification of dorsal *dCCN*/5-HT neurons per cluster (**I**) Quantification of ventral *dCCN*/5-HT neurons per cluster. Error bars denote S.E.M. DP: dorsal protocerebrum; CSD: contra-laterally projecting deutocerebral neuron; SP1: superior protocerebrum, anterior medial protocerebrum, frontal rind, SP2: superior protocerebrum, anterior medial protocerebrum, posterior to SP1; IP: inferior medial protocerebrum; LP1: lateral protocerebrum; LP2: ventrolateral protocerebrum; SEZ1: subesophageal zone; SEZ2: posterior lateral subsophageal zone; SEZ3: posterior subesophageal zone. Nomenclature from Giang et al., 2011.

**Supplemental figure 7:**
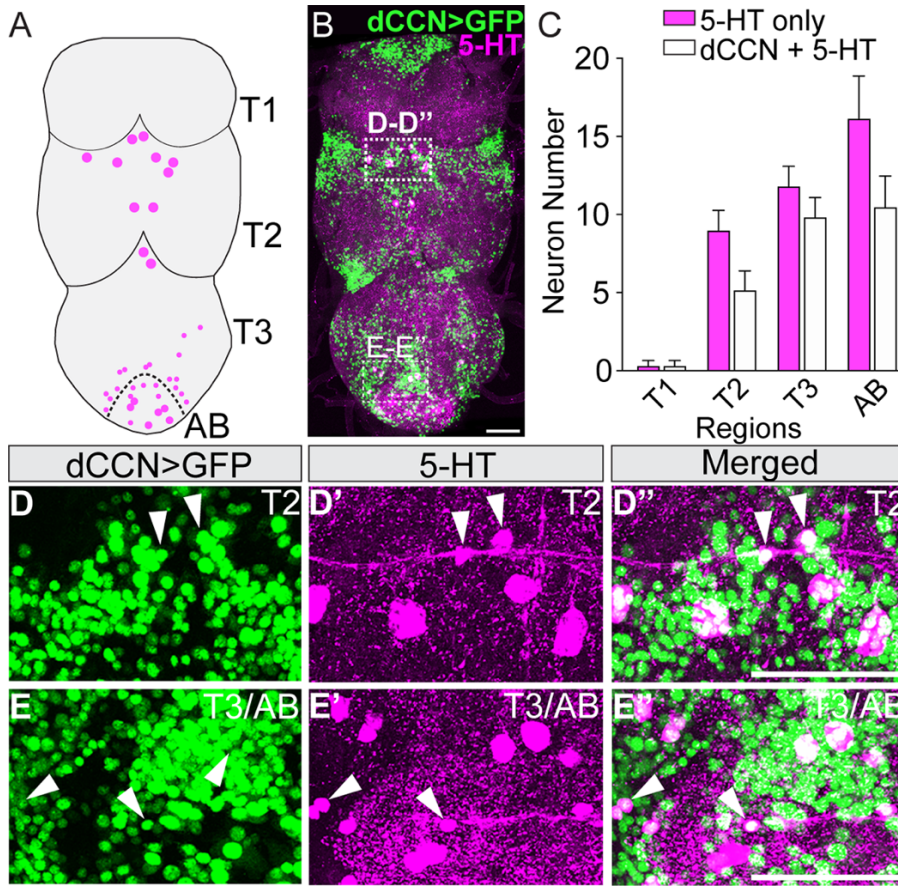
Figure S7: Co-expression of 5-HT and *dCCN* in adult ventral nerve cords. (**A**) A schematic representation of an adult ventral nerve cord (VNC) with magenta dots representing main serotonin (5-HT) neurons. The VNC is divided into regions T1, T2, T3, and AB. (**B**) GFP nuclei of a *dCCN^(Gal4)^>UAS-nlsGFP* VNC is seen. Anti-5-HT staining appears in magenta. (**C**) Quantification of 5-HT only and 5-HT - *dCCN* co-expressing neurons per region. (**D-D''**) A closer examination at the T2 region of the VNC highlighting 5-HT immunoreactive neurons co-expressing *dCCN*. Arrows point to examples of co-expressing neurons. (**E-E''**) A closer examination at the T3/AB region of the VNC highlighting 5-HT immunoreactive neurons co-expressing *dCCN*. Arrows point to examples of co-expressing neurons. Scale bars represent 50 μm.
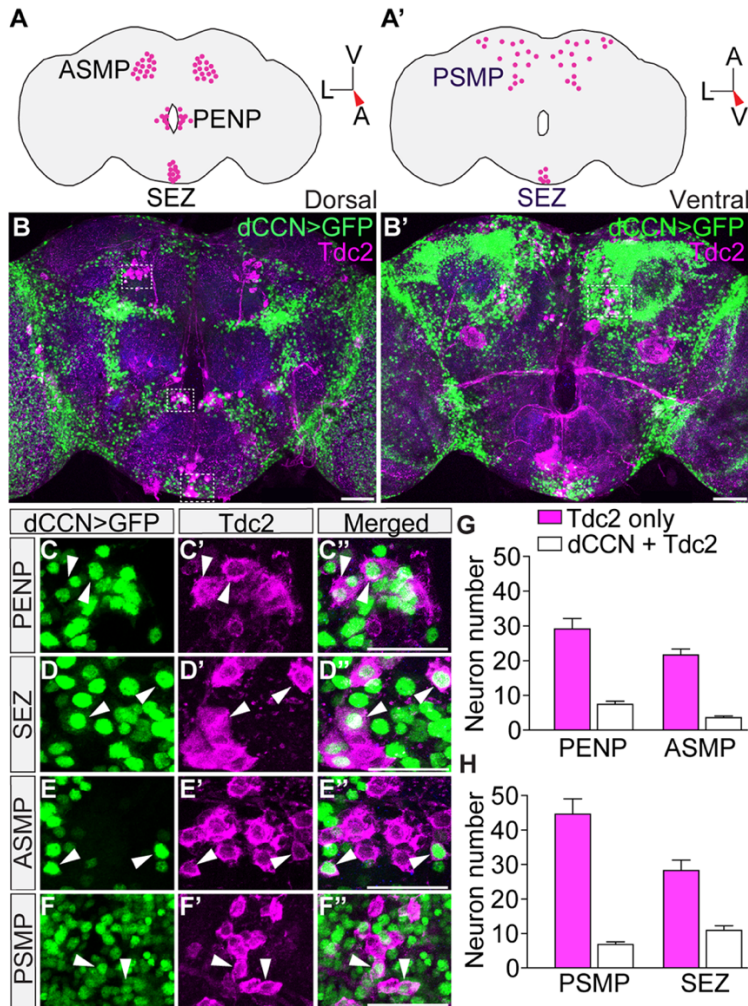
Figure 7:

Figure 7: *dCCN* **is expressed in subsets of OA neurons. (A-A')** Schematic illustrating the dorsal (**A**) and ventral (**A'**) view of major OA neuron clusters. (**B**) Identification of dCCN/OA neurons in the adult brain of *dCCN^{Gal4}>nlsGFP* progeny by immunohistochemistry (anti-Tdc2, magenta; anti-GFP, green; anti-Brp, blue) Dotted boxes in these dorsal optical sections outline higher magnification images of clusters in C, D, and E. (**B'**) *dCCN^{Gal4}>nlsGFP* neurons expressing Tdc2 in ventral sections of the adult brain (anti-Tdc2, magenta; anti-Brp, blue). Dotted boxes outline higher magnification images of clusters in F. (**C-F''**) Co-expression of Tdc2 and *dCCN^{Gal4}>nlsGFP* in higher magnification confocal images from dotted boxes in B-B'. Arrowheads point to dCCN/Tdc2 co-expressing neurons. Scale bars represent 50 μm. (**C-C''**) Co-expression of Tdc2 and *dCCN^{Gal4}>nlsGFP* in the PENP cluster. (**D-D''**) *dCCN^{Gal4} >nlsGFP* express Tdc2 in the SEZ cluster. (**E-E''**) A few Tdc2+ neurons in the ASMP cluster co-expression *dCCN^{Gal4} >nlsGFP*. (**F-F''**) Co-expression of Tdc2 and *dCCN^{Gal4}>nlsGFP* neurons in the PSMP cluster. (**G-H**) Quantification of dorsal and ventral *dCCN*/OA neurons per cluster. Error bars denote S.E.M. SEZ: subesophageal zone, PENP: periesophageal neuropils, ASMP: anterior superior medial protocerebrum, and PSMP: posterior superior medial protocerebrum. Nomenclature from Sherer et al., 2020.

Supplemental figure 8:
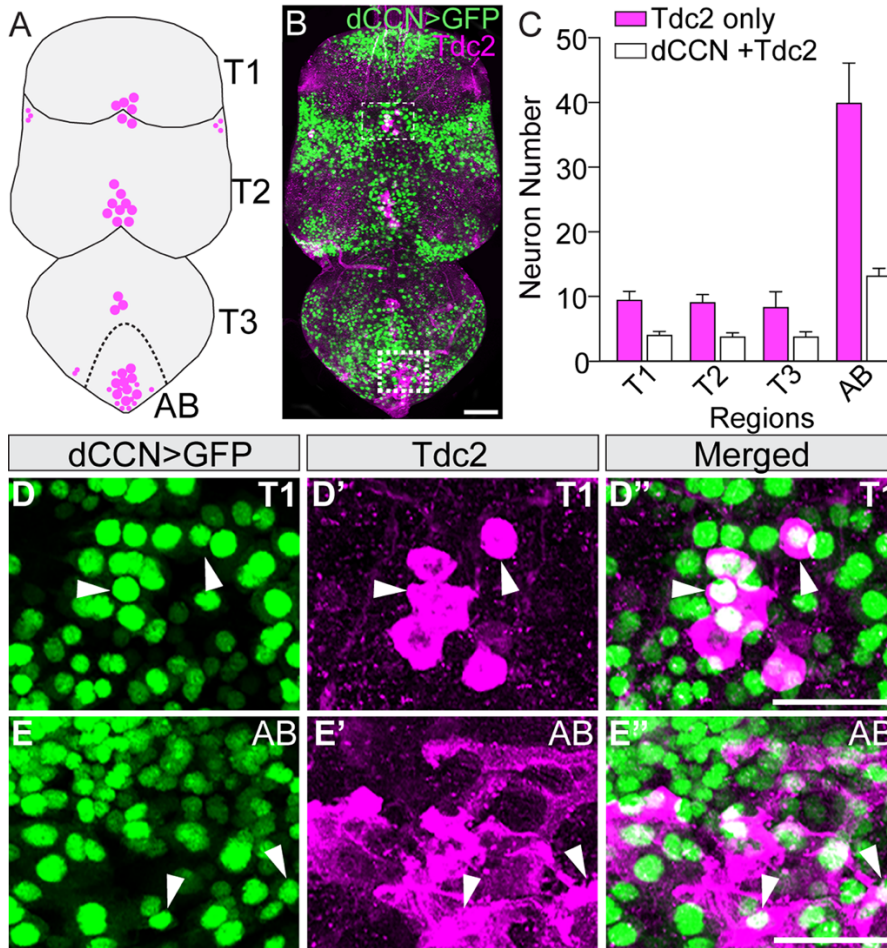
Figure S8: Co-expression of OA and *dCCN* in adult ventral nerve cords. (**A**) A schematic representation of an adult ventral nerve cord (VNC) with magenta dots representing prominent octopamine (OA) neurons. The VNC is divided into regions T1, T2, T3, and AB. (**B**) Green nuclei of a *dCCN^Gal4^>UAS-nlsGFP* VNC labeled with an anti-tdc2 antibody is seen in magenta. (**C**) Quantification of OA only and OA - *dCCN* neurons per region. (**D-D''**) A closer examination at the T2 region highlighting OA VNC neurons co-expressing *dCCN*. (**E-E''**) A closer examination at the T3/AB region highlighting OA VNC neurons co-expressing *dCCN*. Arrows point to co-expressing OA – *dCCN* neurons. Scale bars represent 50 µm.

significant number of neuromodulatory neurons and thus may be required for the development or function of circuits that control sensory processing, mood-related behaviors, and cognition (Monastirioti 1999; Fuxe et al., 2010; Sengupta et al., 2017; Deng et al., 2019).

dCCN is required for female fertility

The location of abdominal ganglion *dCCN*-expressing neurons in the female VNC led us to investigate whether these neurons innervate the female reproductive system. Each insect ovary consists of 15–20 ovarioles surrounded by a contractile meshwork called the peritoneal sheath (Middleton et al., 2006). The peritoneal sheath, lateral oviduct and uterus are innervated by two sets of nerves, branching from the abdominal median ganglion (Monastirioti, 2003; Middleton et al., 2006). Using the *20XUAS-6XGFP* reporter, we found the abdominal ganglion neurons that innervate the ovaries and uterus are indeed *dCCN^{Gal4}* neurons (Fig. 8A-C).

To determine if *dCCN* function is required for female fertility, we quantified egg laying and embryo viability. To reduce *dCCN* function, we assayed females in which a UAS-driven inverted repeat transgene targeting *dCCN* (*UAS-dCCN-RNAi*) was expressed under control of *dCCN^{Gal4}* as well as females homozygous for the severe hypomorphic *dCCN^{Gal4}* allele (Fig. 8D-E, SFig. 2). To ensure copulation success, five wildtype males were placed with a single transgenic control, *dCCN^{Gal4};UAS-dCCN-RNAi,* or *dCCN^{Gal4}/dCCN^{Gal4}* female. After individually mating with wildtype males, the number of embryos laid by single control and experimental females were counted. Embryo number did not differ between transgenic control females or *dCCN^{Gal4};UAS-dCCN-RNAi* females, indicating that reduced *dCCN* function is sufficient for control levels of egg laying (Fig. 8D-E, SFig. 2). However, we found a significant decrease in the number of embryos laid by *dCCN^{Gal4}/dCCN^{Gal4}* homozygous females at day 3 and day 5 post-mating (Fig. 8D-E). Furthermore, embryos laid by *dCCN^{Gal4}/ dCCN^{Gal4}* females did not hatch and were not viable. One possible explanation for a decrease in egg laying is a reduction in successful copulation. To determine copulation success, a sole wildtype male was placed with a single transgenic control or *dCCN^{Gal4}/dCCN^{Gal4}* female, and courtship was recorded for one hour. Although the rate was reduced, successful copulation occurred in ~36% of pairings with

Figure 8:
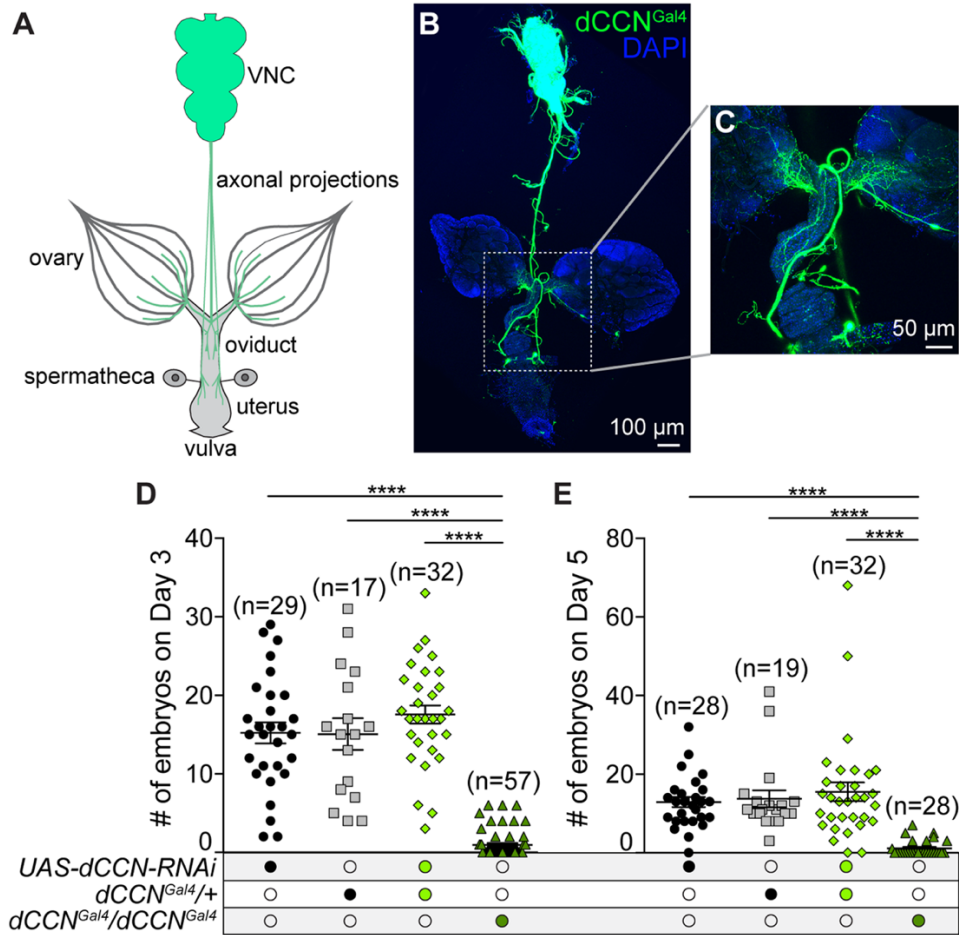
Figure 8: *dCCN* is required for female fertility. (**A**) Schematic illustrating ovaries and uterus innervation by *dCCN^{Gal4}* > *UAS-6X-GFP* neurons located in the VNC. (**B**) Projections of *dCCN^{Gal4}* > *UAS-6X-GFP* innervate the ovaries and uterus of the female reproductive system. Scale bar = 100 μm. Blue represents DAPI staining. (**C**) Higher magnification of *dCCN^{Gal4}* > *UAS-6X-GFP* uterus and ovary innervation from the dotted box region in B. Scale bar represents 50 μm. (**D-E**) *dCCN^{Gal4}/ dCCN^{Gal4}* females laid significantly less embryos than transgenic controls and *dCCN^{Gal4}-dCCN-RNAi* females on day 3 (**D**), and day 5 (**E**). Error bars denote S.E.M. All statistical tests are Kruskal-Wallis with Dunn's multiple comparisons test, (*$p<0.05$, **$p<0.01$, ***$p<0.001$, ****$p<0.0001$).

Supplemental figure 9:
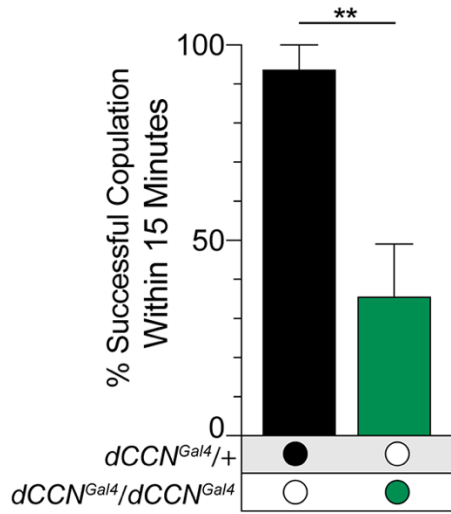
Figure S9: ***dCCN^Gal4* females successfully copulate within 15 minutes**. ~94% of heterozygous *dCCN^Gal4* females and ~36% homozygous *dCCN^Gal4* females successfully copulate within 15 minutes. n=16 for *dCCN^Gal4*/+ and n=14 for *dCCN^Gal4*/*dCCN^Gal4*. Error bars denote S.E.M.

dCCN^{Gal4}/dCCN^{Gal4} females during the first 15 minutes of assay time (SFig. 9). While further experiments are required to determine how *dCCN* is required for the function of ovary and uterus-innervating neurons, CCN vertebrate family members are also required in the female reproductive system for follicular development and ovulation (Winterhager and Gellhaus 2014).

Sex-specific neurons in the adult CNS express *dCCN*

Our finding that *dCCN* is required for female reproduction led us to investigate whether *dCCN* is expressed in other subsets of sex-specific neurons. *fruitless* (*fru*) and *double-sex* (*dsx*) are key genes that specify sex-specific neuron development and circuitry (Lee et al., 2000; Goodwin et al., 2000; Anand et al., 2001; Stockinger et al., 2005; Kimura et al., 2005; Yamamoto, 2007; Rideout et al., 2007; Villella and Hall, 2008; Rideout et al., 2010; Yamamoto, 2008; Sato et al., 2019; Ishii et al., 2020; Sato et al., 2020; Wohl et al., 2020; Chowdhury et al., 2020). Studies have identified at least 12 distinct classes of *fru+* neurons that are sexually dimorphic (Stockinger et al., 2005). These differences include a few neuronal classes that are present in males but lacking in females, such as P1, pIP10, and vPR6, and several others that differ in cell numbers, projections, or arborizations, such as mAL/aDT2, aSP1, and aSP2 (Fig. 9A-B). To determine whether *dCCN* is expressed in *fru+* neurons, a three-part transgenic combination was used: the *fru^{FLP}* allele to drive FLP-mediated recombination specifically in *fru* neurons, the *dCCN^{Gal4}* driver, and the *UAS>stop>mCD8-GFP* reporter which is only expressed in those cells that are labeled by the Gal4 driver and also *fru*, due to FLP-mediated excision of the stop cassette (Theodosiou, 1998). Using *dCCN^{Gal4}* to identify sexually dimorphic cells, we identified female-specific cells in the pL region per hemisphere (Fig. 9B', C', D'), and males have more aSP1 neurons (Fig. 9A, B, D). We also found that *dCCN^{Gal4}* labeled 2 *fru+* neurons in the antenna lobe of the male but not female brain (Fig. 9B, D). Differences in *dCCN/fru* neuron number were also observed between males and females in segment T1, the abdominal ganglion, and the midline of the VNC (SFig 10A-B').

Although *fru* does not have an obvious mammalian homolog, *dsx*-related genes are present in vertebrates where they regulate sex-specific differentiation in many tissues, including the nervous system (Rideout et al., 2007; Villella and Hall, 2008; Rideout et al.,

Figure 9:
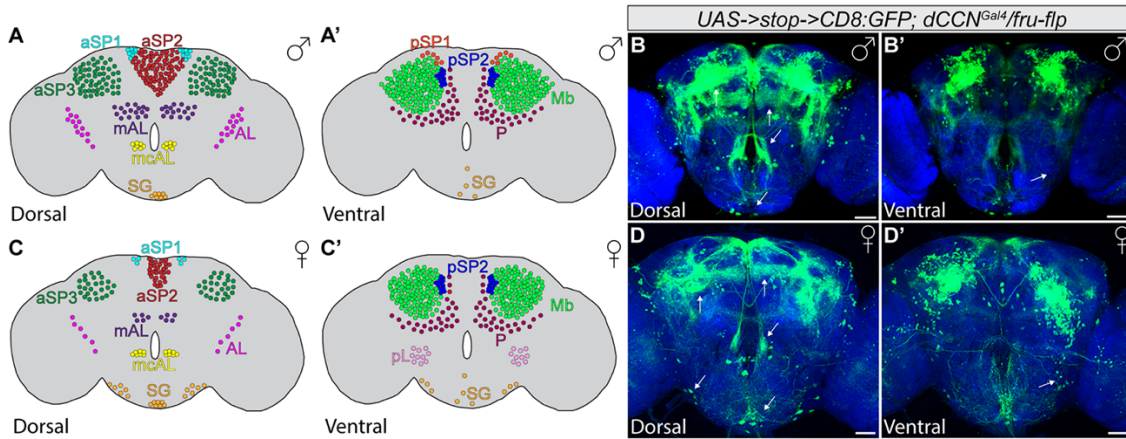
Figure 9: *Fruitless - dCCN* **brain expression is sexually dimorphic.** (**A**) A schematic representation showing prominent dorsal male *fruitless (fru)* neuron clusters of the brain and their anatomical position. (**A'**) A schematic representation showing prominent ventral *fru* neuron clusters. (**B**) The dorsal portion of a brain displaying *dCCN - fru* expressing neurons in GFP of a male *UAS->stop->CD8:GFP; dCCN^Gal4/fru-flp* fly. (**B'**) The ventral portion of the male brain from **B**. (**C**) A schematic representation showing prominent dorsal female *fru* neuron clusters. (**C'**) A schematic representation showing prominent ventral female *fru* neuron clusters. (**D**) The dorsal portion of a brain displaying *dCCN - fru* expressing neurons in GFP of a female *UAS->stop->CD8:GFP; dCCN^Gal4/fru-flp* fly. (**D'**) The ventral portion of a female brain from **D**. Blue represents anti-nC82 staining. Scale bars represent 50 μm. Arrows point to neuronal cell body or axonal differences between male and female *dCCN - fru* expression. *fru* clusters, nomenclature, and anatomical locations were adapted and modified from figure 2 and table 1 of Stockinger et al., 2005.

Supplemental figure 10:
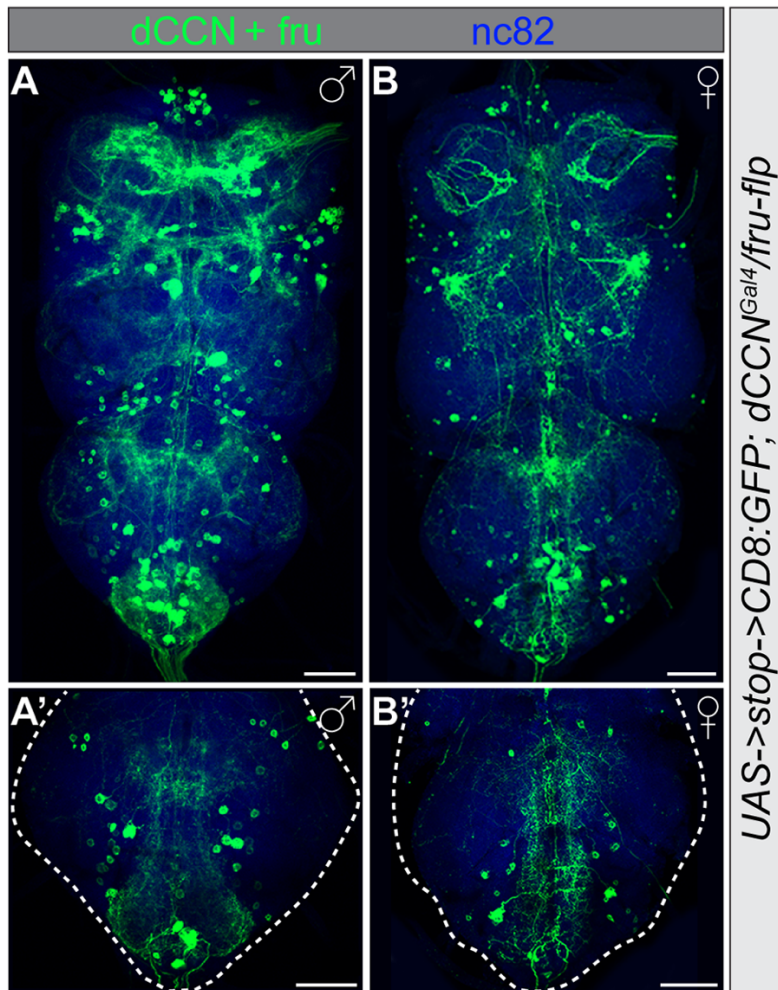
Figure S10: *Fruitless - dCCN* **ventral nerve cord expression is sexually dimorphic**. (**A**) *dCCN – fruitless (fru)* expressing neurons can be seen in GFP in a male *UAS->stop->CD8:GFP; dCCN^Gal4/fru-flp* ventral nerve cord (VNC). (**A'**) A closer examination of neuronal soma in the ventral portion of the male abdominal ganglion (AB). (**B**) *dCCN - fru* expressing neurons can be seen in GFP in a female *UAS->stop->CD8:GFP; dCCN^Gal4/fru-flp* VNC. (**B'**) A closer examination of neuronal soma in the ventral portion of the female AB. For (**A-B'**), an anti-GFP antibody was used to enhance GFP signal. Blue represents anti-brp (nC82) neuropil staining. Scale bars represent 50 μm.

2010; Wohl et al., 2020; Chowdhury et al., 2020). In the adult *Drosophila* brain, 10 major clusters of *dsx*-expressing neurons are present, with males having more neurons per cluster than females (Rideout et al, 2007; Rideout et al., 2010). These clusters consist of the anterior dorsal neurons (aDN), posterior clusters pC1 and pC2, the posterior dorsal cluster (pCd/pC3), and the subesophageal neurons (SN), as well as the posterior medial neurons (pMN1-2), the posterior lateral neurons (pLN), and the subesophageal lateral neurons (SLG) (Fig. 10A, B). We examined *dCCN* expression in *dsx*-positive neurons using the same intersectional genetic approach as above, now with the *dsx^FLP^* transgene (Rezaval et al., 2014) in combination with *dCCN^Gal4^* and the Gal4/FLP-responsive membrane reporter, *UAS>stop>mCD8::GFP*. We observed large numbers of *dCCN/dsx+* neurons in the adult male brain, particularly in the pC1 pC2, and SLG clusters (Fig. 10C-D'), as well as sex-specific differences between the pC1 and pC2 clusters in the female brain (Fig. 10C-D'). In addition, *dCCN/dsx*-positive neurons are found in the thoracic segments of the male VNC, but not the female (SFig. 11A-B'), and sex-specific differences in the abdominal ganglion are also observed in which males have more neurons than females (SFig. 11A', B').

In summation, our results indicate that *dCCN* is expressed in neurons that inform the sexual identity of cells (Verhulst et al., 2010). Sex-specific alternative splicing of both *fru* and *dsx* occurs throughout development and is required for the formation of sex-specific somatic tissues and neuronal circuitry (Salvemini et al., 2010). Furthermore, the expression of sexually-dimorphic *fru* transcript alters the axonal arborizations of pheromone-sensing neurons, a circuit pathway with opposing outcomes in males and females (Cachero et al., 2010; Ruta et al., 2010), and *fru* expression in the interneurons of the protocerebrum has been proposed as a mechanism for altering this logic of male and female circuitry (Kohl et al., 2013). Should *dCCN* be required for the formation of *fru* and *dsx* neurons at multiple stages of development, there may be a profound developmental role for CCN family proteins as key regulators of neuron and circuit identity.

Figure 10:
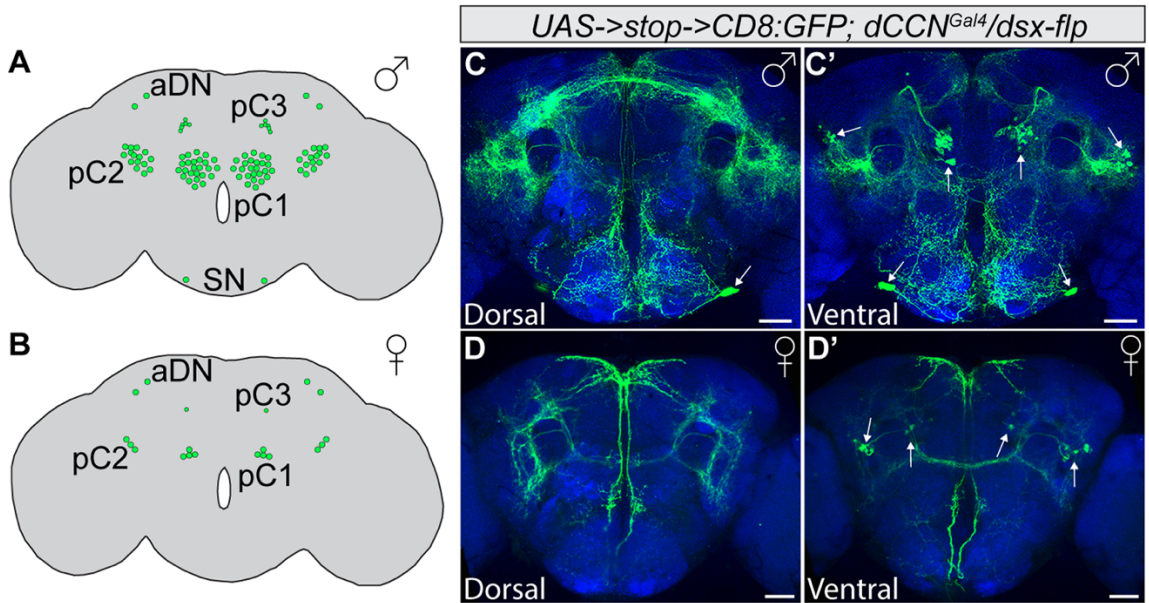
Figure 10: *Double-sex - dCCN* **brain expression is sexually dimorphic.** (**A**) A schematic representation displaying the primary male *double-sex* (*dsx)* neuron clusters of the brain and their anatomical position. (**B**) The dorsal portion of a male *UAS->stop->CD8:GFP; dCCN^Gal4/dsx-flp* brain displaying *dCCN - dsx* expression in GFP. (**B'**) The ventral portion of the same brain in B displaying *dCCN - dsx* expression in GFP. (**C**) A schematic representation displaying the major clusters of female *dsx* neurons and their anatomical position. (**D**) The dorsal portion of a female *UAS->stop->CD8:GFP; dCCN^Gal4/dsx-flp* brain displaying *dCCN - dsx* expression in GFP. (**D'**) The ventral portion of the same brain in D displaying *dCCN - dsx* expression in GFP. For **B-B'**, and **D-D'**, an anti-GFP antibody was used to enhance GFP signal. Blue represents anti-brp (nC82) neuropil staining. Scale bars represent 50 μm. pC1: dorsal inferomedial protocerebrum, pC2: inferolateral protocerebrum, pC3: superomedial protocerebrum, and SN: subesophageal neurons (male specific). *dsx* clusters, nomenclature, and anatomical locations were adapted and modified from figure 2 of Rideout et al., 2010.

Supplemental figure 11:
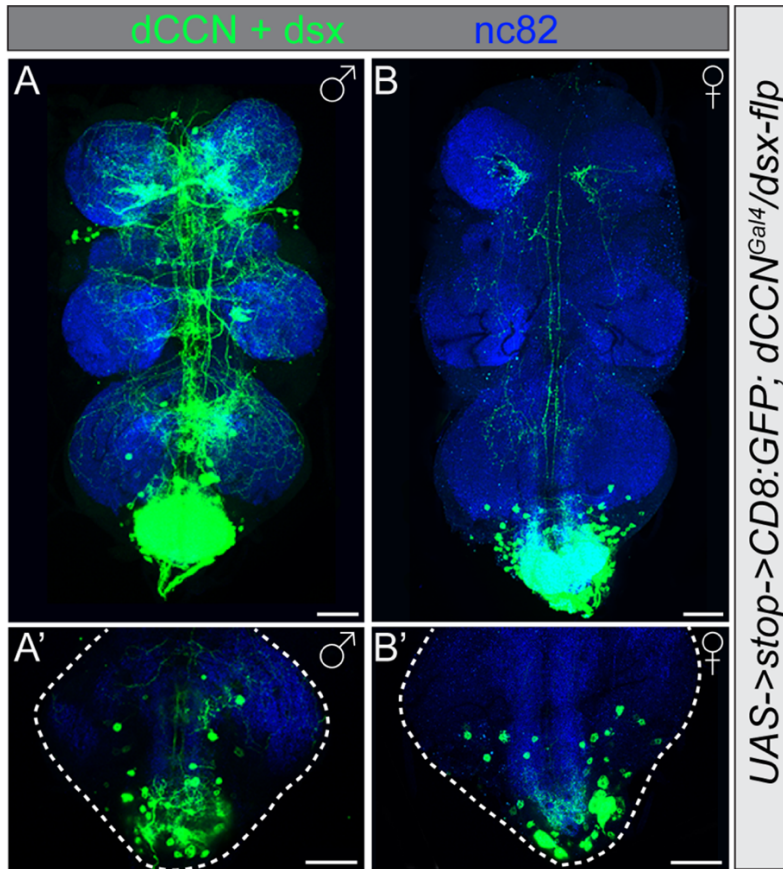
Figure S11: *Double-sex - dCCN* ventral nerve cord expression is sexually dimorphic. (**A**) *dCCN - double-sex (dsx)* expressing neurons can be seen in GFP in a male *UAS->stop->CD8:GFP; dCCN^Gal4/dsx-flp* ventral nerve cord (VNC). (**A'**) A closer examination of neuronal soma in the ventral portion of the male abdominal ganglion (AB). (**B**) *dCCN - dsx* expressing neurons can be seen in GFP in a female *UAS->stop->CD8:GFP; dCCN^Gal4/dsx-flp* VNC. (**B'**) A closer examination of neuronal soma in the ventral portion of the female AB. For (**A-B'**), an anti-GFP antibody was used to enhance GFP signal. Blue represents anti-brp (nC82) neuropil staining. Scale bars represent 50 μm.

Materials and Methods

Drosophila Husbandry and Stocks: All flies were reared on standard cornmeal-based fly food. Unless noted otherwise, during development and post-eclosion, flies were raised and housed at 25 C, ~50% humidity, and a 12:12hr light-dark cycle (1400+200 lx white fluorescent light) in humidity and temperature-controlled incubators. A list of stocks used can be found in the Resource Table.

Generation of *dCCN* line: The *dCCN-Gal4* line was created through MiMIC insertion-conversion at the endogenous *dCCN* chromosomal locus. A protein-trap is generated by converting a MiMIC insertion into the coding region of the endogenous *dCCN* gene.

qPCR: Total RNA from ~40 heads using Direct-zol RNA Miniprep Pluskit (Zymo Research) was purified and treated with DNase I per the manufacturer's protocol. RNA concentrations were measured with a ND-1000 nanodrop spectrometer. Reverse transcription was accomplished using iScript cDNA Synthesis kit (Bio-Rad Laboratories). RT-PCR was performed using 300 ng cDNA added to iTaq Universal SYBR Green Supermix (Bio-Rad Laboratories) and primers in a 20 L reaction volume. All samples were run in triplicate using a Stratagene Mx3005P qPCR System (Agilent Technologies). Expression of ribosomal protein 49 (Rp49) was used as the reference control to normalize expression between genotypes. Expression levels were determined using the $\Delta\Delta CT$ method and results from control ($dCCN^{Gal4}/+$) and experimental ($dCCN^{Gal4}/ dCCN^{Gal4}$) groups were normalized relative to flies in a yellow-white genetic background (yw/+). The following primers were used: Rp49 Forward: 50-CATCCGCCCAGCATACAG-3' Rp49 Reverse: 5'-CCATTTGTGCGACAGCTTAG-3' *dCCN* Forward: 5'-GATGTGGCTATGTGAGAATCCAA-3' *dCCN* Reverse: 5'-GCAAATTGCTCAGTTGATGGC-3'.

In situ analysis and imaging: A modified version of the Ryoo lab protocol was performed and can be found at: http://ryoo-lab.med.nyu.edu/protocols/embryo-situ. On day 1, collected embryos were fixed with 4% paraformaldehyde (Mallinckrodt Chemicals, Cat# 2621-59) in 1% PBS, and incubated overnight in hybridization buffer

and probes specific for *dCCN* on rotation at 4 degrees C. On day 2, three ten-minute washes of PBS were applied to embryos, then embryos are incubated overnight in a rabbit anti-DIG-AP antibody and hybridization buffer at 4 degrees C. On day 3, three ten-minute washes of PBS were applied to the embryos. After washes, a staining solution was applied to the embryos for 4 hours in hybridization buffer. Three additional ten-minute PBS washes were applied, then embryonic brain lobes and nerve cords were dissected, then mounted in Vectashield. Slides are allowed to set for 1 hour before imaging.

Embryo collection: Embryos of 4-22 hours old (stages 9-17) were collected from grape juice agar plates (3% agar) with fresh yeast, dechlorinated for five minutes with 50% chlorox in dH$_2$O, and then washed in cold tap water until chlorox was thoroughly removed. Dechlorinated embryos were fixed in a solution containing 50% freshly made 4% paraformaldehyde (Mallinckrodt Chemicals, Cat# 2621-59) in 1% PBS, and 50% heptane for 20 mins. After fixation, heptane was manually pipetted out, and 100% methanol of equal fixation volume was added to the fixation solution. Embryos were vigorously shaken for 1 min to crack vitelline membranes. Three additional 5 min washes of 100% methanol were added to the mixture of embryos while pipetting off previous supernatants to remove residual PFA, heptane, and cracked vitelline membranes. Embryos were stored in a -20 C freezer in 100% methanol for future use.

Immunohistochemistry and Imaging: Embryos were rehydrated through a series of methanol washes at 70%, 50%, and 30% in 1% PBS for 5 mins at each wash. After rehydration washes, embryos were washed in 1% PBS 2 times, for 10 min each. Following PBS washes, embryos were incubated in blocking solution (2% Normal Goat Serum, 2% Bovine Serum Albumin, 2% Triton-X in 1% PBS) for 2 hours before primary antibodies were applied and incubated on rotation overnight at ~3 C. The primary antibody used was rabbit anti-GFP (3:500; Thermo Fisher Scientific, Cat# G10362), and the secondary antibody was goat anti-rabbit 488 (1:200; Thermo Fisher Scientific, Cat# R37116). Labeled embryos were mounted in Vectashield (Vector Labs, Cat# H1000). For larval imaging, third instar larvae were dissected on ice and fixed with 4% paraformaldehyde (Electron Microscopy Sciences, Cat# 15710) for 30 mins, washed in

PBT three times for 10 mins each, washed in 1% PBS for 5 minutes, then incubated in blocking solution for 2 hours before primary antibodies were applied and incubated overnight on rotation. Primary antibodies used were rabbit anti-CD4 (1:100; Novus Biologicals, Cat# NBP1-86143), rabbit anti-GFP (3:500; Thermo Fisher Scientific, Cat# G10362), and mouse anti-actinin (1:20; DSHB Cat#2G3-3D7). Secondary antibodies included goat anti-rabbit Alexa 488 (1:200, Thermo Fisher Scientific, Cat# R37116), goat anti-rabbit Alexa 594 (1:200, Thermo Fisher Scientific, Cat# A-11012), and goat anti-mouse Alexa 594 (1:200; Thermo Fisher Scientific, Cat# A-21125). Labeled larval CNSs or NMJs were mounted with either Vectashield (Vector Labs, #H1000) or DAPI (Cell Signaling Technology, #8961S), and slides set for one hour before imaging.

For adults, 3-7 day old adult male and female dissected brains, VNCs, maxillary palps, antennas, or gut structures were fixed in 4% paraformaldehyde for 30 minutes. 3-7 day old female reproductive organs were fixed for 60 minutes in 4% paraformaldehyde. 3-7 day old adult legs and proboscis were fixed overnight in 4% paraformaldehyde on rotation at ~3 C. The following primary antibodies were used: rabbit anti-GFP (3:500; Thermo Fisher Scientific, Cat# G10362), rabbit anti-TH (1:200), rabbit anti-5-HT (1:1000; Sigma Aldrich, Cat# S5545), rabbit anti-Tdc2 (3:500; Covalab, Cat# pab0822-P), and mouse anti-bruchpilot (nc82) (1:80; DSHB Cat# nc82). Secondary antibodies conjugated to Alexa 488, Alexa 594, or Alexa 647 were used at a concentration of 1:200 (see resource table). Labeled organs or structures were mounted in either Vectashield (Vector Labs, #H1000) or DAPI (Cell Signaling Technology, #8961S). Slides were allowed to set one hour before imaging.

Imaging: Images were collected on an Olympus Fluoview FV1000 laser scanning confocal mounted on an inverted IX81 microscope or a Zeiss Confocal Microscope. Images were processed using ImageJ (NIH) and Adobe Photoshop (Adobe, CA).

Courtship Assays: A single virgin female of 3-4 days old was paired with an isolated *Canton S* wild type male of similar age, and placed in chamber of a 12 well plate with room temperature standard cornmeal fly food filled to ~80% of the height of the chamber. A camera recorded behavioral engagements for 90 minutes after paired flies

45

were placed into the chamber. iMovie (Apple Inc., 2009) was used to manually analyze courting behaviors, and the times at which copulation did or did not occur was recorded.

Sterility Assays: A single female was paired with five *Canton S* wild type males on the day of eclosion (day 1), and placed into a vial containing standard cornmeal fly food with red food coloring. 24 hours before day 3 and day 5, the single female and five males were transferred into a fresh food vial containing red food coloring. On days 3 and 5 (24 hours after transfer into a fresh vial), the number of embryos was manually counted under a lab bench microscope. Data was collected and entered into Microsoft Excel spreadsheets, and GraphPad Prism for analyses.

Larval NMJ Electrophysiology: Through collaboration, two electrode voltage clamp recording techniques were used to measure excitatory post-synaptic potentials at NMJs of larvae following previously established electrophysiology recording protocols from the McCabe lab (Choi et al., 2014).

Sequence Alignment and Amino Acid Sequences: Sequence alignments were created using NCBI's Protein BLAST's online tool. (Madden T. *The BLAST Sequence Analysis Tool*. 2002 Oct 9 [Updated 2003 Aug 13]. In: McEntyre J, Ostell J, editors. The NCBI Handbook [Internet]. Bethesda (MD): National Center for Biotechnology Information (US); 2002-. Chapter 16. Available from: http://www.ncbi.nlm.nih.gov/books/NBK21097/). Amino acid sequences were obtained from http://www.uniprot.org/.

Neuron quantification: Amine neuron and co-expression counts were conducted in Image J (NIH) by manually scanning and counting fluorescently labeled neurons through stacks of TIFFs. Counts were collected in Microsoft Excel spreadsheets and averaged in GraphPad Prism.

Data Collection, Figure Making, and Data Analysis: Microsoft Excel and GraphPad Prism (version 8.0) were used for data collection and analysis. Image J was used to

process raw confocal images. Adobe Photoshop and Illustrator were used to further process images, and generate figures for publication.

Resource Table

REAGENT, RESOURCE, or PRODUCT	SOURCE	IDENTIFIER
Antibodies		
Mouse anti-Drosophila bruchpilot (nc82)	Developmental Studies Hybridoma Bank (DSHB)	Cat# nc82; RRID: AB_2314866
Mouse anti-Actinin (2G3-3D7)	Developmental Studies Hybridoma Bank (DSHB)	Cat# 2G3-3D7; RRID:AB_2721943
Rabbit anti-GFP	Thermo Fisher Scientific	Cat# G10362, RRID:AB_2536526
Rabbit anti-CD4	Novus Biologicals	Cat# NBP1-86143
Rabbit anti-Tdc2	Covalab	Cat# pab0822-P
Rabbit anti-TH		
Rabbit anti-5-HT	Sigma Aldrich	Cat# S5545
Rat anti-Elav	Developmental Studies Hybridoma Bank (DSHB)	Cat# 7E8A10; RRID: AB_528218
Mouse anti-Repo	Developmental Studies Hybridoma Bank (DSHB)	Cat # 8D12; RRID: AB_528448
Donkey anti-mouse Alexa 647	Thermo Fisher Scientific	Cat# A-31571, RRID:AB_162542
Goat anti-rabbit Alexa 488	Thermo Fisher Scientific	Cat# R37116, RRID:AB_2556544
Goat anti-mouse Alexa 594	Thermo Fisher Scientific	Cat# A-21125, RRID:AB_2535767
Goat anti-rabbit Alexa 594	Thermo Fisher Scientific	Cat# A-11012,
Goat anti rat Alexa 488	Thermo Fisher Scientific	Cat# A-11007;
Mounting Mediums		
Vectashield	Vector Labs	Cat# H1000
DAPI	Cell Signaling Technology	Cat# 8961S
***Drosophila* lines**		
Canton-S	BDSC	RRID: BDSC_64349
dCCNGal4	Dr. Sarah Certel	N/A
UAS-dCCN-RNAi	BDSC	RRID: BDSC_41913
UAS-dCCN:HA	Dr. Sarah Certel	N/A
UAS-CD8-GFP	BDSC	RRID: BDSC_5130
20XUAS-6XGFP		
UAS-dsRed	BDSC	RRID: BDSC_6282
UAS->stop->CD8:GFP		
UAS-GFP.S65T	BDSC	RRID: BDSC_1521
fru-flp		
dsx-flp		
UAS-stinger GFP	Dafni	
UAS-CD4:TdTom	BDSC	RRID: BDSC_35841
repo-FLP (II)		
UAS-HA;;dCCN-DBD	BDSC	RRID: BDSC_70415
dCCN-AD	BDSC	RRID: BDSC_75357
EAAT1-DBD	BDSC	RRID: BDSC_74466
EAAT1-AD	BDSC	RRID: BDSC_71474
Software and Algorithms		
Fiji/ImageJ	National Institutes of Health (NIH)	https://imagej.net/Fiji; RRID: SCR_002285
GraphPad Prism	GraphPad Software	https://www.graphpad.com/; RRID: SCR_002798
Excel 2019	Microsoft Corporation	https://products.office.com/excel
Adobe Illustrator 2020	Adobe	https://www.adobe.com/creativecloud.html
Adobe Photoshop 2020	Adobe	https://www.adobe.com/creativecloud.html

Chapter 3: Dual Neurotransmission Manuscript

Chapter note:

In addition to my thesis work on the *dCCN* project, I significantly contributed to experiments identifying and examining the role of glutamate release from octopamine neurons. As second author on the following publication, I performed key immunohistochemistry experiments, image analysis and figure construction, as well as aggression assays, scoring, and statistical analyses.

RESEARCH ARTICLE

Octopamine neuron dependent aggression requires dVGLUT from dual-transmitting neurons

Lewis M. Sherer [1], Elizabeth Catudio Garrett [1], Hannah R. Morgan [2], Edmond D. Brewer [2], Lucy A. Sirrs [2], Harold K. Shearin [3], Jessica L. Williams [3], Brian D. McCabe [4], R. Steven Stowers [3], Sarah J. Certel [1,2]*

1 Cellular, Molecular and Microbial Biology Graduate Program, University of Montana, Missoula, Montana, United States of America, 2 Division of Biological Sciences, Center for Structural and Functional Neuroscience, University of Montana, Missoula, Montana, United States of America, 3 Cell Biology and Neuroscience Department, Montana State University, Bozeman, Montana, United States of America, 4 Brain Mind Institute, Swiss Federal Institute of Technology (EPFL), Lausanne, Switzerland

* sarah.certel@umontana.edu

Abstract

Neuromodulators such as monoamines are often expressed in neurons that also release at least one fast-acting neurotransmitter. The release of a combination of transmitters provides both "classical" and "modulatory" signals that could produce diverse and/or complementary effects in associated circuits. Here, we establish that the majority of *Drosophila* octopamine (OA) neurons are also glutamatergic and identify the individual contributions of each neurotransmitter on sex-specific behaviors. Males without OA display low levels of aggression and high levels of inter-male courtship. Males deficient for dVGLUT solely in OA-glutamate neurons (OGNs) also exhibit a reduction in aggression, but without a concurrent increase in inter-male courtship. Within OGNs, a portion of VMAT and dVGLUT puncta differ in localization suggesting spatial differences in OA signaling. Our findings establish a previously undetermined role for dVGLUT in OA neurons and suggests that glutamate uncouples aggression from OA-dependent courtship-related behavior. These results indicate that dual neurotransmission can increase the efficacy of individual neurotransmitters while maintaining unique functions within a multi-functional social behavior neuronal network.

Author summary

Neurons communicate with each other via electrical events and the release of chemical signals. An emerging challenge in understanding neuron communication is the realization that many neurons release more than one type of chemical signal or neurotransmitter. Here we ask how does the release of more than one neurotransmitter from a single neuron impact circuits that control behavior? We determined the monoamine octopamine and the classical transmitter glutamate are co-expressed in the *Drosophila* adult CNS. By manipulating the release of glutamate in OA-glutamate neurons, we demonstrated glutamate has both separable actions and complementary actions with OA on

51

aggression and reproductive behaviors respectively. Aggression is a behavior that is highly conserved between organisms and present in many human disease states, including depression and Alzheimer's disease. Our results show that aggressive behavior requires the release of both neurotransmitters in dual-transmitting neurons and suggests within this set of neurons, glutamate may provide a new therapeutic target to modulate aggression in pathological conditions.

Introduction

The classical view of information transfer for many decades was that each neuron released a single neurotransmitter, leading to the 'one neuron, one transmitter' hypothesis [1], formalized by John Eccles as Dale's Principle [2]. Dale himself, however, recognized the possibility that neurons can release more than one molecule [3] and indeed, research from multiple systems and neuronal populations have established that many if not most, neurons release more than one neurotransmitter [4–7]. Dual neurotransmission has the potential to transform the way we consider the computation and transmission of information by neurons, circuits and networks. Presynaptically, the release of two neurotransmitters could impact information transfer by several mechanisms that are not mutually exclusive including; attenuating signals by modulating presynaptic autoreceptors, transmitting spatially distinct signals by segregating specific vesicle populations to different axon terminals, or conveying similar information through the release of both neurotransmitters from the same synaptic vesicle [8–11]. In addition, one vesicular neurotransmitter transporter can increase the packaging of the other neurotransmitter into the same synaptic vesicle (SV), a process called vesicular synergy [4, 12, 13]. At post-synaptic targets, the release of two transmitters can enhance the strength of the same signal and/or convey unique signals through spatially-restricted receptor expression and second messenger cascades [7, 14]. While recent studies have provided insight into these phenomena at the cellular level [11, 12, 15, 16], the behavioral relevance of co-transmission in normal as well as pathological conditions is an area of considerable complexity and interest.

The genetic tools of *Drosophila* provide the ability to genetically dissect the signaling properties of dual transmission on behavioral networks in general and upon the circuits that control aggression in particular. Aggression is a hardwired behavior that has evolved in the framework of defending or obtaining resources [17, 18]. Monoamines such as serotonin (5-HT), dopamine (DA), norepinephrine (NE) and octopamine (OA), the invertebrate homologue of NE, have powerful modulatory effects on aggression in systems ranging from insects and crustaceans to humans [19–23]. In humans, aggressive behavior can be expressed at extreme levels and out of context due to medical, neurologic and or psychiatric disorders including depression and schizophrenia [24–26]. Pharmacological agents that selectively manipulate monoamine signaling are used to treat anxiety and depression, yet these drugs are often ineffective, and in the case of serotonin/norepinephrine reuptake inhibitors (SNRIs) can induce side effects including increased aggression and impulsivity [25, 27–29].

At least two difficulties arise in targeting monoamines to achieve successful outcomes. First, monoamines can be released from synaptic vesicles (SVs) into the presynaptic cleft and by extrasynaptic release from large dense core vesicles (LDCVs) [30–33]. Thus, monoamines are recognized both as neurotransmitters and as neuromodulators that signal via diffusion [34, 35]. The second difficulty is that their effects are likely exerted through interactions with neuropeptides (neuropeptide Y and oxytocin are two examples) and with neurotransmitters including GABA and glutamate [5, 14, 36, 37]. Due in part to recent studies suggesting the

52

expression of vesicular glutamate transporters (VGLUTs) can be altered by psychiatric medications [38–41] and the importance of dopamine neuron glutamate co-transmission on the schizophrenia resilience phenotype in mice [42], we generated new tools to identify and manipulate glutamate function in monoamine-expressing neurons.

We found that the majority of OA neurons within the *Drosophila* nervous system also express the vesicular neurotransmitter transporter for glutamate (dVGlut). Functionally, glutamate (GLU) co-expression could convey the same information by promoting the synaptic vesicle packing of OA or GLU may convey distinct information that is separate from the function of OA. In *Drosophila*, OA synthesis and release are essential for conserved social behaviors; males without OA display low levels of aggression and high levels of inter-male courtship [43–47]. We demonstrate that males deficient for dVGLUT solely in OA-glutamate neurons (OGNs) also exhibit a reduction in aggression, but without a concurrent increase in inter-male courtship. These results indicate both OA and dVGLUT are required in dual-transmitting neurons to promote aggression. However, only OA is required for the suppression of inter-male courtship and thus the function of dVGLUT in OGNs is not limited to vesicular synergy.

To ask if the separable effects of OA on courtship circuitry may be attributable to spatially distinct OA signals, we conditionally expressed a new epitope-tagged version of the *Drosophila* vesicular neurotransmitter transporter for monoamines (V5-tagged VMAT) in OGNs. While the majority of V5-VMAT and dVGLUT expression colocalize, VMAT is detected in distinct puncta without dVGLUT suggesting the possibility of separable signal transmission. Together, these results demonstrate the complex behavior of aggression requires both dVGLUT and OA in dual-transmitting neurons and suggests within monoamine neurons, GLU may provide a therapeutic target to modulate aggression in pathological conditions.

Results

dVGLUT is co-expressed in OA neurons

The co-expression of vesicular neurotransmitter transporters has been primarily used to identify dual-transmitting neurons[48–52]. To examine glutamatergic transmitter expression, we generated a monoclonal dVGLUT antibody and validated its specificity using a new *dVGlut* allele, *dVGlut^{SS1}*. In homozygous *dVGlut^{SS1}* progeny, dVGLUT protein is not detectable (S1 Fig, Methods), thus demonstrating the specificity of the dVGLUT antibody. As dVGLUT expression is widespread and mainly found in synaptic terminals (S1 Fig), we used the Gal4-UAS system to identify monoamine neurons that express GLU. In this study, we focused specifically on OA neurons that co-express dVGLUT (OA-glutamate neurons (OGNs)).

Cell bodies of OGNs were visualized by a *UAS-dsRed.NLS* reporter under control of *dVGlut-gal4* (hereafter referred to as *dVGlut>dsRed*). OGNs were identified by antibodies to tyrosine decarboxylase 2 (TDC2) and tyramine β-hydroxylase (TβH) as OA is synthesized from the amino acid tyrosine via the action of Tdc and Tβh in invertebrates [46]. OGNs from 10 *dVGlut>dsRed* Tdc2-labeled male brains were quantified by the multi-point ImageJ tool followed by manual verification of each optical section. Within the brain, OA neurons that co-express glutamate are found in the subesophageal zone (SEZ), the periesophageal neuropils (PENP), the anterior (ASMP) and posterior superior medial protocerebrum (PSMP), and the protocerebral bridge (Fig 1A–1E, S1 Table). Co-expression occurs in each region of interest (Fig 1A–1E). Tβh and *dVGlut>dsRed* co-localization (S2 Fig) provides further support that glutamate is found in OA-expressing neurons.

In the adult ventral nervous system (VNS), the thoracic Tdc2+ neurons that innervate skeletal muscles express glutamate (S3 Fig). In the abdominal ganglia, all but 2–3 Tdc2+ neurons express dVGlut (S3 Fig) consistent with the previous finding of OA-glutamate co-expression

53
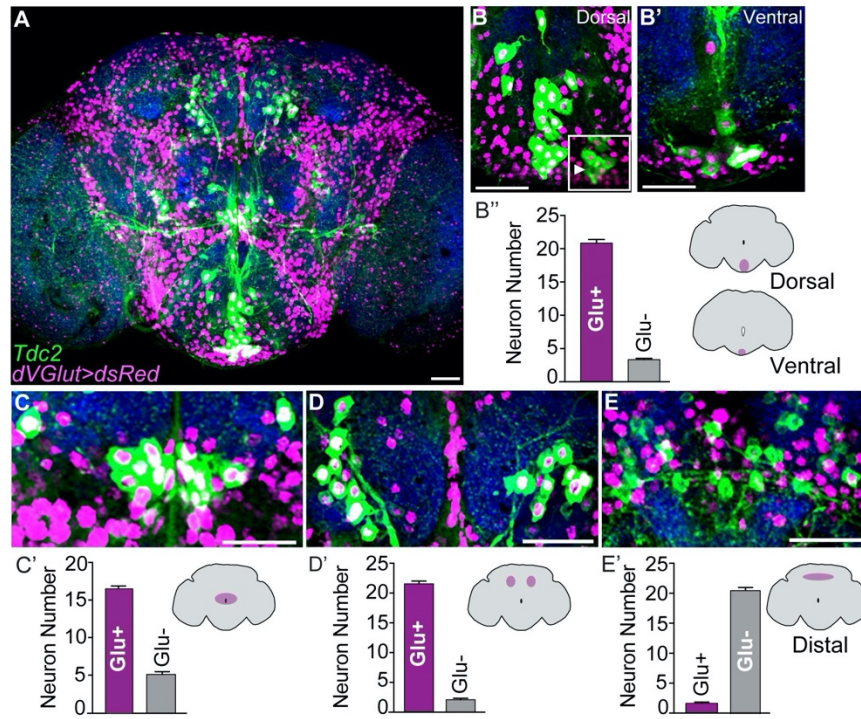
Fig 1. OA neurons co-express glutamate. (A) OA-glutamate co-expression in a *dVGlut>dsRed* male brain labeled with anti-Tdc2 (green). Anti-brp (nc82, blue) labels the neuropil. Scale bar = 10 μm. (**B-B'**) Dorsal (B) and ventral (B') confocal sections of neurons co-expressing OA and dVGlut in the SEZ. Non-dVGlut positive neurons are indicated (B inset, arrowhead). (**B''**) Quantification of OGN SEZ co-expression. (**C-C'**) OGNs in the PENP and quantification. (**D-D'**) *dVGlut>dsRed* neurons expressing Tdc2 in the ASMP and quantification. (**E-E'**) Neurons co-expressing OA and glutamate in the PSMP and quantification. Scale bar = 20 μm for panels B-E.

in abdominal neurons [53]. After detecting no reporter expression from a *Tβh-gal4* driver, dVGLUT cell body expression in OGNs was detected in brains from *tdc2-gal4;UAS-dsRed* adults (S4 Fig). In total, this analysis reveals that of the ~100 OA neurons in the *Drosophila* adult nervous system, about 70% express dVGLUT.

dVGLUT is not required for OA neuron identity

To reduce glutamate function solely in OGNs, a UAS-driven inverted repeat transgene targeting *dVGlut* (*UAS-dVGlut-RNAi*) was expressed under control of the *tdc2-gal4* driver (hereafter *tdc2>dVGlut-RNAi*) (Fig 2A and 2B). The effectiveness of this *UAS-dVGlut-RNAi* line has been verified at the transcript level through RT-qPCR ([12] and S5 Fig) and functionally as the frequency of miniature excitatory postsynaptic potentials (mEPSP) were reduced by this dVGlut RNAi in presynaptic glutamatergic larval motor neurons [12]. As the loss of VGLUT2 in vertebrate dopamine-glutamate dual transmitting neurons impairs survival and

54
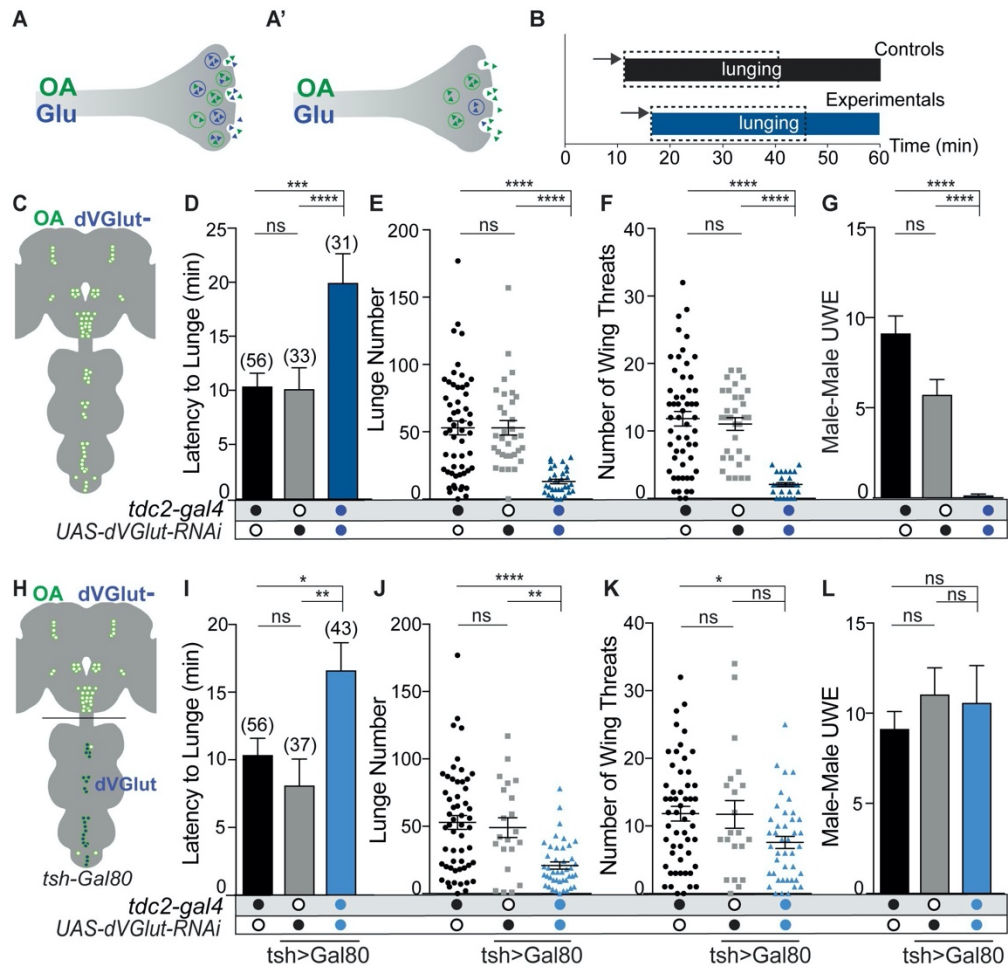
Fig 2. Male aggression requires dVGLUT function in OGNs. (A) dVGLUT reduction in OGNs through RNAi. **(B)** Behaviors for control and experimental male pairs were scored for thirty minutes beginning with the first lunge. **(C)** Schematic illustrating the brain and VNS OGNs. **(D)** Latency to lunge increased in *tdc2>dVGlut-RNAi* males (all statistical tests are Kruskal-Wallis with Dunn's multiple comparisons test, (*p<0.05, **p<0.01, ***p<0.001, ****p<0.0001). **(E)** *tdc2>dVGlut-RNAi* males displayed a decrease in the average number of lunges. **(F)** Wing threats were reduced in *tdc2-dVGlut-RNAi* males. **(G)** *tdc2-dVGlut-RNAi* males did not exhibit inter-male courtship (unilateral wing extensions = UWE). **(H)** Schematic illustrating the addition of *tsh>Gal80* limits dVGLUT reduction to brain OGNs. **(I)** Latency to lunge by *tdc2-gal4/tsh>Gal80;UAS-dVGlut-RNAi* males is significantly longer than controls. **(J)** Lunge number by *tdc2-gal4/tsh>Gal80;UAS-dVGlut-RNAi* males decreases as compared to controls. **(K)** Wing threat number was rescued to *UAS-dVGlut-RNAi* control levels. **(L)** Male-male UWE was rescued to control levels. N values for each genotype, panels D, I. Error bars denote s.e.m.

55

differentiation *in vitro* [49, 54], we examined OGNs in *tdc2>dsRed>dVGlut-RNAi* adults and did not observe obvious changes in OGN survival nor distribution (S5 Fig). In addition, OGN neurotransmitter differentiation was retained as *tdc2>dVGlut-RNAi>dsRed* neurons express Tdc2 (S5 Fig). Neurons labeled by this *tdc2-gal4* whether in the brain or VNS are all Tdc2+ (S6A and S6B Fig).

Reducing glutamate in OGNs decreases male aggression and inter-male courtship

We and others previously demonstrated OA is required for two distinct social male behaviors; the promotion of aggression, and the inhibition of intermale courtship [43, 46, 55, 56]. To address whether dVGLUT performs a related or separable role in these OA-dependent behaviors, we quantified changes in aggression and intermale courtship. Fights between pairs of *tdc2>dVGlut-RNAi* males, and transgenic controls were recorded and multiple agonistic parameters quantified including: latency to the first lunge, number of lunges, and number of agonistic wing threats (Fig 2A, [57, 58]). As behavioral patterns are scored for 30 minutes after the first lunge, each male pair has the same amount of time to exhibit aggressive events or inter-male courtship (Fig 2B).

Males with decreased dVGLUT in OGNs neurons exhibited a significant reduction in aggression as measured by lower numbers of lunges and wing threats, and an increase in the latency to initiate aggression (Fig 2D–2F). These aggression deficits are the same as in males that lack OA [43, 46, 47]. Importantly, the locomotor activity of *tdc2>dVGlut-RNAi* adults during the aggression assay did not differ from *dVGlut-RNAi* controls (S7A Fig).

Interactions between control male pairings within a fight can include low levels of intermale courtship as measured by unilateral wing extensions (UWE, the courtship song motor pattern). Males without OA exhibit high levels of inter-male courtship[43, 55, 56] and previously, we determined the function of three OA-FruM+ neurons is required to suppress intermale courtship [55]. If dVGLUT is only needed to enhance monoamine vesicular packaging and thus modulate OA function, we would expect males with reduced *dVGlut* levels to display the same behavioral deficits, i.e. high levels of inter-male courtship. However, *tdc2>dVGlut-RNAi* males did not exhibit inter-male courtship (Fig 2G). These results suggest; 1) dVGLUT is required in OGNs to promote aggression, and 2) dVGLUT is not required to suppress inter-male courtship.

Aggression requires dVGLUT function in OA-GLU brain neurons

In the adult, motor neurons innervating leg and wing muscles express glutamate [59]. Therefore, the observed behavioral deficits in *tdc2>dVGlut-RNAi* males may reflect impairments at the neuromuscular junction. To address this possibility, we spatially restricted expression of the dVGlut-RNAi transgene to the brain using the *teashirt-lexA 8xlexAop2-IVS-Gal80* (hereafter *tsh>Gal80)* transgenic combination (Fig 2H). The *tsh>Gal80* transgenic combination was effective at blocking Gal4-mediated transcription in the entire VNS including in OGNs that innervate muscles required for courtship and wing threat behaviors (S8 Fig).

With dVGlut function maintained in motor neurons, it was possible all aggressive behaviors would return to control levels. However, latency to initiate aggression remained longer in males with reduced dVGLUT in brain OGNs (*tdc2>tsh>Gal80>dVGlut-RNAi*) and lunge number remained lower when compared to controls (Fig 2I and 2J). Wing threat numbers were at levels lower than one control (Fig 2K) which likely reflects the incompleteness of dVGlut RNAi interference. In contrast, providing dVGLUT function in OGN VNS neurons restored intermale courtship to control levels (Fig 2L). Although total behavioral events by

56
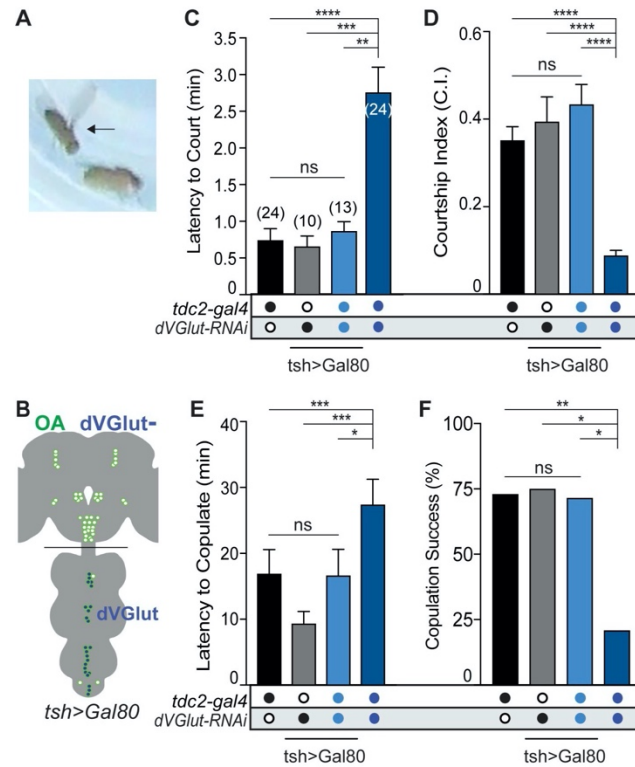
Fig 3. dVGLUT function is required in VNS OGNs for male-female courtship. (A) Male (arrow) to female courtship. **(B)** Schematic illustrating the addition of *tsh>Gal80* limits dVGLUT reduction to brain OGNs. **(C-F)** All parameters of male to female courtship were rescued by restoring glutamate function to OGNs within the VNC. **(C)** The latency to initiate courtship towards a female returned to control levels in males with reduced dVGLUT in brain OGNs. **(D)** The courtship index was restored to control levels in *tdc2-gal4/tsh>Gal80;dVGlut-RNAi* males. **(E)** *tdc2-gal4/tsh>Gal80;dVGlut-RNAi* males exhibited the same latency to copulation as controls. **(F)** The copulation success of males with a dVGLUT reduction in brain OGNs was not significantly different from controls. N values for each genotype located on panel A. All statistical tests are Kruskal-Wallis with Dunn's multiple comparisons test, (*p<0.05, **p<0.01, ***p<0.001, ****p<0.0001.

experimental males (lunges, wing threats, intermale courtship) per minute decreased, overall activity did not (S7 Fig) nor did male-female courtship (Fig 3). These results indicating GLU transport in brain OGNs is required to initiate aggression and for the lunge pattern itself may reflect deficits in the detection of male pheromones as we previously described for OA [43]. Specifically, the suppression of intermale courtship requires the function of three OA-FruM + neurons located in the brain [55] and, aggression requires pheromonal information from Gr32a-expressing chemosensory neurons located in the mouth to OA SEZ neurons [43].

Finally, males with reduced dVGLUT in brain OGNs (*tdc2>tsh>Gal80>dVGlut-RNAi*) performed all measured male-female courtship parameters including latency to court, courtship index, latency to copulation and copulation success at levels indistinguishable from controls (Fig 3). Together, these results indicate dVGlut in OGNs is required in males both for aggression and courtship toward a female and at the behavioral level, the functional requirement for dVGLUT in OGN motor neurons vs. central brain neurons is spatially separable.

Removal of glutamate in OGNs using the *B3RT-vGlut* conditional allele

The experiments above used two different approaches to reduce neurotransmitter levels, but not eliminate dVGLUT. To completely remove glutamate transporter function in OGNs, a conditional allele of *dVGlut*, *B3RT-dVGlut-LexA* (hereafter *B3RT-dVGlut*), was developed via genome editing. Genome edits to the *dVGlut* locus included flanking the dVGlut coding exons with B3 recombination target sites (B3RTs) [60] in the same orientation and inserting the coding sequences of the LexA transcription factor immediately downstream of the 3' B3RT (Fig 4A). With *B3RT-dVGlut*, glutamate function can be temporally and spatially controlled using Gal4 drivers of interest to express the B3 recombinase that in turn catalyzes the *in vivo* excision of DNA between the B3RTs (Fig 4B). Two outcomes result after B3 recombinase-mediated excision; 1) a *dVGlut* null allele is generated solely in the neurons of interest, and 2) a *dVGlut-LexA* driver is created that allows visualization of glutamatergic neurons when a LexAop reporter is present.

To assess the functionality of *dVGlut* within the *B3RT-dVGlut* chromosome pre- and post-excision, the *B3RT-dVGlut* chromosome was crossed with the null allele, *dVGlut^{SS1}* (S1 Fig). In the absence of a Gal4 driver, *vGlut^{SS1}/B3RT-vGlut* progeny are fully viable and no LexAop-driven reporter gene expression is detected (Fig 4C). In contrast, when B3 recombinase (*UAS-B3*) is expressed in the nervous system by the pan-neuronal driver, *n-syb-Gal4*, dVGLUT expression is eliminated and *vGlut^{SS1}/B3RT-dVGlut;UAS-B3/n-syb-Gal4* progeny are inviable (data not shown). These results establish that the *B3RT-dVGlut* genome edits preserve dVGLUT function prior to excision, but after excision, as expected with removal of the entire dVGLUT protein-coding sequence, a *dVGlut* null allele is generated.

To verify the functionality of the *B3RT-dVGlut* chromosome in Tdc2+ neurons, we crossed *tdc2-gal4* with *B3RT-dVGlut;UAS-B3*. Following B3-mediated excision in Tdc2+ neurons, the resulting *dVGlut-lexA* driver is active in OGNs demonstrating the *dVGlut* coding region was removed. The excision of dVGlut and substitution with LexA in the adult nervous system was confirmed by co-localization of nuclear markers (Fig 4D and 4D'). This result provides additional confirmation the majority of Tdc2+ neurons are glutamatergic. In addition, nuclear reporters were used to confirm the loss of dVGLUT does not obviously alter OGN differentiation (S9 Fig).

To completely remove dVGLUT function, we used the *dVGlut^{SS1}* null allele in combination with the *B3RT-dVGlut* conditional null allele. Due to the requirements for GLU in OA-GLU motor neurons, we crossed the *tsh>Gal80* transgenes onto the *B3RT-dVGlut* chromosome. Males with homozygous null *dVGlut* mutations in brain OGNs were generated by driving B3 recombinase with *tdc2-gal4* (*dVGlut^{SS1}/B3RT-dVGlut tsh>Gal80;UAS-B3/tdc2-gal4*). As expected, the complete loss of GLU in brain OGNs reduced male aggression. Specifically, the latency to initiate aggression increased, and lunge numbers decreased (Fig 4E and 4F). Not unexpectedly, the complete elimination of dVGLUT function resulted in aggression deficits significantly worse when compared to the RNAi approach (Fig 4I) including now a reduction in wing threat number (Fig 4G) which demonstrates an advantage in using the conditional null *B3RT-dVGlut* allele. Finally, and significantly, the number of inter-male wing extensions

58
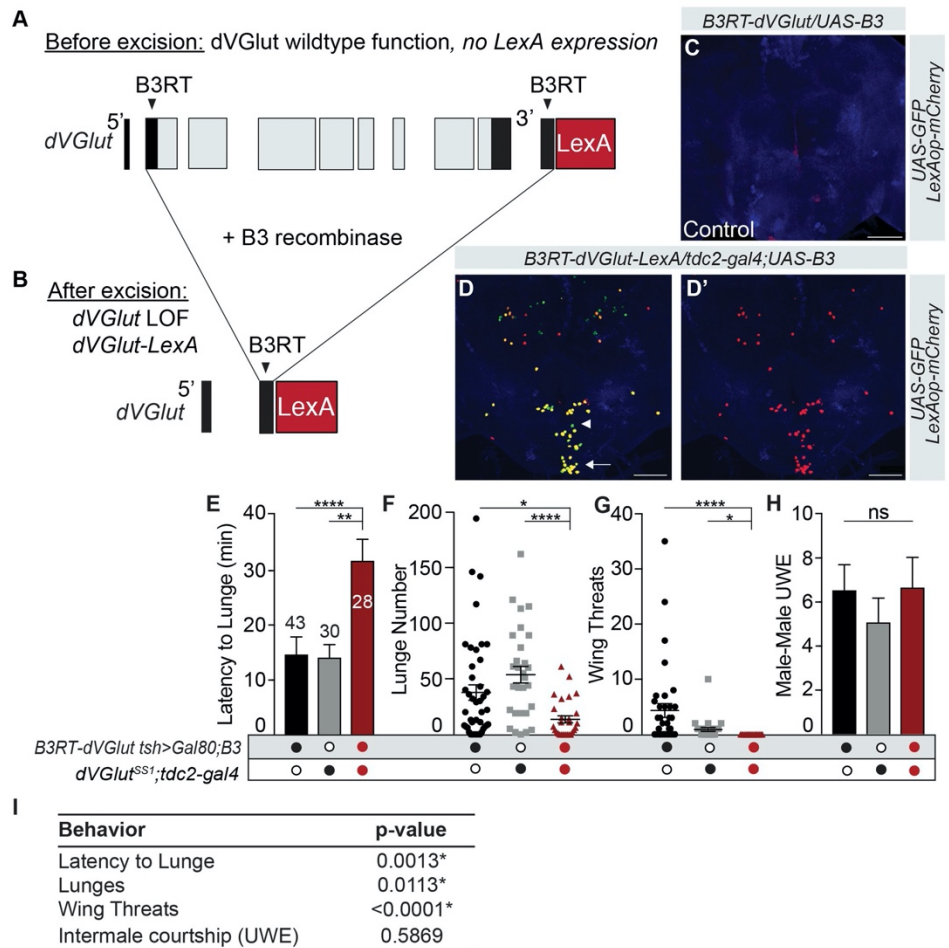
Fig 4. B3-mediated elimination of dVGLUT in OGNs reduces male aggression. (A,B) Schematic of the *B3RT-dVGlut-LexA* conditional allele. B3RTs flank dVGlut coding exons (A) and excise the entire dVGlut coding sequence in a specific subset of neurons upon expression of the B3 recombinase (B). After excision, a *dVGlut* null loss-of-function allele and *dVGlut-LexA* driver is created (B). (C) Control brain demonstrating without a source of Gal4-driven B3 recombinase, excision and therefore LexA expression does not occur. (D-D') *tdc2-gal4* driven B3 recombinase-mediated excision effectively removes *dVGlut* resulting in *B3RT-LexA*-driven mCherry expression is in the majority of OA neurons (yellow). As expected, a few Tdc2+ neurons do not express dVGLUT (arrowhead, green). LexAop reporter expression that does not also show UAS expression may be observed as a result of excisions that occurred during development in former Tdc2+ neurons. (E) Latency to lunge increased in males lacking dVGLUT function (*B3RT-dVGlut tsh>Gal80/dVGlut^SS1; UAS-B3*) in OGNs. (F) Males without dVGLUT function lunged significantly less when compared to controls. (G) Wing threat number decreased in experimental males. (H) No significant differences in male-male courtship. (I) Aggression is significantly reduced by the complete loss of dVGLUT in OGNs as compared to the RNAi-based dVGLUT reduction. All statistical tests are Kruskal-Wallis with Dunn's multiple comparisons test, (*p<0.05, **p<0.01, ***p<0.001, ****p<0.0001. Error bars denote s.e.m. N values for each genotype, panel E.

59

did not differ from controls (Fig 4H) nor from males with a reduction of *dVGlut* in brain OGNs (Fig 2K). In summation, the *dVGlut^{SS1}/B3RT-dVGlut* null combination elegantly and independently validates the aggression phenotypes based on *dVGlut* RNAi-based reduction, demonstrates the applicability of a powerful new conditional genetic tool, and confirms that dVGLUT function in OGNs is not required to regulate intermale courtship.

Reducing GLU by EAAT1 overexpression recapitulates the decrease in aggression

At this point, GLU function within OGNs has been altered by reducing glutamate transport into synaptic vesicles. Whether the aggression phenotypes of OGN dVGLUT mutant males are due to deficits in the concentration of GLU into synaptic vesicles, the packaging of OA, or a reduction of released GLU is not clear. After release, glutamate is rapidly removed from synapses by excitatory amino acid transporters (EAATs) [61, 62]. Therefore, to reduce GLU signaling after release, we increased expression of the only high-affinity glutamate transporter in *Drosophila*, EAAT1 (Fig 5A) [63, 64].

EAAT1 is expressed in glia throughout the nervous system [64]. By examining 2–10 individual EAAT1-GFP clones in ~40 brains, we determined OGN neuronal cell bodies and arborizations are consistently enmeshed by EAAT1-expressing glia (Fig 5B and 5C). To reduce
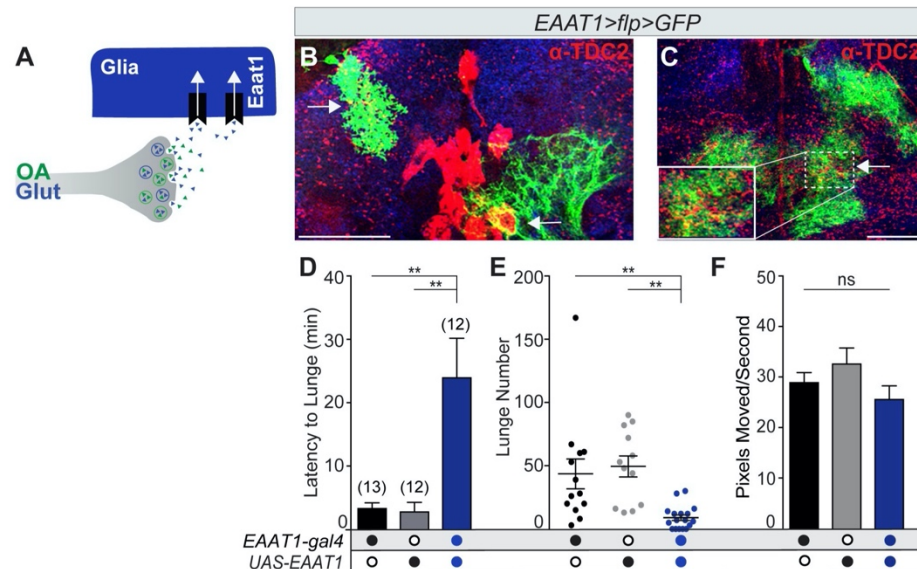
Fig 5. Reducing glutamate function through EAAT1 overexpression decreases male aggression. (A) Glutamate function was reduced by increasing EAAT1 expression in EAAT1-expressing glia. (B, C) GFP-expressing EAAT1 glia (*hs-flp; EAAT1-gal4/UAS>stop>CD8:GFP*) enwrap Tdc2+ neuron cell bodies (arrowhead) and endings (arrow). Higher magnification of dashed box in C. Scale bar = 30 um. (D) The latency to lunge by *EAAT1>Eaat1* males was increased as compared to controls. (E) A decrease in lunge number was exhibited by *EAAT1>Eaat1* males as compared to controls. (F) Locomotor activity during the aggression assay did not differ. All statistical tests are Kruskal-Wallis with Dunn's multiple comparisons tests. N values for each genotype are in panel D.

https://doi.org/10.1371/journal.pgen.1008609.g005

60

glutamate signaling after release, EAAT1 expression was increased via a transgene (*EAAT1-gal4;UAS-EAAT1*). While a loss of EAAT1 impairs larval movement [65], overexpression of EAAT1 has been used in adult long-term memory formation assays which requires locomotion [66]. Similar to the dVGLUT loss-of-function results above, the aggressive behavior of males with reduced GLU signaling by EAAT1 overexpression (*EAAT1-gal4;UAS-EAAT1*) was altered in two parameters: the latency to initiate lunging increased and lunge number decreased (Fig 5D and 5E). Locomotor activity during the aggression assay did not differ (Fig 5F). Although future experiments will be needed to determine if the promotion of aggression requires dVGLUT packaging of OA in synaptic vesicles and OGN glutamate signaling to downstream targets, results from this section support the hypothesis that OGN-mediated aggression requires GLU.

OA and Glu signal to a shared aggression-promoting circuit

If Glu and OA convey signals to separable aggression-promoting circuits, a loss of both neurotransmitters would reduce aggression greater than the loss of either alone (Fig 6A). If, however, Glu and OA signal to a shared circuit or circuits that converge, a loss of both transmitters would reduce aggression to the same levels as the loss of one alone. To address this question,
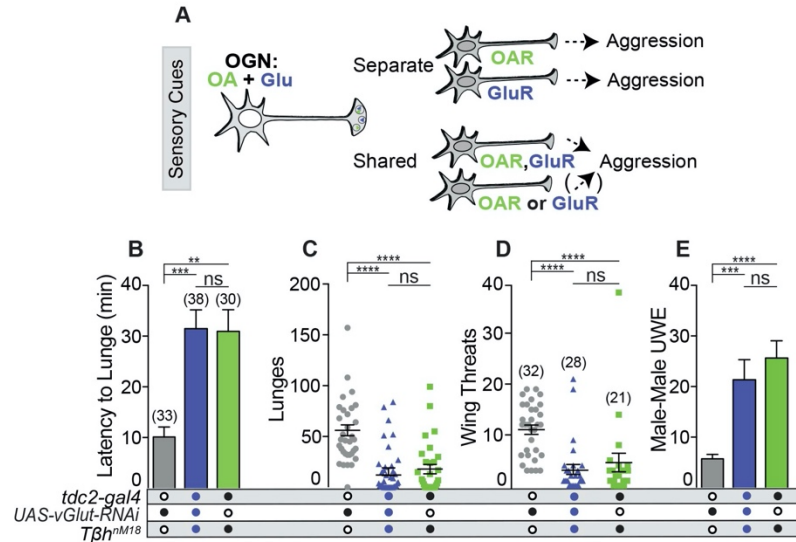
Fig 6. OA and Glu signal to a shared aggression-promoting circuit. (A) OGNs could signal to separate aggression-promoting circuits (resulting in aggression deficits greater than the single mutant) or to a shared or converged circuit. **(B-E)** dVGlut was reduced in OGNs of *TβhM18* males (*TβhM18;tdc2>dVGlut-RNAi*). **(B)** Latency to lunge increased in *TβhM18;tdc2>dVGlut-RNAi* males compared to the transgenic control but not *TβhM18* males. **(C)** Lunge number by males with reduced dVGLUT and lacking OA was not significantly different than *TβhM18* males. **(D)** *TβhM18;tdc2>dVGlut-RNAi* males displayed lower wing threat numbers compared to the transgenic control but not *TβhM18* males. **(E)** Males with reduced dVGLUT and lacking OA (blue column) displayed an increase in inter-male courtship at levels higher than the control but not significantly different from *TβhM18* mutants (green column). All statistical tests are Kruskal-Wallis with Dunn's multiple comparisons test, (*p<0.05, **p<0.01, ***p<0.001, ****p<0.0001. Error bars denote s.e.m.

61

we incorporated the previously described null allele $T\beta h^{nM18}$ [67] and generated $T\beta h^{nM18}$; $tdc2>dVGlut-RNAi$ males. Additive deficits did not occur when males without OA and dVGLUT in OGNs were compared to males lacking only OA (Fig 6B–6D) indicating that both signals, at least partially, converge onto a shared aggression-promoting pathway.

$T\beta h^{nM18}$;$tdc2>vGlut-RNAi$ males displayed levels of male-male courtship that are not significantly different from $T\beta h^{nM18}$ males (blue column, Fig 6E). This result further supports previously published data that OA is required to suppress intermale courtship [43, 55, 56]. Here, increased levels of inter-male courtship due to the absence of OA supersedes or relieves the lack of UWE due to a reduction in dVGlut function (Fig 2). At this point, it is possible the UWE phenotype occurs via OA-modulated circuitry that involves other neurotransmitters [56] or the actions of OA occur at spatially distinct locations.

Spatial segregation of VMAT and dVGLUT within OGN

To compare localization of the two transporters within OGNs, we generated a conditionally expressible epitope-tagged version of VMAT, $RSRT>STOP>RSRT-6XV5-VMAT$, via genome editing. $RSRT>STOP>RSRT-6XV5-VMAT$ has two insertions: 1) a STOP cassette between VMAT coding exons 5 and 6 and, 2) six in-frame tandem copies of a V5 epitope tag within exon 8 which is common to both VMAT-A and VMAT-B isoforms (Fig 7A). The effectiveness of the STOP cassette is confirmed by the lack of V5 expression prior to STOP cassette excision by Gal4-driven R recombinase (S11 Fig) and the effectiveness of the epitope multimerization strategy has also been determined [68]. The conditionality of the $RSRT>STOP>RSRT-6XV5-VMAT$ allele permits visualization of VMAT in subsets of neurons at expression levels driven by the endogenous promoter.

To focus on transporter distribution within OGNs, we expressed $RSRT>STOP>RSRT-6XV5-VMAT$ under control of the split Gal4 combination of $tdc2-Gal4-AD$ and $dVGlut-Gal4-DBD$ ($tdc2-dVGlut-gal4$) which drives expression in OGNs (Fig 7B, S6C–S6F Fig). V5-VMAT was visualized in $tdc2-dVGlut-gal4$; $V5-VMAT UAS-R$ by an antibody to V5 and dVGLUT using mAb dVGLUT (S10 Fig). Fig 7C illustrates that as expected, a large fraction of the V5-VMAT puncta in the AL or SEZ (S11 Fig) either co-localize with dVGLUT or are in close proximity (arrowheads). High resolution images in Fig 7D and 7H, however, reveal V5-VMAT puncta without dVGLUT (arrows). As OA can be found in SVs as well as LDCVs [69, 70], we incorporated a synaptic marker ($UAS-Synaptotagmin$ (Syt):HA) and re-examined V5-VMAT and dVGLUT expression in the AL and SEZ (Fig 7F, S11D Fig). We found V5-VMAT puncta that either co-localize or are in close proximity to Syt:HA and dVGLUT (Fig 7F–7J, S11D–S11H Fig). While the behavioral significance of potential OA synaptic release on aggression circuitry remains to be determined, previous work has demonstrated amine-dependent behaviors can be altered by shifting the balance of OA release from SVs to LDCVs [70]. In addition, as mentioned above, we have previously shown that three OA-FruM^{+} neurons are required to suppress intermale courtship and recent work has identified a small subset of OA receptor OAMB-expressing neurons that when silenced, decrease aggression and increase intermale courtship [56]. The SEZ areas of V5-VMAT and dVGLUT puncta highlighted in Figs 7 and 8 are consistent with projections made by OA-FruM^{+} neurons which are also OGNs (S12 Fig) raising the possibility of distinct OA and GLU inputs to key downstream targets.

Due to the large number of $tdc2-dVGlut-gal4$ neurons, we repeated the experiment using the OA-specific $MB113C-split-gal4$ to drive V5-VMAT in ~2 OGNs (Fig 8A and 8B) [71]. Fig 8C illustrates that as expected, many V5-VMAT puncta in the SEZ either co-localize with dVGLUT or are in close proximity (arrowheads). High resolution images in Fig 8D and 8H,

62
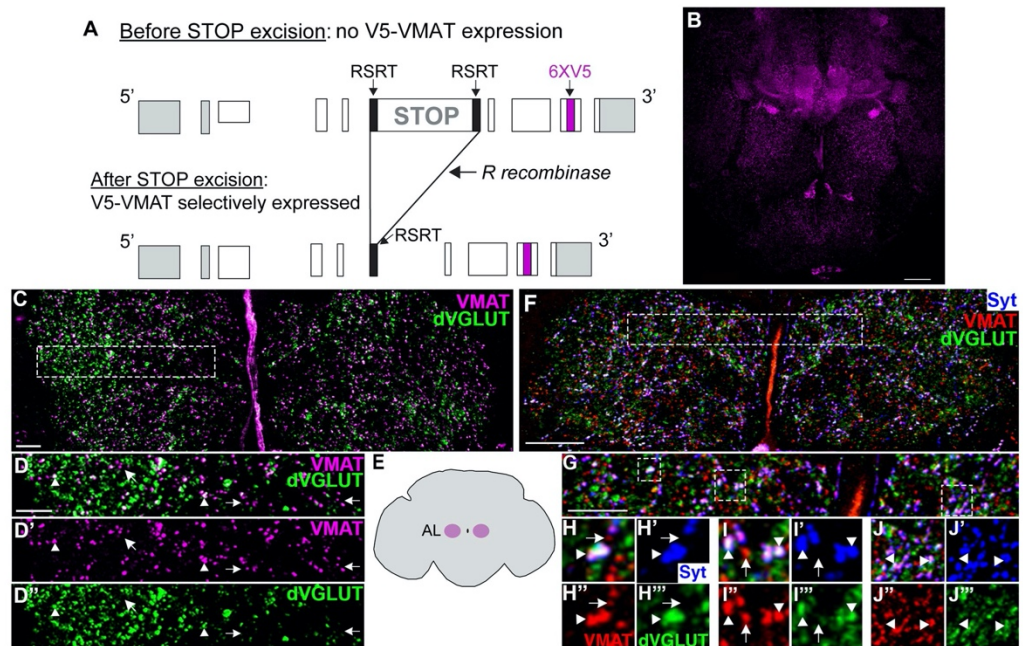
Fig 7. Spatial segregation of VMAT and dVGLUT within OGNs. (A) Schematic of the *RSRT>STOP>RSRT-6XV5-VMAT* conditional allele. RSRTs flank a STOP cassette inserted between VMAT coding exon 5 and 6. Upon Gal4-driven expression of the R recombinase enzyme, the STOP cassette is excised and V5-tagged VMAT expression under control of the endogenous promoter is expressed. **(B)** Representative brain showing V5-VMAT expression in OGNs after excision by *tdc2-dVGlut-gal4* driven R recombinase. The brain is labeled with anti-V5 (magenta) and mAb dVGLUT (green in panels C,D). Scale bar is 30 μm. **(C)** Higher magnification of the antennal lobe region showing dVGLUT expression (green) with V5-VMAT (magenta). Scale bar is 10 μm. **(D)** The region in the dashed box in C showing puncta with dVGLUT and V5-VMAT colocalization (arrowheads) and puncta with only V5-VMAT (arrows). **(E)** Schematic showing the regions of the brain that are depicted in C and F. **(F)** Antennal lobe region of a representative brain with a synaptic marker incorporated (*UAS-synaptotagmin;HA, tdc2-dVGlut split gal4/UAS-R RSRT-STOP-RSRT-6XV5-vMAT*). The brain is labeled with anti-HA (blue), anti-V5 (magenta), and mAb dVGLUT (green). Scale bar is 20 μm. **(G-J''')** Higher magnification of the SEZ region of the AL in F showing dVGLUT expression (green), V5-VMAT (red), and Syt:HA (blue). Arrowheads indicate puncta with dVGLUT, V5-VMAT and Syt:HA and arrows indicate puncta with only V5-VMAT and Syt:HA. The stack for panels C and D contains two optical sections at 0.45 μm. Stacks for panels G-J contain 7 optical sections at 0.5 μm.

https://doi.org/10.1371/journal.pgen.1008609.g007

however, indicate small, but distinct regions that contain V5-VMAT puncta without dVGLUT (arrows). Within the areas of dVGLUT and V5-VMAT possible colocalization, this level of analysis does not indicate whether the two transporters segregate into adjacent but distinct puncta, nor are questions of transporter colocalization on the same vesicles addressed. Nevertheless, our results demonstrate that within OGNs, V5-VMAT and dVGLUT puncta can differ in localization suggesting the aggression vs. intermale courtship phenotype differences may be due to spatial differences in signaling by glutamate and octopamine.

Discussion

Addressing the functional complexities of "one neuron, multiple transmitters" is critical to understanding how neuron communication, circuit computation, and behavior can be

63
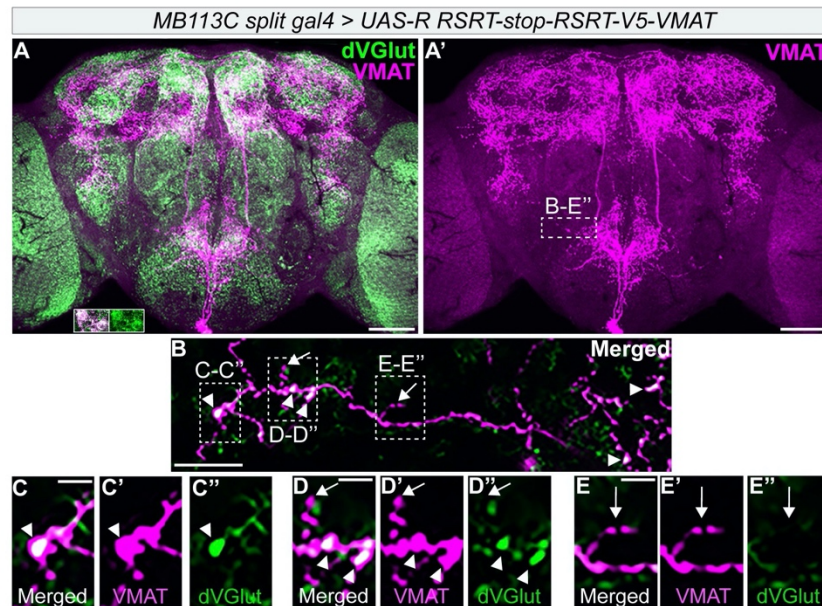
Fig 8. Spatial segregation of VMAT and dVGLUT within two OGNs. (A-A') Representative brain showing V5-VMAT expression in two OGNs after excision by *MB113C-split-gal4* driven R recombinase. The brain is labeled with anti-V5 (magenta) and mAb dVGLUT (green). Scale bar is 50 μm. The inlet in A which is from a separate brain demonstrates this OA neuron driver also expresses dVGLUT (green). **(B-E)** Higher magnification of the SEZ boxed region in A'. Arrowheads point to puncta with V5-VMAT and dVGLUT, arrows indicate V5-VMAT only puncta. Scale bar is 10 μm. **(C-E)** The regions in the dashed boxes in B showing puncta with dVGLUT and V5-VMAT colocalization (arrowheads) and puncta with only V5-VMAT (arrows). Panels B-E contain stacks of four optical sections at 0.45 μm. Scale bar for panels C-E is 5 μm.

regulated by a single neuron. Over many decades, significant progress has been made elucidating the functional properties of neurons co-expressing neuropeptides and small molecule neurotransmitters, where the neuropeptide acts as a co-transmitter and modulates the action of the neurotransmitter [5, 6, 72]. Only recently have studies begun to examine the functional significance of co-transmission by a fast-acting neurotransmitter and a slow-acting monoamine.

In this study, we demonstrated that OA neurons express dVGLUT and utilized a new genetic tool to remove dVGLUT in OA-glutamate neurons. Quantifying changes in the complex social behaviors of aggression and courtship revealed that dVGLUT in brain OGNs is required to promote aggressive behavior and a specific behavioral pattern, the lunge. In contrast, males deficient for dVGLUT function do not exhibit an increase in inter-male courtship. These results establish a previously undetermined role for dVGLUT in OA neurons located in the adult brain and reveal glutamate uncouples aggression from inter-male courtship. It has been suggested that classical neurotransmitters and monoamines present in the same neuron modulate each other's packaging into synaptic vesicles or after release via autoreceptors [9, 49, 73–75]. For example, a reduction of dVGLUT in DA-glutamate neurons resulted in decreased AMPH-stimulated hyperlocomotion in *Drosophila* and mice suggesting a key function of

64

dVGLUT is the mediation of vesicular DA content [12, 49, 76]. In this study, the independent behavioral changes suggests enhancing the packaging of OA into vesicles is not the sole function of dVGLUT co-expression and suggests differences in signaling by OA from OGNs on courtship-related circuitry.

Co-transmission can generate distinct circuit-level effects via multiple mechanisms. One mechanism includes spatial segregation; the release of two neurotransmitters or a neurotransmitter and monoamine from a single neuron occurring at different axon terminals or presynaptic zones. Recent studies examining this possible mechanism have described; (i) the release of GLU and DA from different synaptic vesicles in midbrain dopamine neurons[15, 77] and (ii) the presence of VMAT and VGLUT microdomains in a subset of rodent mesoaccumbens DA neurons[78]. In this study, we expressed a new conditionally expressed epitope-tagged version of VMAT in OGNs and visualized endogenous dVGLUT via antibody labeling. Within OGNs, the colocalization of VMAT and dVGLUT puncta was not complete suggesting the observed behavioral phenotype differences may be due to spatial differences in OA signaling.

A second mechanism by which co-transmission may generate unique functional properties relies on activating distinct postsynaptic receptors. In *Drosophila*, recent work has identified a small population of male-specific neurons that express the alpha-like adrenergic receptor, OAMB, as aggression-promoting circuit-level neuronal targets of OA modulation independent of any effect on arousal[56] and separately knockdown of the *Rdl* GABAa receptor in a specific *doublesex*+ population stimulated male aggression [79]. Future experiments identifying downstream targets that express both glutamate and octopamine receptors would be informative, as well as using additional split-Gal4 lines to determine if segregation of transporters is a hallmark of the majority of OGNs. Finally, a third possible mechanism is Glu may be co-released from OGNs and act on autoreceptors to regulate presynaptic OA release (reviewed in [75]).

Deciphering the signaling complexity that allows neural networks to integrate external stimuli with internal states to generate context-appropriate social behavior is a challenging endeavor. Neuromodulators including monoamines are released to signal changes in an animal's environment and positively or negatively reinforce network output. In invertebrates, a role for OA in responding to external chemosensory cues as well as promoting aggression has been well-established [43, 47, 56, 80–83]. In terms of identifying specific aggression circuit-components that utilize OA, previous results determined OA neurons directly receive male-specific pheromone information [43] and the aSP2 neurons serve as a hub through which OA can bias output from a multi-functional social behavior network towards aggression[56]. The ability of OA to bias behavioral decisions based on positive and negative reinforcement was also recently described for food odors [84]. In vertebrates, it has been proposed that DA-GLU cotransmission in the NAc medial shell might facilitate behavioral switching [85]. Our finding that the majority of OA neurons are glutamatergic, suggests that the complex social behavior of aggression may rely on small subsets of neurons that both signal the rapid temporal coding of critical external stimuli as well as the frequency coding of such stimuli resulting in the enhancement of this behavioral network. One implication of our finding regarding the separable OA-dependent inhibition of inter-male courtship is the possibility of identifying specific synapses or axon terminals that when activated gate two different behavioral outcomes. A second implication is that aggressive behavior in other systems may be modified by targeting GLU function in monoamine neurons.

Finally, monoamine-expressing neurons play key roles in human behavior including aggression and illnesses that have an aggressive component such as depression, addiction, anxiety, and Alzheimer's [86, 87]. While progress is being made in addressing the functional complexities of dual transmission, the possible pathological implications of glutamate co-release by

65

monoamine neurons remains virtually unknown. Analyzing the synaptic vesicle and release properties of monoamine-glutamate neurons could offer new possibilities for therapeutic interventions aimed at controlling out-of-context aggression.

Methods

Drosophila husbandry and stocks

All flies were reared on standard cornmeal-based fly food. Unless noted otherwise, during developmental and post-eclosion, flies were raised at 25°C, ~50% humidity and a 12:12hr light-dark cycle (1400±200 lx white fluorescent light) in humidity and temperature-controlled incubators. A list of stocks can be found in S1 Data.

Aggression assays

Male pupae were isolated and aged individually in 16 x 100mm borosilicate glass tubes containing 1.5ml of standard food medium as previously described [88]. A dab of white or blue acrylic paint was applied to the thorax of two-day old males under CO_2 anesthesia for identification purposes. Flies were returned to their respective isolation tubes for a period of at least 24 hours to allow recovery. For aggression testing, pairs of 3–5 day old, socially naïve adult males were placed in 12-well polystyrene plates (VWR #82050–930) as described previously [43]. All assays were run at 25°C and ~45–50% humidity levels.

Scoring and statistics

All aggression was assayed within first two hours of lights ON time (Zeitgeber hours 0–2) and scored manually using iMovie version 8.0.6. Total number of lunges, wing threats, and unilateral wing extensions were scored for a period of 30 minutes after the first lunge according to the criteria established previously [43, 88]. The time between the aspiration of the flies into the chamber and the first lunge was used for calculating the latency to lunge. Male-male courtship was the number of unilateral wing extensions (singing) followed by abdomen bends or repeated wing extensions. All graphs were generated with Graphpad Prism and Adobe Illustrator CS6. For data that did not meet parametric assumptions, Kruskal-Wallis Test with Dunn's multiple comparison was used unless otherwise specified. A standard unpaired t-test was performed in the case of only two comparisons and a modified chi-square test to compare copulation success.

Activity levels

Activity levels were measured by tracking the flies in each assay using the OpenCV module in the Python programming language to analyze the video and then output XY-coordinate and distance data. The distance traveled was calculated for each fly by determining the starting location followed by the second location after a 250-ms time interval and then taking the sum of the distance traveled in each interval. To calculate pixels moved per second, the distance data was divided by the total time spent tracking.

Immunohistochemistry

Adult male dissected brains were fixed in 4% paraformaldehyde (Electron Microscopy Sciences) for 25 minutes and labeled using a modification of protocols previously described [55]. The following primary antibodies were used: anti-bruchpilot (mAb nc82, 1:30, Developmental Studies Hybridoma Bank developed under the auspices of the NICHD and maintained by the Department of Biology, University of Iowa (Iowa City, IA).), monoclonal rabbit anti-GFP

66

(1:200, Molecular Probes), rat anti-HA 3F10 (1:100, Roche), mAb dVGLUT (1:15), anti-TβH (1:400, [89]), rat anti-V5 (1:200, Biorbyt), and rabbit anti-TDC2 (1:100, Covalab). Secondary antibodies conjugated to Alexa 488, Alexa 594, or Alexa 647 (Molecular Probes) were used at a concentration of 1:200. Labeled brains were mounted in Vectashield (Vector Labs, #H1000). Images were collected on an Olympus Fluoview FV1000 laser scanning confocal mounted on an inverted IX81 microscope and processed using ImageJ (NIH) and Adobe Photoshop (Adobe, CA).

qPCR

Total RNA from ~40 heads using Direct-zol RNA Miniprep Pluskit (Zymo Research)and treated with DNase I per the manufacturer's protocol. RNA concentrations were measured with a ND-1000 nanodrop spectrometer. Reverse transcription was accomplished using iScript cDNA Synthesis kit (Bio-Rad Laboratories). RT-PCR was performed using 300 ng cDNA added to iTaq Universal SYBR Green Supermix (Bio-Rad Laboratories) and primers in a 20 μL reaction volume. All samples were run in triplicate using a Stratagene Mx3005P qPCR System (Agilent Technologies). Expression of *ribosomal protein 49* (*Rp49*) was used as the reference control to normalize expression between genotypes. Expression levels were determined using the ΔΔCT method and results from control (*UAS-dVGlut-RNAi/+*) and experimental (*nsyb-Gal4/UAS-dVGlut-RNAi*) groups were normalized relative to a transgenic control (*nsyb-Gal4/+*). The following primers were used: Rp49 Forward: 50-CATCCGCCCAGCATACAG-3' Rp49 Reverse: 5'-CCATTTGTGCGACAGCTTAG-3' dVGlut Forward: 5'-GCACGGTCAT GTGGTGATTTG-3' dVGlut Reverse: 5'-CCAGAAACGCCAGATACCATGG-3'. Primer designs for all Rp49 and dVGlut primers used have been described previously [12].

Construction of *20XUAS-His2A-GFP*, *13XLexAop2-His2B-mCherry* and *20XUAS-R*

The *20XUAS-His2A-GFP*, *13XLexAop2-His2B-mCherry*, and *20XUAS-R* expression clones were assembled using Gateway MultiSite LR reactions as previously described[90] and as indicated in S2 Table. The *L1-20XUAS-DSCP-L4* and *L1-13XLexAop2-DSCP-L4* entry clones contain 20 copies of UAS and 13 copies of LexAop2 upstream of the *Drosophila* synthetic core promoter (DSCP) [91], respectively. The *R4-His2A-R3* and *R4-His2B-R3* entry clones were generated as previously described [90] using genomic DNA as templates. The *L3-GFP-L2* entry clone was generated from template *pJFRC165*[60] except the PEST sequence is omitted. The *L3-GFP-L2* and *L3-mCherry-HA-L2* entry clones were previously described [92]. The *L1-20XUAS-DSCP-R5* entry clone was previously described [90]. The *pDESTp10aw* destination vector was previously described[93]. Injections were performed by Bestgene, Inc.

Construction of *UAS-B3*

B3 recombinase derived from pJFRC157 [60] was PCR amplified using primers designed to add the syn21 translational enhancer sequence [94] and remove the PEST domain. The verified PCR product was cloned into pENTR (Invtrogen) and subsequently transferred to pBID20xUAS, a derivative of the pBID vector [95] with 20 copies of the UAS binding sequence. Injection of *UAS-B3* was performed by Genetivision into landing site VK31.

Generation of *B3RT-vGlut*

The *B3RT-dVGlut-LexA* chromosome was generated via CRISPR/Cas9 genome editing. Both guide RNAs were incorporated into pCFD4 using previously described methods [96] to

67

produce the double guide RNA plasmid *pCFD4-vGlut1*. The donor plasmid *B3RT-dVGlut-LexA* used the *pHSG298* backbone (Takara Bio) and was generated using NEBuilder HiFi (New England Biolabs). The complete annotated sequence of *B3RT-dVGlut-LexA* is shown in Supplementary Information. *pCFD4-vGlut1/B3RT-dVGlut-LexA* injections were performed by Bestgene, Inc.

To assess the functionality of *dVGlut* on the *B3RT-dVGlut* chromosome pre- and post-excision, the *B3RT-dVGlut* chromosome was crossed with the homozygous lethal *dVGlut* null allele, *dVGlut^{SS1}* in the presence and absence of the pan-neuronal driver *n-syb-Gal4*. In the absence of a Gal4 driver, *dVGlut^{SS1}/B3RT-dVGlut* progeny are fully viable and no LexAop-driven reporter gene expression is detected (Fig 2). When B3 recombinase (*UAS-B3*) is expressed in the nervous system by *n-syb-Gal4*, *dVGlut^{SS1}/B3RT-dVGlut;UAS-B3/n-syb-Gal4* progeny are inviable, therefore after excision, as expected with removal of the entire dVGlut protein-coding sequence, a *dVGlut* null allele results.

Generation of *dVGlut^{SS1}*

The *dVGlut^{SS1}* allele was generated by CRISPR/Cas9 genome editing with the same guide RNAs used to generate *B3RT-dVGlut LexA*. *dVGlut^{SS1}* was identified based on failed complementation with the existing *dVGlut^2* allele[97]. Sequencing of PCR products from this allele indicated a deletion of 2442bp that includes dVGlut amino acids 53–523. Genomic DNA sequence at the breakpoints of the *dVGlut^{SS1}* allele are indicated with the deleted region in bold: GGACCAGGCG**GCGGCCACGC**......**AACCTCCGGC**CGAGGAGCAA.

Generation of the *RSRT-STOP-RSRT-6XV5-vMAT* chromosome

RSRT-STOP-RSRT-6XV5-vMAT was generated via CRISPR/Cas9 genome editing. Both upstream guide RNAs were incorporated into pCFD4-vMAT1 and both downstream guide RNAs were incorporated into pCFD4-vMAT2 as previously described [96]. The *RSRT-STOP-RSRT-6XV5-vMAT* donor plasmid used the *pHSG298* backbone (Takara Bio) and was generated using NEBuilder HiFi (New England Biolabs). The complete annotated sequence of *RSRT-STOP-RSRT-6XV5-vMAT* is shown in Supplementary Information. *pCFD4-vMAT1/pCFD4-vMAT2/RSRT-STOP-RSRT-6XV5-vMAT* injections into the *nos-Cas9* strain *TH_attP2* [98] were performed by Bestgene, Inc.

The R and B3 recombinases from yeast recognize sequence-specific recombination target sites, RSRTs and B3RTs, respectively [60]. These recombinases are highly efficient and highly specific as they exhibit virtually no cross-reactivity with each other's recombinase target sites. When pairs of recombinase target sites are in the same orientation, as is the case for both *B3RT-vGlut-LexA* and *RSRT-STOP-RSRT-6XV5-vMAT*, the recombinases catalyze excision of the intervening DNA and leave behind a single recombinase target site.

dVGlut antibody

Drosophila anti-dVGLUT mouse monoclonal antibodies (10D6G) were generated (Life Technologies Europe) using the C-terminal peptide sequence TQGQMPSYDPQGYQQQ of dVGLUT coupled to KLH.

Supporting information

S1 Fig. Verification of mAb dVGLUT specificity using the null *dVGlut^{SS1}* allele. (A) dVGLUT expression detected by mAb dVGLUT in a heterozygous *yw, dVGlut^{SS1}/+* late stage embryo. **(B)** dVGLUT expression is not detectable by mAb dVGLUT in a homozygous *yw,*

68

dVGlut^{SS1}/ dVGlut^{SS1} late stage embryo.
(TIF)

S2 Fig. Multiple optical sections from *dVGlut>dsRed* male brains labeled with anti-Tβh.
(A-B) Although the Tβh shows weaker immunoreactivity than the anti-Tdc2 antibody, Tβh is mainly detected in *dVGlut>dsRed* neurons at dorsal and ventral positions (A', A", B' and B"). Scale bar = 20 μm.
(TIF)

S3 Fig. (A-A') Schematic showing the regions (boxes) of the VNS imaged in panels B and C. (B-C) A male *dVGlut>dsRed* adult VNS labeled with anti-Tdc2. The majority of dVGLUT + neurons within the thoracic VNS (B) and abdominal VNS (C) express Tdc2 with a few exceptions (arrows). Scale bar = 10 μm.
(TIF)

S4 Fig. (A) Schematic showing the regions imaged in panels B and C (colored boxes). (B-C) The majority of OA neurons within the PENP (B) and SEZ (C) regions co-express dVGLUT as visualized in a male *tdc2>dsRed* adult brain labeled with anti-dVGLUT. Scale bar = 10 μm.
(TIF)

S5 Fig. (A) *dVGlut* transcript levels were decreased in *n-syb-gal4>dVGLUT-RNAi* males as compared to the *n-syb-gal4* control (n = 3; p<0.01). (B-C) Representative images of ventral sections of the SEZ from a *tdc2-gal4>dVGLUT-RNAi;UAS-dsRed* male brain labeled with anti-Tdc2. OGN differentiation as measured by Tdc2 expression is not altered by a reduction of dVGLUT. Scale bar = 10 μm. (D-E) Dorsal sections of the SEZ, PENP and protocerebral bridge region from the same brain as in B. There are no obvious changes in ventral OGN survival and differentiation as measured by Tdc2 expression. Scale bar = 20 μm.
(TIF)

S6 Fig. (A) Verification that each *tdc2>GFP* neuron in the brain and VNS is Tdc2+. The stack for panel A contains 30 optical sections at 1.0 μm. Scale bar = 20 μm. (B) The stack for panel B contains 34 optical sections at 1.0 μm. Scale bar = 20 μm. (C-E) Verification that each *tdc2-dVGlut-split>GFP* neuron is Tdc2+. The stack for panels C-E contains 56 optical sections at 0.5 μm. Scale bar = 20 μm. (F) Schematic showing the locations of Tdc+ clusters in C-E.
(TIF)

S7 Fig. (A) The activity levels of controls and *tdc2>dVGlut-RNAi* males did not differ during the aggression assay as measured by pixels moved/second. (B) Total behavioral events (lunges, wing threats, inter-male courtship) per minute was calculated. The average number of behavioral events per minute exhibited by experimental males (*tdc2>tsh>Gal80>dVGlut-RNAi*) was slightly higher than controls (**p<0.01)
(TIF)

S8 Fig. (A) The VNS of a *tdc2>mtd:HA* male, note the Tdc2+ cell bodies. (B) The addition of *tsh>Gal80* blocked the Gal4-mediated expression of mtd:HA in the majority of Tdc2+ VNS neurons (*tdc2/tsh>Gal80;dsRed*). Axonal projections from brain Tdc2+ neurons are visualized in the VNS. (C) Significantly less Tdc2+ VNS neurons are detected in *tdc2/tsh>Gal80;dsRed* vs. *tdc2>dsRed* males. (Mann Whitney, P = 0.001). (D) The addition of *tsh>Gal80* does not alter brain *tdc2-gal4* reporter driven expression.
(TIF)

S9 Fig. Neuron survival or distribution is not altered by the complete loss of dVGLUT in OGNs (A-D) Representative images of dorsal (A-B) and ventral (C-D) optical sections of the

69

SEZ region from *tdc2-gal4;B3RT-dVGlut/dVGLUT^SS1;UAS-B3 lexAop-His2B-mCherry UAS-His2A-GFP* males. OGNs are visualized by the mCherry reporter and white co-colocalization in the merged channel. Scale bar = 20 μm.
(TIF)

S10 Fig. RSRT>stop>6xV5-VMAT is not expressed without Gal4-mediated excision of the stop cassette. (A-A') In the presence of a Gal4 driver (*tdc2-Gal4-AD dVGlut-Gal4-DBD*) to drive R recombinase (*UAS-R*) expression, the stop cassette of RSRT>stop>6XV5-VMAT is excised and V5-VMAT (magenta) is expressed and visualized by anti-V5. dVGLUT (green) is visualized by mAb dVGLUT. **(B-B')** Without the presence of a Gal4 driver, dVGLUT expression is apparent while expression from RSRT>stop>6XV5-VMAT is not detected by anti-V5. Scale bar = 30 μm.
(TIF)

S11 Fig. (A) Higher magnification of the SEZ region showing V5-VMAT expression in OGNs after excision by *tdc2-dVGlut-gal4* driven R recombinase. The brain is labeled with anti-V5 (magenta) and mAb dVGLUT (green). Scale bar = 15 μm. **(B-B")** Higher magnification of the SEZ region of the region in the dashed box in panel B. Arrowheads indicate puncta with dVGLUT and V5-VMAT colocalization. Arrows indicate puncta with only V5-VMAT (arrows). **(C)** Schematic indicating the location of the SEZ region. **(D)** SEZ region of a representative brain with a synaptic marker incorporated (*UAS-synaptotagmin;HA, tdc2-dVGlut-gal4/UAS-R RSRT-STOP-RSRT-6XV5-vMAT*). The brain is labeled with anti-HA (blue), anti-V5 (magenta), and mAb dVGLUT (green). Scale bar = 20 μm. **(E)** Higher magnification of the SEZ region in D. Scale bar = 10 μm. **(F-H)** Regions of interest from E showing puncta with dVGLUT, V5-VMAT and Syt:HA. The stack for panel B contains two optical sections at 0.45 μm. Six optical sections at 0.45 μm were stacked in panels E-H.
(TIF)

S12 Fig. OGNs include the three OA-FruM+ neurons. (A-C) Brains from *tdc2-dVGlut-split-gal4/UAS>stop>CD8:GFP;fru-flp* males demonstrate OA-FruM+ neurons are also dVGlut+. **(D)** No OGNs in the VNS are FruM+ although as expected the OGN-FruM+ neurons project into the VNS. Scale bar = 20 μm. **(E-G)** OGN-FruM+ neurons (arrow) were also identified in *dVGlut-gal4/UAS>stop>CD8:GFP;fru-flp* male brains labeled with anti-Tdc2 (magenta). Scale bar = 20 μm.
(TIF)

S1 Table. Identified OGNs based on OA neuron nomenclature.
(TIF)

S2 Table. Cloning components used for the construction of the 20XUAS-His2A-GFP and 13XLexAop2-His2B-mCherry lines.
(TIF)

S1 Data.
(TIF)

70

Author Contributions

Conceptualization: Lewis M. Sherer, R. Steven Stowers, Sarah J. Certel.

Data curation: Lewis M. Sherer, Edmond D. Brewer.

Formal analysis: Lewis M. Sherer, Elizabeth Catudio Garrett, Hannah R. Morgan, Lucy A. Sirrs, Sarah J. Certel.

Funding acquisition: R. Steven Stowers, Sarah J. Certel.

Investigation: Lewis M. Sherer, Elizabeth Catudio Garrett, Hannah R. Morgan, Lucy A. Sirrs, R. Steven Stowers, Sarah J. Certel.

Methodology: R. Steven Stowers.

Resources: Harold K. Shearin, Jessica L. Williams, Brian D. McCabe, R. Steven Stowers.

Supervision: Sarah J. Certel.

Visualization: R. Steven Stowers.

Writing – original draft: Sarah J. Certel.

Writing – review & editing: R. Steven Stowers, Sarah J. Certel.

References

1. Dale H. Pharmacology and Nerve-endings (Walter Ernest Dixon Memorial Lecture): (Section of Therapeutics and Pharmacology). Proc R Soc Med. 1935; 28(3):319–32. Epub 1935/01/01. PMID: 19990108; PubMed Central PMCID: PMC2205701.

2. Eccles JC, Fatt P, Koketsu K. Cholinergic and inhibitory synapses in a pathway from motor-axon collaterals to motoneurones. J Physiol. 1954; 126(3):524–62. Epub 1954/12/10. https://doi.org/10.1113/jphysiol.1954.sp005226 PMID: 13222354; PubMed Central PMCID: PMC1365877.

3. Strata P, Harvey R. Dale's principle. Brain Res Bull. 1999; 50(5–6):349–50. Epub 2000/01/22. https://doi.org/10.1016/s0361-9230(99)00100-8 PMID: 10643431.

4. Hnasko TS, Edwards RH. Neurotransmitter corelease: mechanism and physiological role. Annu Rev Physiol. 2012; 74:225–43. Epub 2011/11/08. https://doi.org/10.1146/annurev-physiol-020911-153315 PMID: 22054239; PubMed Central PMCID: PMC4090038.

5. Nassel DR. Substrates for Neuronal Cotransmission With Neuropeptides and Small Molecule Neurotransmitters in Drosophila. Front Cell Neurosci. 2018; 12:83. Epub 2018/04/14. https://doi.org/10.3389/fncel.2018.00083 PMID: 29651236; PubMed Central PMCID: PMC5885757.

6. Nusbaum MP, Blitz DM, Marder E. Functional consequences of neuropeptide and small-molecule cotransmission. Nat Rev Neurosci. 2017; 18(7):389–403. Epub 2017/06/09. https://doi.org/10.1038/nrn.2017.56 PMID: 28592905; PubMed Central PMCID: PMC5547741.

7. Vaaga CE, Borisovska M, Westbrook GL. Dual-transmitter neurons: functional implications of co-release and co-transmission. Curr Opin Neurobiol. 2014; 29:25–32. Epub 2014/05/13. https://doi.org/10.1016/j.conb.2014.04.010 PMID: 24816154; PubMed Central PMCID: PMC4231002.

8. El Mestikawy S, Wallen-Mackenzie A, Fortin GM, Descarries L, Trudeau LE. From glutamate co-release to vesicular synergy: vesicular glutamate transporters. Nat Rev Neurosci. 2011; 12(4):204–16. Epub 2011/03/19. https://doi.org/10.1038/nrn2969 PMID: 21415847.

9. Gras C, Herzog E, Bellenchi GC, Bernard V, Ravassard P, Pohl M, et al. A third vesicular glutamate transporter expressed by cholinergic and serotoninergic neurons. J Neurosci. 2002; 22(13):5442–51. Epub 2002/07/05. https://doi.org/10.1523/JNEUROSCI.22-13-05442.2002 PMID: 12097496.

10. Ottersen OP, Storm-Mathisen J. Glutamate- and GABA-containing neurons in the mouse and rat brain, as demonstrated with a new immunocytochemical technique. J Comp Neurol. 1984; 229(3):374–92. Epub 1984/11/01. https://doi.org/10.1002/cne.902290308 PMID: 6150049.

11. Root DH, Zhang S, Barker DJ, Miranda-Barrientos J, Liu B, Wang HL, et al. Selective Brain Distribution and Distinctive Synaptic Architecture of Dual Glutamatergic-GABAergic Neurons. Cell Rep. 2018; 23 (12):3465–79. Epub 2018/06/21. https://doi.org/10.1016/j.celrep.2018.05.063 PMID: 29924991.

12. Aguilar JI, Dunn M, Mingote S, Karam CS, Farino ZJ, Sonders MS, et al. Neuronal Depolarization Drives Increased Dopamine Synaptic Vesicle Loading via VGLUT. Neuron. 2017; 95(5):1074–88 e7.

71

Epub 2017/08/22. https://doi.org/10.1016/j.neuron.2017.07.038 PMID: 28823729; PubMed Central PMCID: PMC5760215.

13. Lohr KM, Bernstein AI, Stout KA, Dunn AR, Lazo CR, Alter SP, et al. Increased vesicular monoamine transporter enhances dopamine release and opposes Parkinson disease-related neurodegeneration in vivo. Proc Natl Acad Sci U S A. 2014; 111(27):9977–82. Epub 2014/07/01. https://doi.org/10.1073/pnas.1402134111 PMID: 24979780; PubMed Central PMCID: PMC4103325.

14. Trudeau LE, El Mestikawy S. Glutamate Cotransmission in Cholinergic, GABAergic and Monoamine Systems: Contrasts and Commonalities. Front Neural Circuits. 2018; 12:113. Epub 2019/01/09. https://doi.org/10.3389/fncir.2018.00113 PMID: 30618649; PubMed Central PMCID: PMC6305298.

15. Silm K, Yang J, Marcott PF, Asensio CS, Eriksen J, Guthrie DA, et al. Synaptic Vesicle Recycling Pathway Determines Neurotransmitter Content and Release Properties. Neuron. 2019; 102(4):786–800 e5. Epub 2019/04/21. https://doi.org/10.1016/j.neuron.2019.03.031 PMID: 31003725; PubMed Central PMCID: PMC6541489.

16. Zhang Q, Liu B, Wu Q, Liu B, Li Y, Sun S, et al. Differential Co-release of Two Neurotransmitters from a Vesicle Fusion Pore in Mammalian Adrenal Chromaffin Cells. Neuron. 2019; 102(1):173–83 e4. Epub 2019/02/19. https://doi.org/10.1016/j.neuron.2019.01.031 PMID: 30773347.

17. Wrangham RW. Two types of aggression in human evolution. Proc Natl Acad Sci U S A. 2018; 115 (2):245–53. Epub 2017/12/28. https://doi.org/10.1073/pnas.1713611115 PMID: 29279379; PubMed Central PMCID: PMC5777045.

18. Thomas AL, Davis SM, Dierick HA. Of Fighting Flies, Mice, and Men: Are Some of the Molecular and Neuronal Mechanisms of Aggression Universal in the Animal Kingdom? PLoS Genet. 2015; 11(8): e1005416. Epub 2015/08/28. https://doi.org/10.1371/journal.pgen.1005416 PMID: 26312756; PubMed Central PMCID: PMC4551476.

19. Craig IW, Halton KE. Genetics of human aggressive behaviour. Hum Genet. 2009; 126(1):101–13. Epub 2009/06/10. https://doi.org/10.1007/s00439-009-0695-9 PMID: 19506905.

20. Hoopfer ED. Neural control of aggression in Drosophila. Curr Opin Neurobiol. 2016; 38:109–18. Epub 2016/05/18. https://doi.org/10.1016/j.conb.2016.04.007 PMID: 27179788.

21. Kravitz EA, Fernandez Mde L. Aggression in Drosophila. Behav Neurosci. 2015; 129(5):549–63. https://doi.org/10.1037/bne0000089 PMID: 26348714.

22. Nelson RJ, Trainor BC. Neural mechanisms of aggression. Nat Rev Neurosci. 2007; 8(7):536–46. https://doi.org/10.1038/nrn2174 PMID: 17585306.

23. Rillich J, Rillich B, Stevenson PA. Differential modulation of courtship behavior and subsequent aggression by octopamine, dopamine and serotonin in male crickets. Horm Behav. 2019. Epub 2019/06/22. https://doi.org/10.1016/j.yhbeh.2019.06.006 PMID: 31226329.

24. Bruno V, Mancini D, Ghoche R, Arshinoff R, Miyasaki JM. High prevalence of physical and sexual aggression to caregivers in advanced Parkinson's disease. Experience in the Palliative Care Program. Parkinsonism Relat Disord. 2016; 24:141–2. Epub 2016/01/21. https://doi.org/10.1016/j.parkreldis.2016.01.010 PMID: 26786755.

25. Liu CS, Ruthirakuhan M, Chau SA, Herrmann N, Carvalho AF, Lanctot KL. Pharmacological Management of Agitation and Aggression in Alzheimer's Disease: A Review of Current and Novel Treatments. Curr Alzheimer Res. 2016; 13(10):1134–44. Epub 2016/05/04. https://doi.org/10.2174/1567205013666160502122933 PMID: 27137221.

26. Stigler KA, McDougle CJ. Pharmacotherapy of irritability in pervasive developmental disorders. Child Adolesc Psychiatr Clin N Am. 2008; 17(4):739–52, vii-viii. Epub 2008/09/09. https://doi.org/10.1016/j.chc.2008.06.002 PMID: 18775367.

27. Kim S, Boylan K. Effectiveness of Antidepressant Medications for Symptoms of Irritability and Disruptive Behaviors in Children and Adolescents. J Child Adolesc Psychopharmacol. 2016; 26(8):694–704. Epub 2016/08/03. https://doi.org/10.1089/cap.2015.0127 PMID: 27482998.

28. Moret C, Briley M. The importance of norepinephrine in depression. Neuropsychiatr Dis Treat. 2011; 7 (Suppl 1):9–13. Epub 2011/07/14. https://doi.org/10.2147/NDT.S19619 PMID: 21750623; PubMed Central PMCID: PMC3131098.

29. Sharma T, Guski LS, Freund N, Gotzsche PC. Suicidality and aggression during antidepressant treatment: systematic review and meta-analyses based on clinical study reports. BMJ. 2016; 352:i65. Epub 2016/01/29. https://doi.org/10.1136/bmj.i65 PMID: 26819231; PubMed Central PMCID: PMC4729837.

30. Agnati LF, Guidolin D, Guescini M, Genedani S, Fuxe K. Understanding wiring and volume transmission. Brain Res Rev. 2010; 64(1):137–59. Epub 2010/03/30. https://doi.org/10.1016/j.brainresrev.2010.03.003 PMID: 20347870.

72

31. Beaudet A, Descarries L. The monoamine innervation of rat cerebral cortex: synaptic and nonsynaptic axon terminals. Neuroscience. 1978; 3(10):851–60. Epub 1978/01/01. https://doi.org/10.1016/0306-4522(78)90115-x PMID: 215936.

32. Descarries L, Berube-Carriere N, Riad M, Bo GD, Mendez JA, Trudeau LE. Glutamate in dopamine neurons: synaptic versus diffuse transmission. Brain Res Rev. 2008; 58(2):290–302. Epub 2007/11/29. https://doi.org/10.1016/j.brainresrev.2007.10.005 PMID: 18042492.

33. Descarries L, Watkins KC, Lapierre Y. Noradrenergic axon terminals in the cerebral cortex of rat. III. Topometric ultrastructural analysis. Brain Res. 1977; 133(2):197–222. Epub 1977/09/16. https://doi.org/10.1016/0006-8993(77)90759-4 PMID: 902092.

34. De-Miguel FF, Trueta C. Synaptic and extrasynaptic secretion of serotonin. Cell Mol Neurobiol. 2005; 25(2):297–312. https://doi.org/10.1007/s10571-005-3061-z PMID: 16047543.

35. Fuxe K, Agnati LF, Marcoli M, Borroto-Escuela DO. Volume Transmission in Central Dopamine and Noradrenaline Neurons and Its Astroglial Targets. Neurochem Res. 2015; 40(12):2600–14. Epub 2015/04/22. https://doi.org/10.1007/s11064-015-1574-5 PMID: 25894681.

36. Marder E, Thirumalai V. Cellular, synaptic and network effects of neuromodulation. Neural Netw. 2002; 15(4–6):479–93. https://doi.org/10.1016/s0893-6080(02)00043-6 PMID: 12371506.

37. Takahashi A, Quadros IM, de Almeida RM, Miczek KA. Behavioral and pharmacogenetics of aggressive behavior. Curr Top Behav Neurosci. 2012; 12:73–138. https://doi.org/10.1007/7854_2011_191 PMID: 22297576; PubMed Central PMCID: PMC3864145.

38. Moutsimilli L, Farley S, El Khoury MA, Chamot C, Sibarita JB, Racine V, et al. Antipsychotics increase vesicular glutamate transporter 2 (VGLUT2) expression in thalamolimbic pathways. Neuropharmacology. 2008; 54(3):497–508. Epub 2007/12/25. https://doi.org/10.1016/j.neuropharm.2007.10.022 PMID: 18155072.

39. Uezato A, Meador-Woodruff JH, McCullumsmith RE. Vesicular glutamate transporter mRNA expression in the medial temporal lobe in major depressive disorder, bipolar disorder, and schizophrenia. Bipolar Disord. 2009; 11(7):711–25. Epub 2009/10/21. https://doi.org/10.1111/j.1399-5618.2009.00752.x PMID: 19839996.

40. Tordera RM, Pei Q, Sharp T. Evidence for increased expression of the vesicular glutamate transporter, VGLUT1, by a course of antidepressant treatment. J Neurochem. 2005; 94(4):875–83. Epub 2005/07/05. https://doi.org/10.1111/j.1471-4159.2005.03192.x PMID: 15992385.

41. Shan D, Lucas EK, Drummond JB, Haroutunian V, Meador-Woodruff JH, McCullumsmith RE. Abnormal expression of glutamate transporters in temporal lobe areas in elderly patients with schizophrenia. Schizophr Res. 2013; 144(1–3):1–8. Epub 2013/01/30. https://doi.org/10.1016/j.schres.2012.12.019 PMID: 23356950; PubMed Central PMCID: PMC3572263.

42. Mingote S, Chuhma N, Kalmbach A, Thomsen GM, Wang Y, Mihali A, et al. Dopamine neuron dependent behaviors mediated by glutamate cotransmission. Elife. 2017; 6. Epub 2017/07/14. https://doi.org/10.7554/eLife.27566 PMID: 28703706; PubMed Central PMCID: PMC5599237.

43. Andrews JC, Fernandez MP, Yu Q, Leary GP, Leung AK, Kavanaugh MP, et al. Octopamine neuromodulation regulates Gr32a-linked aggression and courtship pathways in Drosophila males. PLoS Genet. 2014; 10(5):e1004356. Epub 2014/05/24. https://doi.org/10.1371/journal.pgen.1004356 PMID: 24852170; PubMed Central PMCID: PMC4031044.

44. Baier A, Wittek B, Brembs B. Drosophila as a new model organism for the neurobiology of aggression? J Exp Biol. 2002; 205(Pt 9):1233–40. PMID: 11948200.

45. Certel SJ, Savella MG, Schlegel DC, Kravitz EA. Modulation of Drosophila male behavioral choice. Proc Natl Acad Sci U S A. 2007; 104(11):4706–11. https://doi.org/10.1073/pnas.0700328104 PMID: 17360588.

46. Hoyer SC, Eckart A, Herrel A, Zars T, Fischer SA, Hardie SL, et al. Octopamine in male aggression of Drosophila. Curr Biol. 2008; 18(3):159–67. https://doi.org/10.1016/j.cub.2007.12.052 PMID: 18249112.

47. Zhou C, Rao Y, Rao Y. A subset of octopaminergic neurons are important for Drosophila aggression. Nat Neurosci. 2008; 11(9):1059–67. https://doi.org/10.1038/nn.2164 PMID: 19160504.

48. Chaudhry FA, Reimer RJ, Bellocchio EE, Danbolt NC, Osen KK, Edwards RH, et al. The vesicular GABA transporter, VGAT, localizes to synaptic vesicles in sets of glycinergic as well as GABAergic neurons. J Neurosci. 1998; 18(23):9733–50. Epub 1998/11/21. https://doi.org/10.1523/JNEUROSCI.18-23-09733.1998 PMID: 9822734.

49. Hnasko TS, Chuhma N, Zhang H, Goh GY, Sulzer D, Palmiter RD, et al. Vesicular glutamate transport promotes dopamine storage and glutamate corelease in vivo. Neuron. 2010; 65(5):643–56. Epub 2010/03/13. https://doi.org/10.1016/j.neuron.2010.02.012 PMID: 20223200; PubMed Central PMCID: PMC2846457.

73

50. Jonas P, Bischofberger J, Sandkuhler J. Corelease of two fast neurotransmitters at a central synapse. Science. 1998; 281(5375):419–24. Epub 1998/07/17. https://doi.org/10.1126/science.281.5375.419 PMID: 9665886.

51. Ren J, Qin C, Hu F, Tan J, Qiu L, Zhao S, et al. Habenula "cholinergic" neurons co-release glutamate and acetylcholine and activate postsynaptic neurons via distinct transmission modes. Neuron. 2011; 69 (3):445–52. Epub 2011/02/15. https://doi.org/10.1016/j.neuron.2010.12.038 PMID: 21315256.

52. Tritsch NX, Ding JB, Sabatini BL. Dopaminergic neurons inhibit striatal output through non-canonical release of GABA. Nature. 2012; 490(7419):262–6. Epub 2012/10/05. https://doi.org/10.1038/nature11466 PMID: 23034651; PubMed Central PMCID: PMC3944587.

53. Rodriguez-Valentin R, Lopez-Gonzalez I, Jorquera R, Labarca P, Zurita M, Reynaud E. Oviduct contraction in Drosophila is modulated by a neural network that is both, octopaminergic and glutamatergic. J Cell Physiol. 2006; 209(1):183–98. https://doi.org/10.1002/jcp.20722 PMID: 16826564.

54. Stuber GD, Hnasko TS, Britt JP, Edwards RH, Bonci A. Dopaminergic terminals in the nucleus accumbens but not the dorsal striatum corelease glutamate. J Neurosci. 2010; 30(24):8229–33. Epub 2010/06/18. https://doi.org/10.1523/JNEUROSCI.1754-10.2010 PMID: 20554874; PubMed Central PMCID: PMC2918390.

55. Certel SJ, Leung A, Lin CY, Perez P, Chiang AS, Kravitz EA. Octopamine neuromodulatory effects on a social behavior decision-making network in Drosophila males. PLoS One. 2010; 5(10):e13248. Epub 2010/10/23. https://doi.org/10.1371/journal.pone.0013248 PMID: 20967276; PubMed Central PMCID: PMC2953509.

56. Watanabe K, Chiu H, Pfeiffer BD, Wong AM, Hoopfer ED, Rubin GM, et al. A Circuit Node that Integrates Convergent Input from Neuromodulatory and Social Behavior-Promoting Neurons to Control Aggression in Drosophila. Neuron. 2017; 95(5):1112–28 e7. Epub 2017/09/01. https://doi.org/10.1016/j.neuron.2017.08.017 PMID: 28858617; PubMed Central PMCID: PMC5588916.

57. Chen S, Lee AY, Bowens NM, Huber R, Kravitz EA. Fighting fruit flies: a model system for the study of aggression. Proc Natl Acad Sci U S A. 2002; 99(8):5664–8. https://doi.org/10.1073/pnas.082102599 PMID: 11960020.

58. Dierick HA. A method for quantifying aggression in male Drosophila melanogaster. Nat Protoc. 2007; 2 (11):2712–8. https://doi.org/10.1038/nprot.2007.404 PMID: 18007606.

59. Baek M, Mann RS. Lineage and birth date specify motor neuron targeting and dendritic architecture in adult Drosophila. J Neurosci. 2009; 29(21):6904–16. Epub 2009/05/29. https://doi.org/10.1523/JNEUROSCI.1585-09.2009 PMID: 19474317.

60. Nern A, Pfeiffer BD, Svoboda K, Rubin GM. Multiple new site-specific recombinases for use in manipulating animal genomes. Proc Natl Acad Sci U S A. 2011; 108(34):14198–203. Epub 2011/08/13. https://doi.org/10.1073/pnas.1111704108 PMID: 21831835; PubMed Central PMCID: PMC3161616.

61. Jensen AA, Fahlke C, Bjorn-Yoshimoto WE, Bunch L. Excitatory amino acid transporters: recent insights into molecular mechanisms, novel modes of modulation and new therapeutic possibilities. Curr Opin Pharmacol. 2015; 20:116–23. Epub 2014/12/04. https://doi.org/10.1016/j.coph.2014.10.008 PMID: 25466154.

62. Martin CA, Krantz DE. Drosophila melanogaster as a genetic model system to study neurotransmitter transporters. Neurochem Int. 2014; 73:71–88. Epub 2014/04/08. https://doi.org/10.1016/j.neuint.2014.03.015 PMID: 24704795; PubMed Central PMCID: PMC4264877.

63. Seal RP, Daniels GM, Wolfgang WJ, Forte MA, Amara SG. Identification and characterization of a cDNA encoding a neuronal glutamate transporter from Drosophila melanogaster. Receptors Channels. 1998; 6(1):51–64. Epub 1998/07/17. PMID: 9664622.

64. Soustelle L, Besson MT, Rival T, Birman S. Terminal glial differentiation involves regulated expression of the excitatory amino acid transporters in the Drosophila embryonic CNS. Dev Biol. 2002; 248(2):294–306. Epub 2002/08/09. https://doi.org/10.1006/dbio.2002.0742 PMID: 12167405.

65. Stacey SM, Muraro NI, Peco E, Labbe A, Thomas GB, Baines RA, et al. Drosophila glial glutamate transporter Eaat1 is regulated by fringe-mediated notch signaling and is essential for larval locomotion. J Neurosci. 2010; 30(43):14446–57. Epub 2010/10/29. https://doi.org/10.1523/JNEUROSCI.1021-10.2010 PMID: 20980602.

66. Matsuno M, Horiuchi J, Ofusa K, Masuda T, Saitoe M. Inhibiting Glutamate Activity during Consolidation Suppresses Age-Related Long-Term Memory Impairment in Drosophila. iScience. 2019; 15:55–65. Epub 2019/04/29. https://doi.org/10.1016/j.isci.2019.04.014 PMID: 31030182; PubMed Central PMCID: PMC6487374.

67. Monastirioti M, Linn CE Jr., White K. Characterization of Drosophila tyramine beta-hydroxylase gene and isolation of mutant flies lacking octopamine. J Neurosci. 1996; 16(12):3900–11. https://doi.org/10.1523/JNEUROSCI.16-12-03900.1996 PMID: 8656284.

74

68. Tison KV, McKinney HM, Stowers RS. Demonstration of a Simple Epitope Tag Multimerization Strategy for Enhancing the Sensitivity of Protein Detection Using Drosophila vAChT. G3 (Bethesda). 2019. Epub 2019/11/27. https://doi.org/10.1534/g3.119.400750 PMID: 31767639.

69. Atwood HL, Govind CK, Wu CF. Differential ultrastructure of synaptic terminals on ventral longitudinal abdominal muscles in Drosophila larvae. J Neurobiol. 1993; 24(8):1008–24. Epub 1993/08/01. https://doi.org/10.1002/neu.480240803 PMID: 8409966.

70. Grygoruk A, Chen A, Martin CA, Lawal HO, Fei H, Gutierrez G, et al. The redistribution of Drosophila vesicular monoamine transporter mutants from synaptic vesicles to large dense-core vesicles impairs amine-dependent behaviors. J Neurosci. 2014; 34(20):6924–37. Epub 2014/05/16. https://doi.org/10.1523/JNEUROSCI.0694-14.2014 PMID: 24828646; PubMed Central PMCID: PMC4019805.

71. Sujkowski A, Ramesh D, Brockmann A, Wessells R. Octopamine Drives Endurance Exercise Adaptations in Drosophila. Cell Rep. 2017; 21(7):1809–23. Epub 2017/11/16. https://doi.org/10.1016/j.celrep.2017.10.065 PMID: 29141215; PubMed Central PMCID: PMC5693351.

72. Brewer JC, Olson AC, Collins KM, Koelle MR. Serotonin and neuropeptides are both released by the HSN command neuron to initiate Caenorhabditis elegans egg laying. PLoS Genet. 2019; 15(1):e1007896. Epub 2019/01/25. https://doi.org/10.1371/journal.pgen.1007896 PMID: 30677018; PubMed Central PMCID: PMC6363226.

73. Amilhon B, Lepicard E, Renoir T, Mongeau R, Popa D, Poirel O, et al. VGLUT3 (vesicular glutamate transporter type 3) contribution to the regulation of serotonergic transmission and anxiety. J Neurosci. 2010; 30(6):2198–210. Epub 2010/02/12. https://doi.org/10.1523/JNEUROSCI.5196-09.2010 PMID: 20147547.

74. Ciranna L. Serotonin as a modulator of glutamate- and GABA-mediated neurotransmission: implications in physiological functions and in pathology. Curr Neuropharmacol. 2006; 4(2):101–14. Epub 2008/07/11. https://doi.org/10.2174/157015906776359540 PMID: 18615128; PubMed Central PMCID: PMC2430669.

75. Pittaluga A. Presynaptic Release-Regulating mGlu1 Receptors in Central Nervous System. Front Pharmacol. 2016; 7:295. Epub 2016/09/16. https://doi.org/10.3389/fphar.2016.00295 PMID: 27630571; PubMed Central PMCID: PMC5006178.

76. Birgner C, Nordenankar K, Lundblad M, Mendez JA, Smith C, le Greves M, et al. VGLUT2 in dopamine neurons is required for psychostimulant-induced behavioral activation. Proc Natl Acad Sci U S A. 2010; 107(1):389–94. Epub 2009/12/19. https://doi.org/10.1073/pnas.0910986107 PMID: 20018672; PubMed Central PMCID: PMC2806710.

77. Fortin GM, Ducrot C, Giguere N, Kouwenhoven WM, Bourque MJ, Pacelli C, et al. Segregation of dopamine and glutamate release sites in dopamine neuron axons: regulation by striatal target cells. FASEB J. 2019; 33(1):400–17. Epub 2018/07/17. https://doi.org/10.1096/fj.201800713RR PMID: 30011230.

78. Zhang S, Qi J, Li X, Wang HL, Britt JP, Hoffman AF, et al. Dopaminergic and glutamatergic microdomains in a subset of rodent mesoaccumbens axons. Nat Neurosci. 2015; 18(3):386–92. Epub 2015/02/11. https://doi.org/10.1038/nn.3945 PMID: 25664911; PubMed Central PMCID: PMC4340758.

79. Koganezawa M, Kimura K, Yamamoto D. The Neural Circuitry that Functions as a Switch for Courtship versus Aggression in Drosophila Males. Curr Biol. 2016; 26(11):1395–403. Epub 2016/05/18. https://doi.org/10.1016/j.cub.2016.04.017 PMID: 27185554.

80. Crocker A, Sehgal A. Octopamine regulates sleep in Drosophila through protein kinase A-dependent mechanisms. J Neurosci. 2008; 28(38):9377–85. https://doi.org/10.1523/JNEUROSCI.3072-08a.2008 PMID: 18799671.

81. Scheiner R, Steinbach A, Classen G, Strudthoff N, Scholz H. Octopamine indirectly affects proboscis extension response habituation in Drosophila melanogaster by controlling sucrose responsiveness. J Insect Physiol. 2014; 69:107–17. Epub 2014/05/14. https://doi.org/10.1016/j.jinsphys.2014.03.011 PMID: 24819202.

82. Stevenson PA, Dyakonova V, Rillich J, Schildberger K. Octopamine and experience-dependent modulation of aggression in crickets. J Neurosci. 2005; 25(6):1431–41. https://doi.org/10.1523/JNEUROSCI.4258-04.2005 PMID: 15703397.

83. Youn H, Kirkhart C, Chia J, Scott K. A subset of octopaminergic neurons that promotes feeding initiation in Drosophila melanogaster. PLoS One. 2018; 13(6):e0198362. Epub 2018/06/28. https://doi.org/10.1371/journal.pone.0198362 PMID: 29949586; PubMed Central PMCID: PMC6021039.

84. Classen G, Scholz H. Octopamine Shifts the Behavioral Response From Indecision to Approach or Aversion in Drosophila melanogaster. Front Behav Neurosci. 2018; 12:131. Epub 2018/07/19. https://doi.org/10.3389/fnbeh.2018.00131 PMID: 30018540; PubMed Central PMCID: PMC6037846.

85. Mingote S, Amsellem A, Kempf A, Rayport S, Chuhma N. Dopamine-glutamate neuron projections to the nucleus accumbens medial shell and behavioral switching. Neurochem Int. 2019; 129:104482. Epub 2019/06/07. https://doi.org/10.1016/j.neuint.2019.104482 PMID: 31170424.

75

86. Manchia M, Carpiniello B, Valtorta F, Comai S. Serotonin Dysfunction, Aggressive Behavior, and Mental Illness: Exploring the Link Using a Dimensional Approach. ACS Chem Neurosci. 2017; 8(5):961–72. Epub 2017/04/06. https://doi.org/10.1021/acschemneuro.6b00427 PMID: 28378993.

87. Vermeiren Y, Van Dam D, Aerts T, Engelborghs S, De Deyn PP. Monoaminergic neurotransmitter alterations in postmortem brain regions of depressed and aggressive patients with Alzheimer's disease. Neurobiol Aging. 2014; 35(12):2691–700. Epub 2014/07/07. https://doi.org/10.1016/j.neurobiolaging.2014.05.031 PMID: 24997673.

88. Certel SJ, Kravitz EA. Scoring and analyzing aggression in Drosophila. Cold Spring Harb Protoc. 2012; 2012(3):319–25. Epub 2012/03/03. https://doi.org/10.1101/pdb.prot068130 PMID: 22383642.

89. Koon AC, Ashley J, Barria R, DasGupta S, Brain R, Waddell S, et al. Autoregulatory and paracrine control of synaptic and behavioral plasticity by octopaminergic signaling. Nat Neurosci. 2011; 14(2):190–9. Epub 2010/12/28. nn.2716 [pii] https://doi.org/10.1038/nn.2716 PMID: 21186359.

90. Petersen LK, Stowers RS. A Gateway MultiSite recombination cloning toolkit. PLoS One. 2011; 6(9): e24531. Epub 2011/09/21. https://doi.org/10.1371/journal.pone.0024531 PMID: 21931740; PubMed Central PMCID: PMC3170369.

91. Pfeiffer BD, Jenett A, Hammonds AS, Ngo TT, Misra S, Murphy C, et al. Tools for neuroanatomy and neurogenetics in Drosophila. Proc Natl Acad Sci U S A. 2008; 105(28):9715–20. https://doi.org/10.1073/pnas.0803697105 PMID: 18621688.

92. Williams JL, Shearin HK, Stowers RS. Conditional Synaptic Vesicle Markers for Drosophila. G3 (Bethesda). 2019. Epub 2019/01/13. https://doi.org/10.1534/g3.118.200975 PMID: 30635441.

93. Shearin HK, Dvarishkis AR, Kozeluh CD, Stowers RS. Expansion of the gateway multisite recombination cloning toolkit. PLoS One. 2013; 8(10):e77724. Epub 2013/11/10. https://doi.org/10.1371/journal.pone.0077724 PMID: 24204935; PubMed Central PMCID: PMC3799639.

94. Pfeiffer BD, Truman JW, Rubin GM. Using translational enhancers to increase transgene expression in Drosophila. Proc Natl Acad Sci U S A. 2012; 109(17):6626–31. Epub 2012/04/12. https://doi.org/10.1073/pnas.1204520109 PMID: 22493255; PubMed Central PMCID: PMC3340069.

95. Wang JW, Beck ES, McCabe BD. A modular toolset for recombination transgenesis and neurogenetic analysis of Drosophila. PLoS One. 2012; 7(7):e42102. Epub 2012/08/01. https://doi.org/10.1371/journal.pone.0042102 PMID: 22848718; PubMed Central PMCID: PMC3405054.

96. Port F, Chen HM, Lee T, Bullock SL. Optimized CRISPR/Cas tools for efficient germline and somatic genome engineering in Drosophila. Proc Natl Acad Sci U S A. 2014; 111(29):E2967–76. Epub 2014/07/09. https://doi.org/10.1073/pnas.1405500111 PMID: 25002478; PubMed Central PMCID: PMC4115528.

97. Daniels RW, Collins CA, Chen K, Gelfand MV, Featherstone DE, DiAntonio A. A single vesicular glutamate transporter is sufficient to fill a synaptic vesicle. Neuron. 2006; 49(1):11–6. Epub 2006/01/03. https://doi.org/10.1016/j.neuron.2005.11.032 PMID: 16387635; PubMed Central PMCID: PMC2248602.

98. Ren X, Sun J, Housden BE, Hu Y, Roesel C, Lin S, et al. Optimized gene editing technology for Drosophila melanogaster using germ line-specific Cas9. Proc Natl Acad Sci U S A. 2013; 110(47):19012–7. Epub 2013/11/06. https://doi.org/10.1073/pnas.1318481110 PMID: 24191015; PubMed Central PMCID: PMC3839733.

76

Chapter 4: Discussion

Neuron Communication

The over-arching theme of my master's research has been to understand the mechanisms that underlie neuron communication in the developing and adult brain. Neuronal communication is made possible by the neuron's specialized structures and the combination of electrical events called 'action potentials' and chemical neurotransmitters. At the synaptic junction between two neurons, an action potential causes the pre-synaptic neuron to release a chemical neurotransmitter. An ever-growing challenge in understanding neuron communication is the realization that many neurons release more than one type of chemical signal or neurotransmitter. In the collaborative dual transmission publication, we asked: *how does the release of more than one neurotransmitter from a single neuron impact circuits that control behavior*? We determined the monoamine octopamine (OA) and the classical transmitter glutamate are co-expressed in the *Drosophila* adult central nervous system (CNS). By manipulating the release of glutamate in OA-glutamate neurons, we demonstrated glutamate has both separable actions and complementary actions with OA on aggression and reproductive behaviors respectively. Aggression is a behavior that is highly conserved between organisms and present in many human disease states, including traumatic brain injuries (TBIs), depression, and Alzheimer's disease (Takahashi and Miczek, 2014; Thomas et al., 2015; Wrangham, 2018; Svensson et al., 2018). Our results show that aggressive behavior requires the release of both neurotransmitters in dual-transmitting neurons and suggests within this set of neurons, glutamate may provide a new therapeutic target to modulate aggression in pathological conditions.

A second emerging area of neuron communication that is also complex and still largely unknown, is the impact of the extracellular space surrounding neurons and glia on brain function. With the emergence of new technologies in combination with decades of research, a picture is developing that shows the narrow intercellular space to be a complex microenvironment essential to neuronal function, a signaling pathway in its own right, and an important conduit for drug delivery. The requirement for components of this extracellular space has been the core of my thesis project with the study of the matricellular protein (MCP) family member, *dCCN*. The connection that binds both projects together is our ultimate goal: determine how the complex signaling capabilities

of monoamine neurotransmitters modulate circuits that control behavior, namely aggression.

dCCN Discussion

The CCN family of MCPs are a group of highly conserved, non-structural ECM proteins that are critical for modulating intercellular signaling and trafficking (Bornstein and Sage, 2002; Rachfal, 2005; Katsube et al., 2009; Chen and Lau, 2009; Bornstein, 2009; Perbal, 2013; Adams, 2018; Perbal, 2018). The four well conserved functional domains of CCN proteins enable a single family member the ability to interact with a multitude of signaling partners that initiate many biological processes (Holbourn et al., 2008; Malik et al., 2015; Hu et al., 2019). A variety of tissues express the CCN family of MCPs, and numerous pathologies, developmental deficiencies, diseases, psychiatric conditions, cancers, and many other disorders result from disruptions in CCN:ECM or CCN:cell communication (Jun et al., 2011; Malik et al., 2015; Perbal, 2018; Hu et al., 2019). However, the requirements for CCN function in the nervous system, aside from a few studies, remains poorly understood.

In this study, I examined the sole CCN family member encoded by the *Drosophila melanogaster* genome, which we refer to as *dCCN*. We have shown that *dCCN* is expressed in the CNS at each developmental stage. Widespread, but not ubiquitous *dCCN* expression begins in the CNS of the embryo, is present in the CNS and motor neurons of larvae, and *dCCN* CNS widespread expression is maintained to adulthood. We predict that *dCCN* is important for development and critical for the remodeling and growth of the CNS within the *Drosophila* organism as the CNS undergoes immense morphological changes from an embryo, to a larvae, and finally, to an adult fly. We identified *dCCN* expressing sensory neurons of the peripheral nervous system (PNS) including the proboscis, maxillary palps, antennae, legs, and wings. We also discovered *dCCN* expressing projections innervating the crop and proventriculus structures of the gastrointestinal system. These sensory neurons are important for collecting internal and external stimuli, and are responsible for conveying this information back to the central brain. Additionally, we found *dCCN* expressing projections innervating the ovaries and uterus. We identified monoamine neuronal

populations that co-express *dCCN*, of which include the monoamines serotonin (5-HT), dopamine (DA), and OA. In addition, we found that *dCCN* is expressed in sexually dimorphic populations of neurons critical for sex-specific behaviors, of which include *fruitless* (*fru*) and *double-sex* (*dsx*). Lastly, we have demonstrated for the first time, that *dCCN* is required for neurotransmission at the larval neuromuscular junction (NMJ) and for female sterility. To conclude, *dCCN* is an incredibly important MCP of the CNS and contributes to synaptic neurotransmission and nervous system function.

We found that *dCCN* is expressed in the monoamine neurons DA, 5-HT, and OA. Monoamine neurons are important for regulating an immense variety of physiological processes, moods, and is known to govern behaviors (Dishman 1997; Libersat and Pflueger 2004; Kamhi and Traniello 2013; Bubak et al., 2014; De Boer et al., 2015; Swallow et al., 2016). A previous study by Hori et al. also demonstrated monoamine and CCN protein interactions in which CCN2 production is upregulated when 5-HT receptors are stimulated in chondrocytes (Hori et al, 2017). As MCPs do not have a structural role in the extracellular space (ECS), MCPs, and in particular *dCCN*, may indirectly impact the signaling of monoamine neurotransmitters released from synaptic sites and extra-synaptic sites by interacting with integrins as one example to stabilize neuronal junctions, bouton architecture, and potentially vesicle release.

We found sexually dimorphic *dCCN* expression in *fru* and *dsx* neurons. *Fru* and d*sx* are have different sets of neurons, cells, and expression patterns between males and females. Previous work demonstrated that *fru* neurons are important for male specific behaviors such as courtship and aggression (Lee et al., 2000; Goodwin et al., 2000; Anand et al., 2001; Stockinger et al., 2005; Kimura et al., 2005; Yamamoto, 2007; Rideout et al., 2007; Yamamoto, 2008; Villella and Hall, 2008; Sato et al., 2019; Ishii et al., 2020; Sato et al., 2020; Wohl et al., 2020). *Dsx* is important for male courting, specifically for performing sine song and copulatory behaviors, and initiating aggression towards males (Rideout et al., 2007; Rideout et al., 2010; Ishii et al., 2020). Additionally, both *fru* and *dsx* is essential for receptivity in females during courting events (Rideout et al., 2007; Villella and Hall, 2008; Rideout et al., 2010; Chowdhury et al, 2020). We predict that *dCCN* expression within *fru* and *dsx* may be to contribute to the development of sex specific neurons and cells, to give cells and neurons a sexual identity, and to

contribute to the health and maintenance of reproductive organs and the formation of offspring. *dCCN* may possibly impact behavior, but additional experiments are needed to separate out a developmental role.

Future Directions

There are two questions that can now be addressed after this work. First, it is necessary to examine the developmental vs. mature nervous system function of *dCCN*. While it has been demonstrated that the delicate balance of structural remodeling and stabilization of neuronal networks requires cell:ECM interactions changes over the life-span of an organism, to date, separating the role of CCN proteins during development vs. the mature cell/tissue has yet to be addressed in any system. This information is key to identifying temporally-regulated ECM or signaling factors that interact with CCN proteins as well as determining how CCN proteins contribute to neurotransmission changes in disease states. The second question is location: separating the nuclear vs. secreted function of CCN proteins. This question can be addressed by generating genome-edited fly strains to tag the *dCCN* endogenous protein and prevent secretion.

Significance

During development and in the adult, the ECS provides multiple cues that promote synaptic plasticity on the one hand, and maintenance of the homeostasis of neural circuitries on the other. The importance of the ECM for both of these processes indicate that it could have a pivotal role in the pathogenesis of neurological and neuropsychiatric disorders. Indeed, recent studies support the view that ECM aberrations are likely to contribute to imbalanced synaptic function in epilepsy, Alzheimer's disease, and other neurodegenerative disorders, TBI, and depression (Jun et al., 2011; Malik et al., 2015; Perbal, 2018; Dazzan et al., 2018; Davies, 2019). Results from this thesis project has provided new information on the sexually dimorphic expression and function of CCN family members and demonstrated a requirement for CCN proteins in synaptic transmission. There is still much to unravel in the quest to understand the specific functional contributions of the CCN family of MCPs within the CNS and PNS, and soon these roles will be elucidated. The findings of this work and future aims of this study will

81

lead to data that could be applied in potential therapeutic applications that may aid in CNS injury repair, microenvironment re-assembly, tissue regeneration and organ growing, electrophysiology treatments, TBI treatments, and numerous other clinical applications.

References

Abu Hamdeh S, Shevchenko G, Mi J, Musunuri S, Bergquist J, & Marklund N. *Proteomic differences between focal and diffuse traumatic brain injury in human brain tissue*. Sci Rep. 2018;8(1):6807. Published 2018 May 1. doi:10.1038/s41598-018-25060-0

Adams JC. *Matricellular Proteins: Functional Insights From Non-mammalian Animal Models*. Curr Top Dev Biol. 2018;130:39-105. doi: 10.1016/bs.ctdb.2018.02.003. Epub 2018 Mar 26.

Alberts B, Johnson A, Lewis J, et al. Molecular Biology of the Cell. 4th edition. New York: Garland Science; 2002. *The Extracellular Matrix of Animals*. Available from: https://www.ncbi.nlm.nih.gov/books/NBK26810/

Albrecht, C., von Der Kammer, H., Mayhaus, M., Klaudiny, J., Schweizer, M., & Nitsch, R. M. *Muscarinic acetylcholine receptors induce the expression of the immediate early growth regulatory gene CYR61*. (2000). J. Biol. Chem. 275, 28929–28936. doi: 10.1074/jbc.m003053200

Anand A, Villella A, Ryner LC, Carlo T, Goodwin SF, Song HJ, Gailey DA, Morales A, Hall JC, Baker BS, & Taylor BJ. *Molecular genetic dissection of the sex-specific and vital functions of the Drosophila melanogaster sex determination gene fruitless*. Genetics. 2001 Aug;158(4):1569-95.

Barnes JM, Przybyla L, Weaver VM. *Tissue mechanics regulate brain development, homeostasis and disease*. J Cell Sci. 2017;130(1):71-82. doi:10.1242/jcs.191742

Bork P. *The modular architecture of a new family of growth regulators related to connective tissue growth factor*. 1993. FEBS Lett 327: 125–130.

Bornstein P. *Diversity of function is inherent in matricellular proteins: an appraisal of thrombospondin 1*. J Cell Biol. 1995;130(3):503-506. doi:10.1083/jcb.130.3.503

Bornstein P, & Sage EH. *Matricellular proteins: extracellular modulators of cell function*. Current Opinion in Cell Biology. Volume 14. Issue 5. 2002. Pages 608-616. ISSN 0955-0674. https://doi.org/10.1016/S0955-0674(02)00361-7

Bornstein, P. *Matricellular proteins: an overview*. J. Cell Commun. Signal. 3, 163 (2009). https://doi.org/10.1007/s12079-009-0069-z

Borroto-Escuela DO, Agnati LF, Bechter K, Jansson A, Tarakanov AO, & Fuxe K. *The role of transmitter diffusion and flow versus extracellular vesicles in volume transmission in the brain neural-glial networks*. Philos Trans R Soc Lond B Biol Sci. 2015;370(1672):20140183. doi:10.1098/rstb.2014.0183

Bradshaw AD. *Diverse biological functions of the SPARC family of proteins*. Int J Biochem Cell Biol. 2012;44(3):480–488. doi:10.1016/j.biocel.2011.12.021

Brigstock DR, Goldshemeding R, Katsube K, Lam SC, Lau LF, Lyons K, Naus C, Perbal B, Riser B, Takigawa M, Yeger H. (2003). *Proposal for a unified CCN nomenclature*. Mol Pathol 56:127–128

Bruno V, Mancini D, Ghoche R, Arshinoff R, Miyasaki JM. *High prevalence of physical and sexual aggression to caregivers in advanced Parkinson's disease*. Experience in the Palliative Care Program. Parkinsonism Relat Disord. 2016;24:141–2. Epub 2016/01/21. pmid:26786755.

Bubak, AN., Jaime L. Grace, Michael J. Watt, Kenneth J. Renner, & John G. Swallow. *Neurochemistry as a bridge between morphology and behavior: Perspectives on aggression in insects.* Current Zoology, Volume 60, Issue 6, 1 December 2014, Pages 778–790, https://doi.org/10.1093/czoolo/60.6.778

Burrows M., G. J. Laurent, and L. H. Field. 1988. *Proprioceptive inputs to nonspiking local interneurons contribute to local reflexes of a locust hindleg.* J Neurosci 8: 3085–3093. https://doi.org/10.1523/jneurosci.08-08-03085.1988

Cachero S., A. D. Ostrovsky, J. Y. Yu, B. J. Dickson, and G. S. X. E. Jefferis. 2010. *Sexual dimorphism in the fly brain.* Curr Biol 20: 1589–1601. https://doi.org/10.1016/j.cub.2010.07.045

Chalasani SH, Kato S, Albrecht DR, Nakagawa T, Abbott LF, Bargmann CI. *Neuropeptide feedback modifies odor-evoked dynamics in Caenorhabditis elegans olfactory neurons.* Nat Neurosci. 2010;13(5):615–621. doi:10.1038/nn.2526

Chaqour B, & Goppelt-Struebe M. *Mechanical regulation of the Cyr61/CCN1 and CTGF/CCN2 proteins.* FEBS J. 2006 Aug;273(16):3639-49. Epub 2006 Jul 19.

Chen L, Brigstock DR. *Analysis of Pathological Activities of CCN Proteins in Fibrotic Diseases: Liver Fibrosis.* Methods Mol Biol. 2017;1489:445–463. doi:10.1007/978-1-4939-6430-7_37

Chen C.-L., L. Hermans, M. C. Viswanathan, D. Fortun, F. Aymanns, et al. 2018. *Imaging neural activity in the ventral nerve cord of behaving adult Drosophila.* Nat Commun 9: 4390. https://doi.org/10.1038/s41467-018-06857-z

Chen CC, & Lau LF. *Functions and mechanisms of action of CCN matricellular proteins.* Int J Biochem Cell Biol. 2009;41(4):771-783. doi:10.1016/j.biocel.2008.07.025

Chen PC, Cheng HC, Yang SF, Lin CW, Tang CH. *The CCN family proteins: modulators of bone development and novel targets in bone-associated tumors.* Biomed Res Int. 2014;2014:437096. doi:10.1155/2014/437096

Choi BJ, Imlach WL, Jiao W, Wolfram V, Wu Y, Grbic M, Cela C, Baines RA, Nitabach MN, & McCabe BD. *Miniature neurotransmission regulates Drosophila synaptic structural maturation.* Neuron. 2014;82(3):618-634. doi:10.1016/j.neuron.2014.03.012

Chowdhury T, Calhoun RM, Bruch K, & Moehring AJ. *The fruitless gene affects female receptivity and species isolation.* Proc Biol Sci. 2020 Mar 25;287(1923):20192765. doi: 10.1098/rspb.2019.2765. Epub 2020 Mar 25.

Chung, K. C., and Ahn, Y. S. *Expression of immediate early gene cyr61 during the differentiation of immortalized embryonic hippocampal neuronal cells.* (1998). Neurosci. Lett. 255, 155–158. doi: 10.1016/s0304-3940(98)00733-2

Cook CN, Brent CS, Breed MD. *Octopamine and tyramine modulate the thermoregulatory fanning response in honey bees (Apis mellifera).* J Exp Biol. 2017 May 15;220(Pt 10):1925-1930. doi: 10.1242/jeb.149203. Epub 2017 Mar 17.

Court R., S. Namiki, J. D. Armstrong, J. Börner, G. Card, et al., 2020. *A Systematic Nomenclature for the Drosophila Ventral Nervous System.* bioRxiv 122952. https://doi.org/10.1101/122952

Dacks A. M., D. S. Green, C. M. Root, A. J. Nighorn, and J. W. Wang, 2009. *Serotonin Modulates Olfactory Processing in the Antennal Lobe of Drosophila.* J Neurogenet 23: 366–377. https://doi.org/10.3109/01677060903085722

Davies, W. *An Analysis of Cellular Communication Network Factor Proteins as Candidate Mediators of Postpartum Psychosis Risk*. Front Psychiatry. 2019;10:876. Published 2019 Nov 26. doi:10.3389/fpsyt.2019.00876

Dazzan P, Fusté M, Davies W. *Do Defective Immune System-Mediated Myelination Processes Increase Postpartum Psychosis Risk?*. Trends Mol Med. 2018;24(11):942-949. doi:10.1016/j.molmed.2018.09.002

de Boer SF, Olivier B, Veening J, & Koolhaas JM. *The neurobiology of offensive aggression: Revealing a modular view*. Physiol Behav. 2015 Jul 1;146:111-27.

De-Miguel FF, & Trueta C. *Synaptic and extrasynaptic secretion of serotonin*. Cell Mol Neurobiol. 2005 Mar;25(2):297-312.

De-Miguel FF, Leon-Pinzon C, Noguez P, & Mendez B. *Serotonin release from the neuronal cell body and its long-lasting effects on the nervous system*. Philos Trans R Soc Lond B Biol Sci. 2015;370(1672):20140196. doi:10.1098/rstb.2014.0196

De-Miguel FF, Nicholls JG. *Release of chemical transmitters from cell bodies and dendrites of nerve cells*. Philos Trans R Soc Lond B Biol Sci. 2015;370(1672):20140181. doi:10.1098/rstb.2014.0181

Deng B., Q. Li, X. Liu, Y. Cao, B. Li, et al., 2019. *Chemoconnectomics: mapping chemical transmission in Drosophila*. Neuron 101: 876-893.e4. https://doi.org/10.1016/J.NEURON.2019.01.045

DeVries S, Li W, & Saszik S. *Parallel Processing in Two Transmitter Microenvironments at the Cone Photoreceptor Synapse*. Neuron. Volume 50, Issue 5, 1 June 2006, Pages 735-748.

Dhar A, & Ray A. *The CCN family proteins in carcinogenesis*. Exp Oncol. 2010 Mar;32(1):2-9.

Diao F., H. Ironfield, H. Luan, F. Diao, W. C. Shropshire, et al., 2015. *Plug-and-play genetic access to Drosophila cell types using exchangeable exon cassettes*. Cell Rep 10: 1410–1421. https://doi.org/10.1016/j.celrep.2015.01.059

Díez J, González A, & Ravassa S. Understanding the Role of CCN Matricellular Proteins in Myocardial Fibrosis. J Am Coll Cardiol. 2016 Apr, 67 (13) 1569-1571.

Dishman RK. Brain monoamines, exercise, and behavioral stress: animal models. Med Sci Sports Exerc. 1997 Jan;29(1):63-74.

Dori I. E., A. Dinopoulos, and J. G. Parnavelas, 1998. *The development of the synaptic organization of the serotonergic system differs in brain areas with different functions*. Exp Neurol 154: 113–125. https://doi.org/10.1006/exnr.1998.6937

Dougherty DA. *Cation-π Interactions Involving Aromatic Amino Acids*. The Journal of Nutrition. Volume 137, Issue 6. June 2007. Pages 1504S–1508S, https://doi.org/10.1093/jn/137.6.1504S

Dyakonova TL, Sultanakhmetov GS, Mezheritskiy MI, Sakharov DA, & Dyakonova VE. *Storage and erasure of behavioural experiences at the single neuron level*. Sci Rep 9, 14733 (2019). https://doi.org/10.1038/s41598-019-51331-5

Elaine Del-Bel & Francisco F. De-Miguel. *Extrasynaptic Neurotransmission Mediated by Exocytosis and Diffusive Release of Transmitter Substances*. Front Synaptic Neurosci. 2018; 10: 13. Published online 2018 Jun 8. doi: 10.3389/fnsyn.2018.00013

Eroglu C., 2009. *The role of astrocyte-secreted matricellular proteins in central nervous system development and function*. J Cell Commun Signal 3: 167–176.

Fan P., D. S. Manoli, O. M. Ahmed, Y. Chen, N. Agarwal, et al., 2013. *Genetic and neural mechanisms that inhibit drosophila from mating with other species*. Cell 154: 89–102. https://doi.org/10.1016/j.cell.2013.06.008

Frangogiannis, NG. *Matricellular proteins in cardiac adaptation and disease*. Physiol Rev. 2012;92(2):635–688. doi:10.1152/physrev.00008.2011

Frantz C, Stewart KM, Weaver VM. *The extracellular matrix at a glance*. J Cell Sci. 2010;123(Pt 24):4195-4200. doi:10.1242/jcs.023820

Friggi-Grelin F, Coulom H, Meller M, Gomez D, Hirsh J, & Birman S. *Targeted gene expression in Drosophila dopaminergic cells using regulatory sequences from tyrosine hydroxylase*. J Neurobiol. 2003 Mar;54(4):618-27.

Fuxe K., A. B. Dahlström, G. Jonsson, D. Marcellino, M. Guescini, et al., 2010. *The discovery of central monoamine neurons gave volume transmission to the wired brain*. Prog Neurobiol 90: 82–100. Fuxe K, Agnati LF, Marcoli M, & Borroto-Escuela DO. Volume Transmission in Central Dopamine and Noradrenaline Neurons and Its Astroglial Targets. Neurochem Res. 2015 Dec;40(12):2600-14. doi: 10.1007/s11064-015-1574-5. Epub 2015 Apr 17.

García-Fuster MJ, & García-Sevilla JA. *Monoamine receptor agonists, acting preferentially at presynaptic autoreceptors and heteroreceptors, downregulate the cell fate adaptor FADD in rat brain cortex*. Neuropharmacology. 2015 Feb;89:204-14. doi: 10.1016/j.neuropharm.2014.09.018. Epub 2014 Oct 5.

Giang T, Ritze Y, Rauchfuss S, Ogueta M, & Scholz H. *The serotonin transporter expression in Drosophila melanogaster*. J Neurogenet. 2011 Mar;25(1-2):17-26. doi: 10.3109/01677063.2011.553002. Epub 2011 Feb 14.

Gilloteaux J. *Histochemical detection of monoamine oxidase activity in smooth muscle and epithelial tissues of Mytilus edulis L. and Mytilus galloprovincialis Lmk*. Acta Histochem. 1979;65(1):15-24. doi: 10.1016/S0065-1281(79)80028-8.

Goodwin SF, Taylor BJ, Villella A, Foss M, Ryner LC, Baker BS, & Hall JC. *Aberrant splicing and altered spatial expression patterns in fruitless mutants of Drosophila melanogaster*. Genetics. 2000 Feb;154(2):725-45.

Göthert, M. *Role of autoreceptors in the function of the peripheral and central nervous system*. Arzneimittelforschung. 1985;35(12A):1909-16.

Gnerer JP, Venken KJ, Dierick HA. *Gene-specific cell labeling using MiMIC transposons*. Nucleic Acids Res. 2015;43(8):e56. doi:10.1093/nar/gkv113

Graeme Eisenhofer, Anders Åneman, Peter Friberg, Douglas Hooper, Lars Fåndriks, Hans Lonroth, Béla Hunyady, Eva Mezey. *Substantial Production of Dopamine in the Human Gastrointestinal Tract*. The Journal of Clinical Endocrinology & Metabolism, Volume 82, Issue 11, 1 November 1997, Pages 3864–3871, https://doi.org/10.1210/jcem.82.11.4339.

Grouleff J, Ladefoged L, Koldsø H, and Schiøtt B. *Monoamine transporters: Insights from molecular dynamics simulations*. Frontiers in pharmacology. (2015). 6. 235. 10.3389/fphar.2015.00235.

Grygoruk A, Chen A, Martin CA, Lawal HO, Fei H, Gutierrez G, et al. *The redistribution of Drosophila vesicular monoamine transporter mutants from synaptic vesicles to large dense-core vesicles impairs amine-dependent behaviors*. J Neurosci. 2014;34(20):6924–37. Epub 2014/05/16. pmid:24828646; PubMed Central PMCID: PMC4019805.

Hamon M, & Blier P. *Monoamine neurocircuitry in depression and strategies for new treatments*. Prog Neuropsychopharmacol Biol Psychiatry. 2013. Aug 1;45:54-63. doi: 10.1016/j.pnpbp.2013.04.009. Epub 2013 Apr 19.

Hann S, Kvenvold L, Newby BN, Hong M, Warman ML. *A Wisp3 Cre-knockin allele produces efficient recombination in spermatocytes during early prophase of meiosis I*. PLoS One. 2013;8(9):e75116. Published 2013 Sep 10. doi:10.1371/journal.pone.0075116

Hansson, SR., Barbara Bottalico, Vera Noskova, & Bertil Casslén. *Monoamine transporters in human endometrium and decidua*. Human Reproduction Update, Volume 15, Issue 2, March-April 2009, Pages 249–260, https://doi.org/10.1093/humupd/dmn048

Hartenstein V., L. Cruz, J. K. Lovick, and M. Guo, 2017. *Developmental analysis of the dopamine-containing neurons of the Drosophila brain*. J Comp Neurol 525: 363–379. https://doi.org/10.1002/cne.24069

Hawrylycz, M.J. et al. (2012). *An anatomically comprehensive atlas of the adult human transcriptome*. Nature 489: 391-399. doi:10.1038/nature11405

He Z., Y. Luo, X. Shang, J. S. Sun, and J. R. Carlson, 2019. *Chemosensory sensilla of the Drosophila wing express a candidate ionotropic pheromone receptor*. PLoS Biol 17. https://doi.org/10.1371/journal.pbio.2006619

Hnasko TS, & Edwards RH. *Neurotransmitter corelease: mechanism and physiological role*. Annu Rev Physiol. 2012;74:225–43.

Hertel M, Tretter Y, Alzheimer C, & Werner S. *Connective tissue growth factor: a novel player in tissue reorganization after brain injury?*. European Journal of Neuroscience. 2000 Jan;12(1):376-80.

Holbourn K. P., K. R. Acharya, and B. Perbal, 2008. *The CCN family of proteins: structure-function relationships*. Trends Biochem Sci 33: 461–473.

Hurvitz JR, Suwairi WM, Van Hul W, El-Shanti H, Superti-Furga A, Roudier J, Holderbaum D, Pauli RM, Herd JK, Van Hul EV, Rezai-Delui H, Legius E, Le Merrer M, Al-Alami J, Bahabri SA, Warman ML. *Mutations in the CCN gene family member WISP3 cause progressive pseudorheumatoid dysplasia*. Nat Genet. 1999 Sep;23(1):94-8.

Hori A, Nishida T, Takashiba S, Kubota S, & Takigawa M. *Regulatory mechanism of CCN2 production by serotonin (5-HT) via 5-HT2A and 5-HT2B receptors in chondrocytes*. PLoS One. 2017;12(11):e0188014. Published 2017 Nov 16. doi:10.1371/journal.pone.0188014

Hu K., Y. Tao, J. Li, Z. Liu, X. Zhu, et al., 2019. *A comparative genomic and phylogenetic analysis of the origin and evolution of the CCN gene family*. Biomed Res Int 2019. https://doi.org/10.1155/2019/8620878

Inoshita T., and T. Tanimura, 2006. *Cellular identification of water gustatory receptor neurons and their central projection pattern in Drosophila*. Proc Natl Acad Sci U S A 103: 1094–1099. https://doi.org/10.1073/pnas.0502376103

Ishida J, Kurozumi K, Ichikawa T, Otani Y, Onishi M, Fujii K, Shimazu Y, Oka T, Shimizu T, & Date I. *Evaluation of extracellular matrix protein CCN1 as a prognostic factor for glioblastoma*. (2015). Brain Tumor Pathol 32(4):245–252

Ishii K, Wohl M, DeSouza A, & Asahina K. *Sex-determining genes distinctly regulate courtship capability and target preference via sexually dimorphic neurons*. Elife. 2020 Apr 21;9. pii: e52701. doi: 10.7554/eLife.52701.

Issa F, Gerhardt GA, Bartko JJ, Suddath RL, Lynch M, Gamache PH, Freedman R, Wyatt RJ, & Kirch DG. *A multidimensional approach to analysis of cerebrospinal fluid biogenic amines in schizophrenia: I. Comparisons with healthy control subjects and neuroleptic-treated/unmedicated pairs analyses.* Psychiatry Res. 1994 Jun;52(3):237-49.

Ito T, Hiraoka S, Kuroda Y, Ishii S, Umino A, Kashiwa A, Yamamoto N, Kurumaji A, & Nishikawa T. *Effects of schizophrenomimetics on the expression of the CCN1 (CYR 61) gene encoding a matricellular protein in the infant and adult neocortex of the mouse and rat.* Int J Neuropsychopharmacol. 2007 Dec;10(6):717-25. Epub 2007 Jul 4.

Jayakumar A. R., A. Apeksha, and M. D. Norenberg, 2017. *Role of Matricellular Proteins in Disorders of the Central Nervous System.* Neurochem Res 42: 858–875. https://doi.org/10.1007/s11064-016-2088-5

Jeong Y. T., S. M. Oh, J. Shim, J. T. Seo, J. Y. Kwon, et al., 2016. *Mechanosensory neurons control sweet sensing in Drosophila.* Nat Commun 7: 1–9. https://doi.org/10.1038/ncomms12872

Jones EV, & Bouvier DS. Astrocyte-Secreted Matricellular Proteins in CNS Remodelling during Development and Disease. *Glia and the Synapse: Plasticity and Disease.* Volume 2014, Article ID 321209, 12 pages. https://doi.org/10.1155/2014/321209

Jun J. Il, and L. F. Lau, 2011. *Taking aim at the extracellular matrix: CCN proteins as emerging therapeutic targets.* Nat Rev Drug Discov 10: 945–963.

Kamhi JF, & Traniello JF. *Biogenic amines and collective organization in a superorganism: neuromodulation of social behavior in ants.* Brain Behav Evol. 2013;82(4):220-36. doi: 10.1159/000356091. Epub 2013 Nov 21.

Kamhi JF, Arganda S, Moreau CS, Traniello JFA. *Origins of Aminergic Regulation of Behavior in Complex Insect Social Systems.* Front Syst Neurosci. 2017;11:74. Published 2017 Oct 10. doi:10.3389/fnsys.2017.00074.

Kaplow M. E., A. H. Korayem, and T. R. Venkatesh, 2008. *Regulation of glia number in drosophila by Rap/Fzr, an activator of the anaphase-promoting complex, and loco, an RGS protein.* Genetics 178: 2003–2016. https://doi.org/10.1534/genetics.107.086397

Kasture A. S., T. Hummel, S. Sucic, and M. Freissmuth, 2018. *Big lessons from tiny flies: Drosophila melanogaster as a model to explore dysfunction of dopaminergic and serotonergic neurotransmitter systems.* Int J Mol Sci 19: 1788.

Katsube K, Sakamoto K, Tamamura Y, & Yamaguchi A. *Role of CCN, a vertebrate specific gene family, in development. Dev Growth Differ.* 2009 Jan;51(1):55-67. doi: 10.1111/j.1440-169X.2009.01077.x.

Kawagoe KT, Garris PA, Wiedemann DJ, & Wightman RM. *Regulation of transient dopamine concentration gradients in the microenvironment surrounding nerve terminals in the rat striatum.* Neuroscience. 1992 Nov;51(1):55-64.

Keshishian H., K. Broadie, A. Chiba, and M. Bate, 1996. *The Drosophila neuromuscular junction: a model system for studying synaptic development and function.* Annu Rev Neurosci 19: 545–575. https://doi.org/10.1146/annurev.ne.19.030196.002553

Khodosevich K., F. Lazarini, J. vonEngelhardt, H. Kaneko, P. M. Lledo, et al., 2013. *Connective tissue growth factor regulates interneuron survival and information processing in the olfactory bulb.* Neuron 79: 1136–1151. https://doi.org/10.1016/j.neuron.2013.07.011

Kim H, Son S, Shin I. *Role of the CCN protein family in cancer*. BMB Rep. 2018;51(10):486–492. doi:10.5483/BMBRep.2018.51.10.192

Kimura K, Ote M, Tazawa T, & Yamamoto D. *Fruitless specifies sexually dimorphic neural circuitry in the Drosophila brain*. Nature. 2005 Nov 10;438(7065):229-33.

Kivelä R, Kyröläinen H, Selänne H, Komi PV, Kainulainen H, & Vihko V. *A single bout of exercise with high mechanical loading induces the expression of Cyr61/CCN1 and CTGF/CCN2 in human skeletal muscle*. J Appl Physiol (1985). 2007 Oct;103(4):1395-401. Epub 2007 Aug 2.

Klenotic PA, Zhang C, & Lin Z. *Emerging roles of CCN proteins in vascular development and pathology*. J Cell Commun Signal. 2016;10(3):251-257. doi:10.1007/s12079-016-0332-z

Kohl J., A. D. Ostrovsky, S. Frechter, and G. S. X. E. Jefferis, 2013. *A Bidirectional Circuit Switch Reroutes Pheromone Signals in Male and Female Brains*. Cell 155: 1610–1623. https://doi.org/10.1016/j.cell.2013.11.025

Kondo Y., T. Nakanishi, M. Takigawa, and N. Ogawa, 1999. *Immunohistochemical localization of connective tissue growth factor in the rat central nervous system*. Brain Res 834: 146–151. https://doi.org/10.1016/S0006-8993(99)01517-6

Koushika S. P., M. J. Lisbin, and K. White, 1996. *ELAV, a Drosophila neuron-specific protein, mediates the generation of an alternatively spliced neural protein isoform*. Curr Biol 6: 1634–1641. https://doi.org/10.1016/S0960-9822(02)70787-2

Kravitz E, and Huber R. *Aggression in invertebrates*. Current Opinion in Neurobiology, Volume 13, Issue 6, 2003, Pages 736-743, ISSN 0959-4388, https://doi.org/10.1016/j.conb.2003.10.003.

Krupska I., E. A. Bruford, and B. Chaqour, 2015. *Eyeing the Cyr61/CTGF/NOV (CCN) group of genes in development and diseases: highlights of their structural likenesses and functional dissimilarities*. Hum Genomics 9: 24.

Kubota S, & Takigawa M. *The role of CCN2 in cartilage and bone development*. (2011). J Cell Commun Signal 5:209–217

Kubota S, & Takigawa M. *The CCN family acting throughout the body: recent research developments*. Biomolecular Concepts. Volume 4, Issue 5. Pages 477–494. doi: https://doi.org/10.1515/bmc-2013-0018

Kubota S, & Takigawa M. *Cellular and molecular actions of CCN2/CTGF and their role under physiological and pathological conditions*. (2015). Clin Sci 128:181–196

Kular L., J. Pakradouni, P. Kitabgi, M. Laurent, and C. Martinerie, 2011. *The CCN family: A new class of inflammation modulators?* Biochimie 93: 377–388.

Kular, J. K., Basu, S., & Sharma, R. I. (2014). *The extracellular matrix: Structure, composition, age-related differences, tools for analysis and applications for tissue engineering*. Journal of Tissue Engineering. https://doi.org/10.1177/2041731414557112

Kusindarta DL & Wihadmadyatami H. *The Role of Extracellular Matrix in Tissue Regeneration. Tissue Regeneration*. (March 29th 2018). Hussein Abdel hay El-Sayed Kaoud. IntechOpen. doi: 10.5772/intechopen.75728. Available from: https://www.intechopen.com/books/tissue-regeneration/the-role-of-extracellular-matrix-in-tissue-regeneration

Kutz WE, Gong Y, Warman ML. *WISP3, the gene responsible for the human skeletal disease progressive pseudorheumatoid dysplasia, is not essential for skeletal function in mice*. Mol Cell Biol. 2005;25(1):414–421. doi:10.1128/MCB.25.1.414-421.2005

Landgraf M., T. Bossing, G. M. Technau, and M. Bate, 1997. *The origin, location, and projections of the embryonic abdominal motorneurons of Drosophila*. J Neurosci 17: 9642–9655. https://doi.org/10.1523/jneurosci.17-24-09642.1997

Landgraf M., V. Jeffrey, M. Fujioka, J. B. Jaynes, and M. Bate, 2003. *Embryonic origins of a motor system: motor dendrites form a myotopic map in Drosophila*. (Thomas M. Jessell, Ed.). PLoS Biol 1: e41. https://doi.org/10.1371/journal.pbio.0000041

Landgraf M., and S. Thor, 2006. *Development of Drosophila motoneurons: Specification and morphology*. Semin Cell Dev Biol 17: 3–11.

Langer SZ. *Presynaptic autoreceptors regulating transmitter release*. Neurochem Int. 2008 Jan;52(1-2):26-30. Epub 2007 May 16.

Latinkic B. V., S. Mercurio, B. Bennett, E. M. A. Hirst, Q. Xu, et al., 2003. *Xenopus Cyr61 regulates gastrulation movements and modulates Wnt signalling*. Development 130: 2429–2441.

Laurent G., and M. Burrows, 1988. *A population of ascending intersegmental interneurones in the locust with mechanosensory inputs from a hind leg*. J Comp Neurol 275: 1–12. https://doi.org/10.1002/cne.902750102

Laurent, M., Le Dréau, G., Guillonneau, X., Lelièvre, E., Slembrouck, A., Goureau, O., et al. *Temporal and spatial expression of CCN3 during retina development*. (2012). Dev. Neurobiol. 72, 1363–1375. doi: 10.1002/dneu.20994

Le Dréau, G., Nicot, A., Bénard, M., Thibout, H., Vaudry, D., Martinerie, C., et al. *NOV/CCN3 promotes maturation of cerebellar granule neuron precursors*. (2010). Mol. Cell. Neurosci. 43, 60–71. doi: 10.1016/j.mcn.2009.02.011

Le Dréau G, Kular L, Nicot AB, Calmel C, Melik-Parsadaniantz S, Kitabgi P, Laurent M, & Martinerie C. *NOV/CCN3 upregulates CCL2 and CXCL1 expression in astrocytes through beta1 and beta5 integrins*. (2010a). Glia 58(12):1510–1521

Leask A, & Abraham DJ. *All in the CCN family: essential matricellular signaling modulators emerge from the bunker*. Journal of Cell Science 2006 119: 4803-4810; doi: 10.1242/jcs.03270

Lee G, Foss M, Goodwin SF, Carlo T, Taylor BJ, & Hall JC. *Spatial, temporal, and sexually dimorphic expression patterns of the fruitless gene in the Drosophila central nervous system*. J Neurobiol. 2000 Jun 15;43(4):404-26.

Lein, E.S. et al. *Genome-wide atlas of gene expression in the adult mouse brain*. 2007. Nature 445: 168-176. doi:10.1038/nature05453

Leppik L, Kriisa, Koido Kati, Koch Kadri, Kajalaid Kärolin, Haring Liina, Vasar Eero, & Zilmer Mihkel. *Profiling of Amino Acids and Their Derivatives Biogenic Amines Before and After Antipsychotic Treatment in First-Episode Psychosis. Frontiers in Psychiatry*. 2018(9):155. https://www.frontiersin.org/article/10.3389/fpsyt.2018.00155. doi: 10.3389/fpsyt.2018.00155

Li J, Ye L, Owen S, Weeks HP, Zhang Z, & Jiang WG. *Emerging role of CCN family proteins in tumorigenesis and cancer metastasis (Review)*. Int J Mol Med. 2015;36(6):1451-1463. doi:10.3892/ijmm.2015.2390

Libersat, F., and Pflueger, HJ. *Monoamines and the Orchestration of Behavior*. BioScience, Volume 54, Issue 1, January 2004, Pages 17–25, https://doi.org/10.1641/0006-3568(2004)054[0017:MATOOB]2.0.CO;2

Lin S, Senapati B, Tsao CH. *Neural basis of hunger-driven behaviour in Drosophila*. Open Biol. 2019;9(3):180259. doi:10.1098/rsob.180259

Ling F., A. Dahanukar, L. A. Weiss, J. Y. Kwon, and J. R. Carlson, 2014. *The molecular and cellular basis of taste coding in the legs of Drosophila*. J Neurosci 34: 7148–7164. https://doi.org/10.1523/JNEUROSCI.0649-14.2014

Liu CS, Ruthirakuhan M, Chau SA, Herrmann N, Carvalho AF, Lanctot KL. *Pharmacological Management of Agitation and Aggression in Alzheimer's Disease: A Review of Current and Novel Treatments*. Curr Alzheimer Res. 2016;13(10):1134–44. Epub 2016/05/04. pmid:27137221.

Ludwig, M., Leng, G. *Dendritic peptide release and peptide-dependent behaviours*. Nat Rev Neurosci 7, 126–136 (2006). https://doi.org/10.1038/nrn1845

Ludwig T., Kirmse R., Poole K., & Schwarz U. *Probing cellular microenvironments and tissue remodeling by atomic force microscopy*. Pflugers Arch - Eur J Physiol 456, 29–49 (2008). https://doi.org/10.1007/s00424-007-0398-9

Malik AR, Urbanska M, Gozdz A, et al. *Cyr61, a matricellular protein, is needed for dendritic arborization of hippocampal neurons*. J Biol Chem. 2013;288(12):8544-8559. doi:10.1074/jbc.M112.411629

Malik, A., Ewa Liszewska, Jacek Jaworski. *Matricellular proteins of the Cyr61/CTGF/NOV (CCN) family and the nervous system*. Front Cell Neurosci. 2015; 9: 237. Published online 2015 Jun 24.

Manor, S Tyano, E Mel, J Eisenberg, R Bachner-Melman, M Kotler & R P Ebstein. *Family-based and association studies of monoamine oxidase A and attention deficit hyperactivity disorder (ADHD): preferential transmission of the long promoter-region repeat and its association with impaired performance on a continuous performance test (TOVA)*. Mol Psychiatry 7, 626–632 (2002). https://doi.org/10.1038/sj.mp.4001037

Mao Z., and R. L. Davis, 2009. *Eight different types of dopaminergic neurons innervate the Drosophila mushroom body neuropil: anatomical and physiological heterogeneity*. Front Neural Circuits 3: 5. https://doi.org/10.3389/neuro.04.005.2009

Marder E, & Thirumalai V. *Cellular, synaptic and network effects of neuromodulation*. Neural Netw. 2002 Jun-Jul;15(4-6):479-93.

Martin A, Scahill L, Kratochvil C. *The 5-HT3 receptor is the only monoamine receptor coupled to an ion channel, probably a Ca2+ channel. Pediatric Psychopharmacology*. Oxford University Press. 2010. p. 31. ISBN 9780199842667.

Masuzzo A., G. Manière, A. Viallat-Lieutaud, É. Avazeri, O. Zugasti, et al., 2019. *Peptidoglycan-dependent NF-κB activation in a small subset of brain octopaminergic neurons controls female oviposition*. Elife 8: e50559. https://doi.org/10.7554/eLife.50559

Meirieu O, Pairet M, Sutra JF, & Ruckebusch M. *Local release of monoamines in the gastrointestinal tract: an in vivo study in rabbits*. Life Sci. 1986 Mar 3;38(9):827-34.

Middleton C. A., U. Nongthomba, K. Parry, S. T. Sweeney, J. C. Sparrow, et al., 2006. *Neuromuscular organization and aminergic modulation of contractions in the Drosophila ovary*. BMC Biol 4. https://doi.org/10.1186/1741-7007-4-17

Mittal R, Debs L, Patel A, Nguyen D, Patel K, O'Connor G, Grati M, Mittal J, Yan D, Eshraghi A, Deo S, Daunert S, and Liu X. *Neurotransmitters: The critical modulators regulating gut-brain axis*. J Cell Physiol. 2017 Sep; 232(9): 2359–2372. Published online 2017 Apr 10. doi: 10.1002/jcp.25518

Mo FE, Muntean AG, Chen CC, Stolz DB, Watkins SC, Lau LF. *CYR61 (CCN1) is essential for placental development and vascular integrity*. Mol Cell Biol. 2002;22(24):8709–8720. doi:10.1128/mcb.22.24.8709-8720.2002

Monastirioti M. *Biogenic amine systems in the fruit fly Drosophila melanogaster.* 1999. Microsc Res Tech 45: 106–121. https://doi.org/10.1002/(SICI)1097-0029(19990415)45:2<106::AID-JEMT5>3.0.CO;2-3

Monastirioti M. *Distinct octopamine cell population residing in the CNS abdominal ganglion controls ovulation in Drosophila melanogaster*. 2003. Dev Biol 264: 38–49. https://doi.org/10.1016/j.ydbio.2003.07.019

Moons T, Hert MD, Gellens E, Gielen L, Sweers K, Jacqmaert S, van Winkel R, Vandekerckhove P, & Claes S. *Genetic Evaluation of Schizophrenia Using the Illumina HumanExome Chip*. PLoS One. 2016;11(3):e0150464. Published 2016 Mar 30. doi:10.1371/journal.pone.0150464

Morris AH, & Kyriakides TR. *Matricellular proteins and biomaterials*. Matrix Biol. 2014;37:183-191. doi:10.1016/j.matbio.2014.03.002

Murphy-Ullrich JE, & Sage EH. *Revisiting the matricellular concept*. Matrix Biol. 2014;37:1-14. doi:10.1016/j.matbio.2014.07.005

Nakamura Y, Cui Y, Fernando C, Kutz WE, & Warman ML. *Normal growth and development in mice over-expressing the CCN family member WISP3*. J Cell Commun Signal. 2009; 3: 105–113.pmid:19401829

Naskar K, and Stern J. *A functional coupling between extrasynaptic NMDA receptors and A-type K+ channels under astrocyte control regulates hypothalamic neurosecretory neuronal activity*. J Physiol 592.13 (2014) pp 2813–2827

Nässel D. R., and K. Elekes. *Aminergic neurons in the brain of blowflies and Drosophila: dopamine- and tyrosine hydroxylase-immunoreactive neurons and their relationship with putative histaminergic neurons*. 1992. Cell Tissue Res 267: 147–167. https://doi.org/10.1007/BF00318701

Nässel DR. *Substrates for Neuronal Cotransmission With Neuropeptides and Small Molecule Neurotransmitters in Drosophila*. Front Neurosci. 2018;12:83.

National Cancer Institute. "*Intercellular Signaling.*" National Cancer Institute Dictionary of Cancer Terms, NIH, 23 Apr. 2020, www.cancer.gov/publications/dictionaries/cancer-terms/def/intercellular-communication.

Niens J., F. Reh, B. Çoban, K. Cichewicz, J. Eckardt, et al., 2017. *Dopamine Modulates Serotonin Innervation in the Drosophila Brain*. Front Syst Neurosci 11: 76. https://doi.org/10.3389/fnsys.2017.00076

Nicholson C, & Rice ME. *The migration of substances in the neuronal microenvironment*. Ann NY Acad Sci 481: 55–71, 1986

Nicholson C, & Rice ME. *Diffusion of ions and transmitters in the brain cell microenvironment*. In: Volume Transmission in the Brain: Novel Mechanisms for Neural Transmission, edited by Fuxe K and Agnati LF. New York: Raven, 1991, p. 279–294.

Nicholson C, Hrabětová S. *Brain Extracellular Space: The Final Frontier of Neuroscience*. Biophys J. 2017;113(10):2133-2142. doi:10.1016/j.bpj.2017.06.052

Noureddine Lazar, Cristina Manara, Samuel Navarro, Anne-Marie Bleau, Antonio Llombart-Bosch, Katia Scotlandi, Nathalie Planque, Bernard Perbal. *Domain-specific CCN3 antibodies as unique tools for structural and functional studies*. J Cell Commun Signal. 2007 Sep; 1(2): 91–102. Published online 2007 Sep 8.

Nusbaum MP, Blitz DM, Marder E. *Functional consequences of neuropeptide and small-molecule co-transmission*. Nat Rev Neurosci. 2017;18(7):389–403.

Nutt DJ. *Relationship of neurotransmitters to the symptoms of major depressive disorder*. J Clin Psychiatry. 2008;69 Suppl E1:4-7.

Okaty B. W., K. G. Commons, and S. M. Dymecki, 2019. *Embracing diversity in the 5-HT neuronal system*. Nat Rev Neurosci 1. https://doi.org/10.1038/s41583-019-0151-3

Okubo Y, Iino M. Visualization of glutamate as a volume transmitter. J Physiol. 2011;589(Pt 3):481-488. doi:10.1113/jphysiol.2010.199539

Ono M., A. Masaki, A. Maeda, T. M. Kilts, E. S. Hara, et al., 2018. *CCN4/WISP1 controls cutaneous wound healing by modulating proliferation, migration and ECM expression in dermal fibroblasts via α5β1 and TNFα*. Matrix Biol 68–69: 533–546. https://doi.org/10.1016/j.matbio.2018.01.004

Pauls D., C. Blechschmidt, F. Frantzmann, B. el Jundi, and M. Selcho, 2018. *A comprehensive anatomical map of the peripheral octopaminergic/tyraminergic system of Drosophila melanogaster*. Sci Rep 8: 15314. https://doi.org/10.1038/s41598-018-33686-3

Perbal B., 2004. *CCN proteins: Multifunctional signalling regulators*. Lancet 363: 62–64.

Perbal, B. *CCN3: Doctor Jekyll and Mister Hyde*. J Cell Commun Signal. 2008 Jun; 2(1-2): 3–7. Published online 2008 Sep 12.

Perbal, B. *CCN proteins: A centralized communication network*. J Cell Commun Signal. 2013 Aug; 7(3): 169–177. Published online 2013 Feb 19.

Perbal, B. *The concept of the CCN protein family revisited: a centralized coordination network*. J Cell Commun Signal. 2018 Mar; 2(1): 3–12. Published online 2018 Feb 22.

Perbal, B., Susan Tweedie, Elspeth Bruford. *The official unified nomenclature adopted by the HGNC calls for the use of the acronyms, CCN1–6, and discontinuation in the use of CYR61, CTGF, NOV and WISP 1–3 respectively*. J Cell Commun Signal. 2018 Dec; 12(4): 625–629. Published online 2018 Nov 5.

Planque, N., Perbal, B. *A structural approach to the role of CCN (CYR61/CTGF/NOV) proteins in tumourigenesis*. Cancer Cell Int 3, 15 (2003). https://doi.org/10.1186/1475-2867-3-15

Raad H., J. F. Ferveur, N. Ledger, M. Capovilla, and A. Robichon, 2016. *Functional Gustatory Role of Chemoreceptors in Drosophila Wings*. Cell Rep 15: 1442–1454. https://doi.org/10.1016/j.celrep.2016.04.040

Rachfal AW, & Brigstock DR. *Structural and Functional Properties of CCN Proteins. Vitamins & Hormones*. Volume 70, 2005, Pages 69-103. https://doi.org/10.1016/S0083-6729(05)70003-0

Reddy, DS. *Current pharmacotherapy of attention deficit hyperactivity disorder*. Drugs Today (Barc). 2013 Oct;49(10):647-65. doi: 10.1358/dot.2013.49.10.2008996.

Rideout EJ, Billeter JC, & Goodwin SF. *The sex-determination genes fruitless and doublesex specify a neural substrate required for courtship song*. Curr Biol. 2007;17(17):1473-1478. doi:10.1016/j.cub.2007.07.047

Rideout EJ, Dornan AJ, Neville MC, Eadie S, & Goodwin SF. *Control of sexual differentiation and behavior by the doublesex gene in Drosophila melanogaster*. Nat Neurosci. 2010;13(4):458-466. doi:10.1038/nn.2515

Ridet JL, Rajaofetra N, Teilhac JR, Geffard M, Privat A. *Evidence for nonsynaptic serotonergic and noradrenergic innervation of the rat dorsal horn and possible involvement of neuron-glia interactions*. Neuroscience. 1993 Jan;52(1):143-57.

Rohrbough J., E. Rushton, E. Woodruff, T. Fergestad, K. Vigneswaran, et al., 2007. *Presynaptic establishment of the synaptic cleft extracellular matrix is required for post-synaptic differentiation*. Genes Dev 21: 2607–2628. https://doi.org/10.1101/gad.1574107

Ruta V., S. R. Datta, M. L. Vasconcelos, J. Freeland, L. L. Looger, et al., 2010. *A dimorphic pheromone circuit in Drosophila from sensory input to descending output*. Nature 468: 686–690. https://doi.org/10.1038/nature09554

Rutigliano G, Accorroni A, & Zucchi R. *The Case for TAAR1 as a Modulator of Central Nervous System Function*. Frontiers in Pharmacology. Volume 8. 2018. Pg. 987. https://www.frontiersin.org/article/10.3389/fphar.2017.00987. doi:10.3389/fphar.2017.00987

Sakamoto, K., Yamaguchi, S., Ando, R., Miyawaki, A., Kabasawa, Y., Takagi, M., et al. *The nephroblastoma overexpressed gene (NOV/ccn3) protein associates with Notch1 extracellular domain and inhibits myoblast differentiation via Notch signaling pathway*. 2002. J. Biol. Chem. 277, 29399–29405. doi: 10.1074/jbc.m203727200

Sakuma, K., Komatsu, H., Maruyama, M., Imaichi, S., Habata, Y., & Mori, M. *Temporal and Spatial Transcriptional Fingerprints by Antipsychotic or Propsychotic Drugs in Mouse Brain*. 2015. PLoS One 10:e118510. doi: 10. 1371/journal.pone.0118510

Salvemini M., C. Polito, and G. Saccone, 2010. *fruitless alternative splicing and sex behaviour in insects: an ancient and unforgettable love story?* J Genet 89: 287–299.

Sato K, Tanaka R, Ishikawa Y, & Yamamoto D. *Behavioral Evolution of Drosophila: Unraveling the Circuit Basis*. Genes (Basel). 2020 Feb 1;11(2). pii: E157. doi: 10.3390/genes11020157.

Sato K, Goto J, & Yamamoto D. *Sex Mysteries of the Fly Courtship Master Regulator Fruitless*. Front Behav Neurosci. 2019 Oct 18;13:245. doi: 10.3389/fnbeh.2019.00245. eCollection 2019.

Sawai K, Mukoyama M, Mori K, Kasahara M, Koshikawa M, Yokoi H, Yoshioka T, Ogawa Y, Sugawara A, Nishiyama H, Yamada S, Kuwahara T, Saleem MA, Shiota K, Ogawa O, Miyazato M, Kangawa K, & Nakao K. *Expression of CCN1 (CYR61) in developing, normal, and diseased human kidney*. Am J Physiol Renal Physiol. 2007 Oct;293(4):F1363-72. Epub 2007 Aug 15.

Sayin S, De Backer JF, Siju KP, et al. *A Neural Circuit Arbitrates between Persistence and Withdrawal in Hungry Drosophila*. Neuron. 2019;104(3):544-558.e6. doi:10.1016/j.neuron.2019.07.028

Schultz GS, Davidson JM, Kirsner RS, Bornstein P, & Herman IM. *Dynamic reciprocity in the wound microenvironment*. Wound Repair Regen. 2011;19(2):134-148. doi:10.1111/j.1524-475X.2011.00673.x

Schwab J. M., E. Postler, T. D. Nguyen, M. Mittelbronn, R. Meyermann, et al., 2000. *Connective tissue growth factor is expressed by a subset of reactive astrocytes in human cerebral infarction*. Neuropathol Appl Neurobiol 26: 434–440. https://doi.org/10.1046/j.1365-2990.2000.00271.x

Schwab J. M., R. Beschorner, T. D. Nguyen, R. Meyermann, and H. J. Schluesener, 2001. *Differential cellular accumulation of connective tissue growth factor defines a subset of reactive astrocytes, invading fibroblasts, and endothelial cells following central nervous system injury in rats and humans*. J Neurotrauma 18: 377–388. https://doi.org/10.1089/089771501750170930

Sedvall G. *Monoamines and schizophrenia*. Acta Psychiatr. Scand. Suppl., 358 (1990), pp. 7-13

Sengupta A., M. Bocchio, D. M. Bannerman, T. Sharp, and M. Capogna, 2017. *Control of amygdala circuits by 5-HT neurons via 5-HT and glutamate cotransmission*. J Neurosci 37: 1785–1796. https://doi.org/10.1523/JNEUROSCI.2238-16.2016

Sigvardt KA, Rothman BS, Brown RO, Mayeri E. *The bag cells of Aplysia as a multitransmitter system: identification of alpha bag cell peptide as a second neurotransmitter*. J Neurosci. 1986;6(3):803–813. doi:10.1523/JNEUROSCI.06-03-00803.1986

Sinakevitch IT, Wolff GH, Pflüger HJ, Smith BH. *Editorial: Biogenic Amines and Neuromodulation of Animal Behavior*. Front Syst Neurosci. 2018;12:31. Published 2018 Jul 13. doi:10.3389/fnsys.2018.00031

Spielman SJ, Kumar K, & Wilke CO. *Comprehensive, structurally-informed alignment and phylogeny of vertebrate biogenic amine receptors*. PeerJ. 2015;3:e773. Published 2015 Feb 17. doi:10.7717/peerj.773

Stenina-Adognravi O. *Invoking the power of thrombospondins: regulation of thrombospondins expression*. Matrix Biol. 2014;37:69–82. doi:10.1016/j.matbio.2014.02.001

Stockinger P, Kvitsiani D, Rotkopf S, Tirián L, & Dickson BJ. *Neural circuitry that governs Drosophila male courtship behavior*. Cell. 2005 Jun 3;121(5):795-807.

Sun J, Zhang W, Tan Z, et al. *Zika virus promotes CCN1 expression via the CaMKIIα-CREB pathway in astrocytes*. Virulence. 2020;11(1):113-131. doi:10.1080/21505594.2020.1715189

Svensson E, Apergis-Schoute J, Burnstock G, Nusbaum MP, Parker D, Schiöth HB. *General Principles of Neuronal Co-transmission: Insights From Multiple Model Systems*. Front Neural Circuits. 2019;12:117. Published 2019 Jan 21. doi:10.3389/fncir.2018.00117

Swallow JG, Bubak AN, Grace JL; Guest Editors. *The role of monoamines in modulating behavior*. Curr Zool. 2016;62(3):253–255. doi:10.1093/cz/zow046

Taber KH, Hurley RA. *Volume transmission in the brain: beyond the synapse*. J Neuropsychiatry Clin Neurosci. 2014;26(1):iv-4. doi:10.1176/appi.neuropsych.13110351

Takahashi A, & Miczek KA. *Neurogenetics of aggressive behavior: studies in rodents*. Curr Top Behav Neurosci. 2014;17:3-44. doi:10.1007/7854_2013_263

Takigawa M. *The CCN Proteins: An Overview*. Methods Mol Biol. 2017;1489:1-8.

Takigawa M. *CCN2: a master regulator of the genesis of bone and cartilage*. (2013). J Cell Commun Signal 7:191–201

Tao J, Bulgari D, Berkhoudt DA, et al. *Drosophila Ptp4E regulates vesicular packaging for monoamine-neuropeptide co-transmission*. J Cell Sci. 2019;132(7):jcs224568. Published 2019 Apr 3. doi:10.1242/jcs.224568

Theodosiou NA, Xu T. *Use of FLP/FRT system to study Drosophila development*. Methods. 1998;14(4):355-365. doi:10.1006/meth.1998.0591

Thomas AL, Davis SM, Dierick HA. *Of Fighting Flies, Mice, and Men: Are Some of the Molecular and Neuronal Mechanisms of Aggression Universal in the Animal Kingdom?*. PLoS Genet. 2015;11(8):e1005416. Epub 2015/08/28.

Timmermans, P. B. M. W. M., & Thoolen, M. J. M. C. *Autoreceptors in the central nervous system*. Medicinal research reviews. (1987). 7(3), 307-332.

Tritsch NX, Sabatini BL. *Dopaminergic modulation of synaptic transmission in cortex and striatum*. Neuron. 2012;76(1):33–50. doi:10.1016/j.neuron.2012.09.023

Trudeau LE, El Mestikawy S. *Glutamate Cotransmission in Cholinergic, GABAergic and Monoamine Systems: Contrasts and Commonalities*. Front Neural Circuits. 2018;12:113. Published 2018 Dec 18. doi:10.3389/fncir.2018.00113

Trueta C, De-Miguel FF. *Extrasynaptic exocytosis and its mechanisms: a source of molecules mediating volume transmission in the nervous system*. Front Physiol. 2012;3:319. Published 2012 Sep 4. doi:10.3389/fphys.2012.00319

Tsao CH, Chen CC, Lin CH, Yang HY, & Lin S. *Drosophila mushroom bodies integrate hunger and satiety signals to control innate food-seeking behavior*. eLife 2018;7:e35264 DOI: 10.7554/eLife.35264

Ueberham U, Ueberham E, Gruschka H, & Arendt T. *Connective tissue growth factor in Alzheimer's disease*. Neuroscience. 2003;116(1):1-6.

Vaaga CE, Borisovska M, Westbrook GL. *Dual-transmitter neurons: functional implications of co-release and co-transmission*. Curr Opin Neurobiol. 2014;29:25–32. doi:10.1016/j.conb.2014.04.010

Van Bockstaele EJ, Pickel VM. *Ultrastructure of serotonin-immunoreactive terminals in the core and shell of the rat nucleus accumbens: cellular substrates for interactions with catecholamine afferents*. J Comp Neurol. 1993 Aug 22;334(4):603-17.

Venkatasubramanian L., and R. S. Mann, 2019. *The development and assembly of the Drosophila adult ventral nerve cord*. Curr Opin Neurobiol 56: 135–143.

Verhulst E. C., L. van de Zande, and L. W. Beukeboom, 2010. *Insect sex determination: It all evolves around transformer*. Curr Opin Genet Dev 20: 376–383.

Villella A, & Hall JC. *Neurogenetics of courtship and mating in Drosophila*. Adv Genet. 2008;62:67-184. doi: 10.1016/S0065-2660(08)00603-2.

Walderhaug E, Varga M, Pedro MS, Hu J, & Neumeister A. *The role of the aminergic systems in the pathophysiology of bipolar disorder*. Curr Top Behav Neurosci. 2011;5:107-26. doi:10.1007/7854_2010_72.

Wang J, Yin L, & Chen Z. *New insights into the altered fibronectin matrix and extrasynaptic transmission in the aging brain*. Journal of Clinical Gerontology and Geriatrics. Volume 2, Issue 2, June 2011, Pages 35-41. https://doi.org/10.1016/j.jcgg.2010.12.002

Watson CJ, Baghdoyan HA, Lydic R. *Neuropharmacology of Sleep and Wakefulness*. Sleep Med Clin. 2010;5(4):513–528. doi:10.1016/j.jsmc.2010.08.003

Watts WW, Morrison SF, Davis RP, and Barman SM. *Serotonin and Blood Pressure Regulation*. Pharmacol Rev. 2012 Apr; 64(2): 359–388. doi: 10.1124/pr.111.004697

Winterhager E., and A. Gellhaus, 2014. *The role of the CCN family of proteins in female reproduction*. Cell Mol Life Sci 71: 2299–2311.

Wohl M, Ishii K, & Asahina K. *Layered roles of fruitless isoforms in specification and function of male aggression-promoting neurons in Drosophila*. Elife. 2020 Apr 21;9. pii: e52702. doi: 10.7554/eLife.52702.

Wong GS, Rustgi AK. *Matricellular proteins: priming the tumour microenvironment for cancer development and metastasis*. Br J. 2013;108(4):755-761. doi:10.1038/bjc.2012.592

Wrangham RW. *Two types of aggression in human evolution*. Proc Natl Acad Sci U S A. 2018;115(2):245–53. Epub 2017/12/28.

Xia YF, Chang J, Yang JF, & Zhang LM. *Research on WISP1 in Lung Disease*. 2016. J Anesth Crit Care Open Access 4(2): 00133. DOI: 10.15406/jaccoa.2016.04.00133

Xie Z, Westmoreland SV, Miller GM. *Modulation of monoamine transporters by common biogenic amines via trace amine-associated receptor 1 and monoamine autoreceptors in human embryonic kidney 293 cells and brain synaptosomes*. J Pharmacol Exp Ther. 2008 May;325(2):629-40. doi: 10.1124/jpet.107.135079. Epub 2008 Feb 29.

Yamamoto D. *The neural and genetic substrates of sexual behavior in Drosophila*. Adv Genet. 2007;59:39-66.

Yamamoto D. *Brain sex differences and function of the fruitless gene in Drosophila*. J Neurogenet. 2008;22(3):309-32. doi.1080/01677060802298491.

Yeger, H., & Perbal, B. *The CCN family of genes: a perspective on CCN biology and therapeutic potential*. J Cell Commun Signal. 2007 Dec; 1(3): 159–164. Published online 2008 Jun 21.

Yellman C., H. Tao, B. He, and J. Hirsh, 1997. *Conserved and sexually dimorphic behavioral responses to biogenic amines in decapitated Drosophila*. Proc Natl Acad Sci U S A 94: 4131–4136. https://doi.org/10.1073/pnas.94.8.4131

Yukiori Goto, Young-A Lee, Yoshie Yamaguchi, & Emanuel Jas. *Biological mechanisms underlying evolutionary origins of psychotic and mood disorders*. Neuroscience Research, 10.1016/j.neures.2016.04.007, 111, (13-24), (2016).

Libersat, F., and Pflueger, HJ. *Monoamines and the Orchestration of Behavior*. BioScience, Volume 54, Issue 1, January 2004, Pages 17–25, https://doi.org/10.1641/0006-3568(2004)054[0017:MATOOB]2.0.CO;2

Zhan, Y., Liu, L. & Zhu, Y. *Taotie neurons regulate appetite in Drosophila*. Nat Commun 7, 13633 (2016). https://doi.org/10.1038/ncomms13633

Zhao Z, Ho L, Wang J, Qin W, Festa ED, Mobbs C, Hof P, Rocher A, Masur S, Haroutunian V, & Pasinetti GM. *Connective tissue growth factor (CTGF) expression in the brain is a downstream effector of insulin resistance- associated promotion of Alzheimer's disease beta-amyloid neuropathology*. FASEB J. 2005 Dec;19(14):2081-2. Epub 2005 Sep 26